Mixed Sediment Dynamics at a Tide-Dominated Confluence

A case study on Yangon Estuary, Myanmar

Master Thesis

R. A. (Rutger) Bax

Royal HaskoningDHV

TU Delft

Boskalis

Mixed-Sediment Dynamics at a Tide-Dominated Confluence

A case study on Yangon Estuary, Myanmar

By

Rutger Bax

in partial fulfilment of the requirements for the degree of

Master of Science
In Civil Engineering

at the Delft University of Technology,
to be defended publicly on Wednesday July 17, 2019 at 11:00 AM.

Supervisor:	Prof. dr. ir. S.G.J. Aarninkhof	TU Delft
Thesis committee:	Dr. ir. A. Blom	TU Delft
	Dr. D.S. van Maren	TU Delft
	Ir. F. Schuurman	RHDHV
	Ir. M.P.J. Janssen	Boskalis

Boskalis   TUDelft   Royal HaskoningDHV
Enhancing Society Together

Preface

This thesis finalises my Master of Science program at the Delft University of Technology in Hydraulic Engineering and was carried out as a graduation internship at Boskalis in Papendrecht.

I would like to express my gratitude to all members of my thesis committee for their profitable discussions and critical feedback during the meetings. A special thanks to my daily supervisor at Boskalis Merijn for helping me improving my technical writing skills and for his support during the project. Additionally, I would like to express my gratitude towards Boskalis for its hospitality and towards all the colleagues and students at Boskalis who contributed to the pleasure I have experienced during the project. I would like to thank Filip and RHDHV for the opportunity to continue working with their numerical models and the lessons learned.

Finally, thanks to my friends and family for the support you gave me during the whole study program.

Rutger Bax

Rotterdam, July 2019

Summary

This thesis research has been conducted to analyse the sediment dynamics in the Yangon Estuary in order to define the cause for the sedimentation in Monkey Point Channel. Monkey Point Channel is a dredged channel through a shoal (Inner Bar) that separates the deep estuary channels between Yangon Port with the Andaman Sea. The shoal is located at the bay head of the estuary where the estuary splits in the Yangon River and the Bago River. The tidal range at the confluence is 4 m, resulting in strong bidirectional currents. Nevertheless, almost daily dredging of Monkey Point Channel is required in order to keep Yangon Port accessible. Multiple dredging projects turned out to be ineffective and hence, more knowledge on the sediment dynamics is required to find a long term solution to reduce the amount of sedimentation in the navigation channel.

In order to investigate the cause of sedimentation in Monkey Point Channel a conceptual model has been developed. The conceptual model is a graphical visualisation of system functions, including dominant processes, providing a framework for thinking, interpretation and communication. The design of the conceptual model is built up in three stages. All three stages contain a version of the dry season and of the monsoon season. In the first stage the system conditions are defined by means of a study area analysis. In the second stage important processes are linked to these conditions based on a literature study to estuarine, riverine and sediment processes. In the third stage the numerical models SOBEK and MIKE are used to calculate discharges, water levels, flow velocities, bed shear stresses and sediment transport within a 2DH framework. The model results are linked to the important processes of the second stage conceptual model. With the quantitative information on the dynamics in the estuary system, the final conceptual model is made. The findings of this conceptual model are described in the subsequent paragraph.

Main characteristics of Yangon Estuary are the macro-tidal regime, the monsoon climate, the presence of a confluence with large tidal range, and high suspended sediment concentrations (SSC) in the system. During the monsoon season, the SSC in the Irrawaddy exceeds 1 g/l and the SSC in the estuary is also around 1 g/l. About 20% of the sediment in the Irrawaddy is smaller than 1 µm, indicating the amount of fine sediments transported towards the Yangon Estuary. During the dry season, the discharge in the Irrawaddy reduces and the SSC falls to 0.1 g/l. At the same time the SSC in the estuary exceeds 6 g/l during spring tides, but less than 1 g/l during neap tides. The SSC are therefore expected to be determined by the tide.

By means of estuary classification, it is showed that Yangon Estuary has a typical morphology of a tide-dominated system with amongst others, tidal sand ridges, a funnel shape, flanking wetlands with mangroves and a bay head delta. In tide-dominated systems, the sediment distribution is controlled by the tidal currents. Important sediment dynamics related processes in tide-dominated estuaries are the formation of an Estuarine Turbidity Maximum (ETM), a flood-dominant tide and spring/neap variations in the Suspended Solids Concentration (SSC).

Further research to flood-dominance is done by the application of the numerical models. The model results show that the tide is flood-dominant during the dry season and becomes ebb

dominant during the monsoon season. The residual sediment transport is therefore expected to be landward during the dry season and seaward during the monsoon season.

Commonly, such high concentrations are related to the presence of an ETM. Basically, there are two forms of an ETM; tide-related and density-related. At a tide-related ETM, sediment gets trapped at the location of the tidal node and at a density-related ETM, sediment gets trapped at the density node. However, the analysis to the salt and tidal intrusion length pointed out that the potential location of the ETM would be more than 30 km upstream of the measured SSC location. Therefore, the SSC are not likely to be caused by these forms of an ETM. A more probable cause for the high SSC is the erosion of mud layers which are formed during neap tides. This process is derived from the Severn Estuary where the SSC is dominated by the spring/neap variation in tidal currents. Numerical model results show that during neap tides, mud is indeed able to settle on the shoals, but during spring tides the bed shear stress exceeds the critical shear stress for the erosion of consolidated mud causing for suspension of fine sediments into the water column.

The analysis to the dynamics at a confluence and bifurcation showed that both during flood and ebb a zone is created with very low flow velocities; stagnation-zone (confluence) and drive-up-zone (bifurcation). Monkey Point Channel is located in the middle of this area and therefore further research was done. The model results showed that the bed shear stresses in the channel are almost constant below the critical shear stress for the erosion of freshly deposited mud (τ_e= 0.2 N/m2). Hence, the mud is able to consolidate, which eventually becomes problematic for ship traffic when the density exceeds 1250 kg/m3. Due to the high SSC values around the Inner Bar, a lot of fine sediment is able to settle in Monkey Point Channel.

By means of nautical charts, the historical morphological development of the estuary has been analysed. In addition, calculations with the sediment model have been made to determine the morphological response to a uniform bed after 10 years. Based on literature study, the analysis to the nautical maps and the model results, it is concluded that the Inner Bar is formed by the deposition of sand originating from the rivers more than 200 years ago. Furthermore, the Inner Bar is stable over the last years, pointing on the balance between erosion and deposition. The erosion is expected to be caused by the strong tidal current and deposition is expected to be caused by the mid-channel bar growth principle.

Dredged material from Monkey Point Channel showed that the slopes consist of medium sand and the sediment in the middle of the channel consists of very soft clayey fine sand. With the final version of the conceptual model it was concluded that the medium sand from the slopes can be related to the historical development of the Inner Bar by sand deposition and the very soft clayey fine sand can be related to the deposition of the high concentrations fine sediments due to the low bed shear stresses in the stagnation zone. To verify this, an estimation on the sediment balance for the Monkey Point Channel is calculated. The calculation showed the same order size of sedimentation as the reported yearly dredging volumes. Hence, the expectation is confirmed by this estimation.

In addition, research to potential solutions for the sedimentation problem is performed. Based on the results it can be concluded that relocation of the navigation channel outside the stagnation-zone is the best option in relation to sedimentation rates. The combination of land reclamation at the western bank in combination with a new dredged channel shows the most promising results.

List of Figures

List of Tables

Contents

1 Introduction

The topic of this MSc thesis is introduced in this chapter. First, the problem is introduced. Next the research questions are defined and finally the methodology is explained.

1.1 Problem definition

Estuaries are a frequent location for ports where transhipment of cargo between inland vessels and sea-going vessels occurs. Because of the ever growing ship sizes, depth limits have been a frequent problem to the accessibility of ports. In order to increase the accessibility of those ports, estuaries have been modified in the past by interventions such as channel deepening and straightening. Such interventions can have large impact on the estuary hydrodynamics and morphodynamics and when the consequences are not considered in advance, new sedimentation problems can occur. Hence, a proper understanding of the sediment dynamics in an estuary is key to an effective solution to sedimentation problems.

This holds also for the sedimentation problem in the navigation channel to Yangon Port. For years, the port of Yangon has been struggling with high sedimentation rates in the navigation channel. The sedimentation is limiting the size and the amount of ships that is able to call for Yangon Port. In order to increase the accessibility of the port, several dredging activities have been carried out. Unfortunately, these projects proved ineffective in the long term, since high sedimentation rates remained. Currently, the navigation channel is being dredged by local dredgers on a daily basis to ensure the navigation channel remains its function (JICA, 2014). Consequently, every year a volume of 2 million cube needs to be dredged, which almost equals the volume of the channel (L = 2000 m, B = 100 m, d = -9.0 m +MSL).

Yangon Port is located at the Yangon River (see Figure 1.2). Ships with a maximum draft of 9 m can sail from the Andaman Sea, through the Yangon Estuary up to the Yangon River (Oosterwegel, 2018). The natural depth of the estuary channels provides a good navigation channel towards Yangon River, but on this route there are two shoals that need to be passed; the Inner Bar and the Outer Bar. The Inner Bar is located just downstream of the confluence and because of the interest in a confluence within a tidal zone, it is decided to focus on the sedimentation problem at the Inner Bar. In order to let ships pass the Inner Bar, Monkey Point Channel has been dredged. Monkey Point Channel was dredged on this location because it is the shortest distance between the Yangon River and the estuary channel just downstream of the Bago River mouth (Myanmar Port Authority, Monkey Point Channel, 2019).

Yangon Port is the major gateway of Myanmar, handling 90% of its cargo transport. Since the fall of the military regime in 2009, followed by a turnover from a closed market to an open market, Myanmar is experiencing a huge economic growth (World Bank, 2018). Related to this economic growth, the demand for cargo transport is also growing rapidly. But due to the limited accessibility of the port, the amount of cargo transport is being limited as well. Consequently, the economic growth is threatened to be hindered by the limited cargo transport. Multiple researches to improve the port system of Myanmar, like the realisation of an offshore port, has been done but these projects are not likely to happen in the near future (Oosterwegel, 2018). Therefore, the Myanmar Port Authority (MPA) wants to optimize the utilization of Yangon Port by improving the current navigation channel.

Currently, there is an ongoing tender from the MPA for a capital dredging project combined with five year of maintenance. Maintaining the navigation channel in the current state has proven to be ineffective. In order to make the tender profitable for contractors, the amount of maintenance should be minimalised. The problem is that the current knowledge is insufficient in order to determine the cause for sedimentation. Hence, a mitigation to minimalise the sedimentation cannot yet be made. Therefore, more research to the sediment dynamics in the estuary is required. Once the cause of the sedimentation is known, one can investigate what kind of mitigation is most effective.

Figure 1.1: Location of the Yangon Estuary in the Irrawaddy Delta.
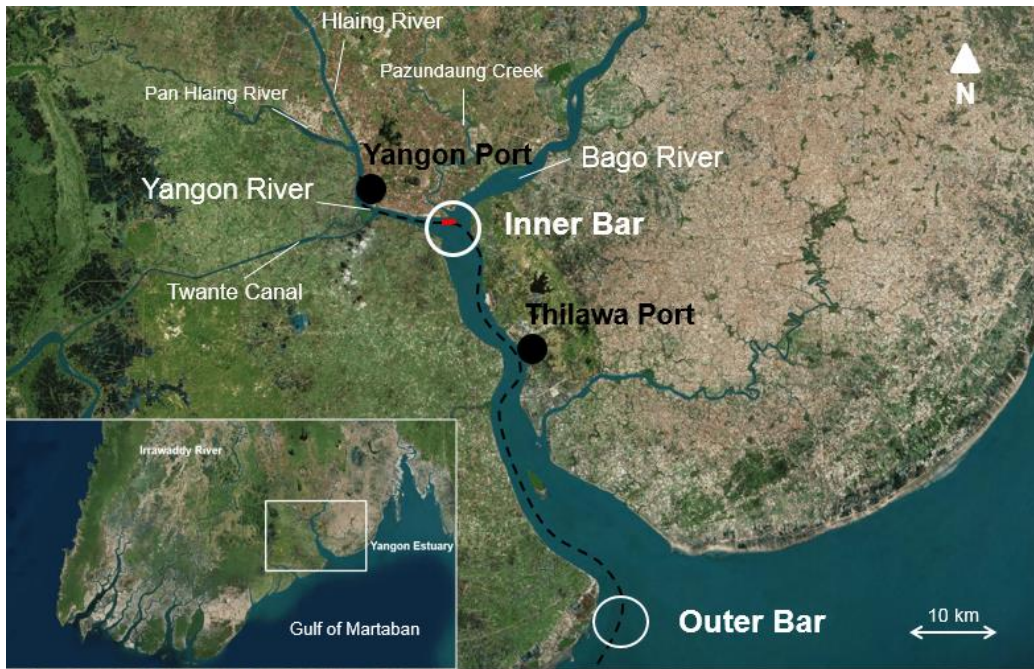
Figure 1.2: Yangon Estuary with the Inner Bar and Outer Bar. The black dashed line shows the navigation channel. The red line shows the location of Monkey Point Channel.

1.2 Research questions

A better understanding of the sediment dynamics in estuaries could seriously contribute to the effectiveness of adjustments that have to increase the accessibility of ports. Furthermore, the In addition the following main research questions is defined:

Which mechanisms are responsible for sedimentation at the confluence of the Bago and Yangon rivers, and how can sedimentation be mitigated?

The research question is approached by answering the following sub-questions:

1. *Which hydrodynamic processes are important in relation to the sediment transport in the estuary?*
2. *How do sand and mud contribute to the sediment dynamics in the estuary?*
3. *Why does sedimentation occur in the navigation channel at the confluence of the Bago and Yangon rivers?*
4. *How can the sedimentation, and therefore the maintenance, in the navigation channel be reduced?*

1.3 Methodology

As already mentioned in **Error! Reference source not found.**, multiple studies have been done to the sediment dynamics of the Yangon Estuary, but the cause for the sedimentation in Monkey Point Channel has not been found yet. Based on the available knowledge and data of the estuary system, it is decided to set up a conceptual model. A conceptual model is a graphical visualisation of system functions, including relevant conditions and dominant processes, providing a framework for thinking, interpretation, and communication. The goal of the conceptual model is, by clustering the processes and conditions into one framework, to find relations and interaction between the processes, which combination forms a potential cause for the sedimentation in Monkey Point Channel. The set-up of the conceptual model is divided in three stages. Because two seasons are dominant in the Yangon Estuary, each stage is provided with a dry season model and a monsoon season model. The framework consists of a top-view of the estuary system in which information is provided numbers and symbols in order to show order sizes and directions.

In the first stage the hydraulic conditions, sediment conditions and morphologic conditions are defined by means of a study area analysis. These conditions are integrated in the conceptual model in order to clarify the variations in space and time. In this way, the estuary conditions give a first indication on which processes need to be considered in the second stage. In addition, estuary classification is applied in order to get a better focus on the relevant processes for the Yangon Estuary.

In the second stage a literature study is done to estuarine, riverine and sediment processes. By defining the interaction between the analysed processes and the estuarine conditions it is considered which processes are dominant regarding the sedimentation in Monkey Point Channel.

In the third stage, numerical models are used in order to get more quantitative insight in the processes that are considered dominant in the second stage. By means of the numerical model results, one is able to show the time and spatial variance of for instance the discharges, flow velocities and water levels. The model results are used as feedback on the conceptual model in order to set-up the final version. Based on this version of the conceptual model, the research question will be answered.

Based on the conceptual model multiple mitigations are defined with the goal to reduce the sedimentation in the navigation channel. The numerical model is used to calculate the impact of the mitigation on the sedimentation rate in the navigation channel. In addition, the effect of the mitigation on the whole system is considered by using the conceptual model.
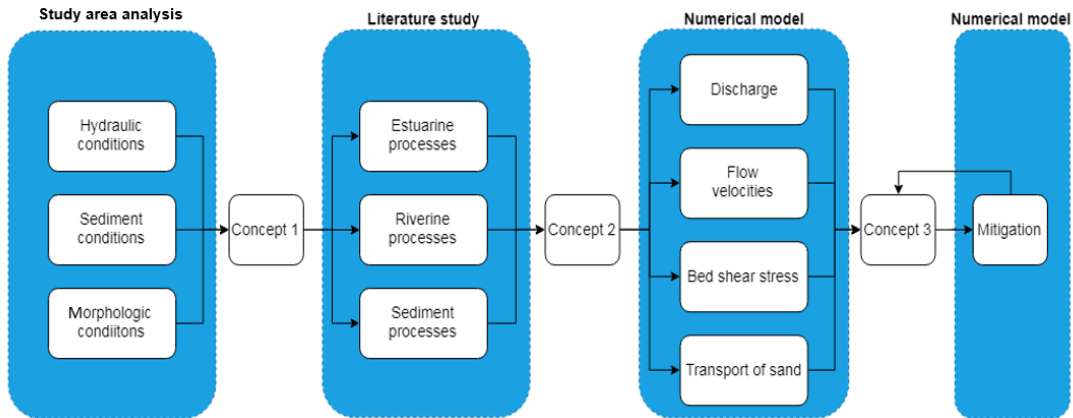
Figure 1.3: Research Methodology

1.4 Research approach

The report outline is similar to the research methodology. The study area analysis is done in Chapter 2. Chapter 2 is finalised with the first stage conceptual model. In Chapter 3 estuary classification is applied in order to refine the scope on which processes need to be considered within the literature study. Chapter 4 contains the literature study which is divided in the estuarine, riverine and sediment processes. Chapter 4 ends with the second stage conceptual model. The numerical model analysis is separated in two chapters. Chapter 5 contains the hydrodynamic model, Chapter 6 contains the sediment model. Chapter 5 and 6 consists both of a model set up and the analysis of the model results. In Chapter 7 the third stage conceptual model is set up based on the combination of the first two conceptual models and the numerical model results. By means of this conceptual model the processes and their relation to the sedimentation in Monkey Point Channel are discussed. Based on this discussion, multiple mitigations are tested and discussed in Chapter 8. In Chapter 9 the critical decisions made during this research are discussed. The final answers to the research question is given in Chapter 10 (Conclusions) after which in Chapter 11 recommendations are made for future research and dredging strategies for Yangon Estuary and its navigation channel.

2 Study area analysis

In this chapter the first stage version of the conceptual model is created. First, an overview of the river network is presented, followed by the hydraulic conditions. Next, the sediment and morphologic conditions are defined. Finally, these conditions are clustered in the conceptual model.

The Yangon Estuary is the most easterly branch of the Irrawaddy River, the largest river of Myanmar and one of the largest sediment transporting rivers of the world (Robinson, 2007). The Irrawaddy River rises from the Himalayas in the north of Myanmar, crosses Myanmar and flows into the Andaman Sea through multiple branches called the Irrawaddy Delta (See Figure 1.1). The Yangon Estuary is connected to the Irrawaddy by the Upper Hlaing River, the Nyaungdon River and the Twante Canal.
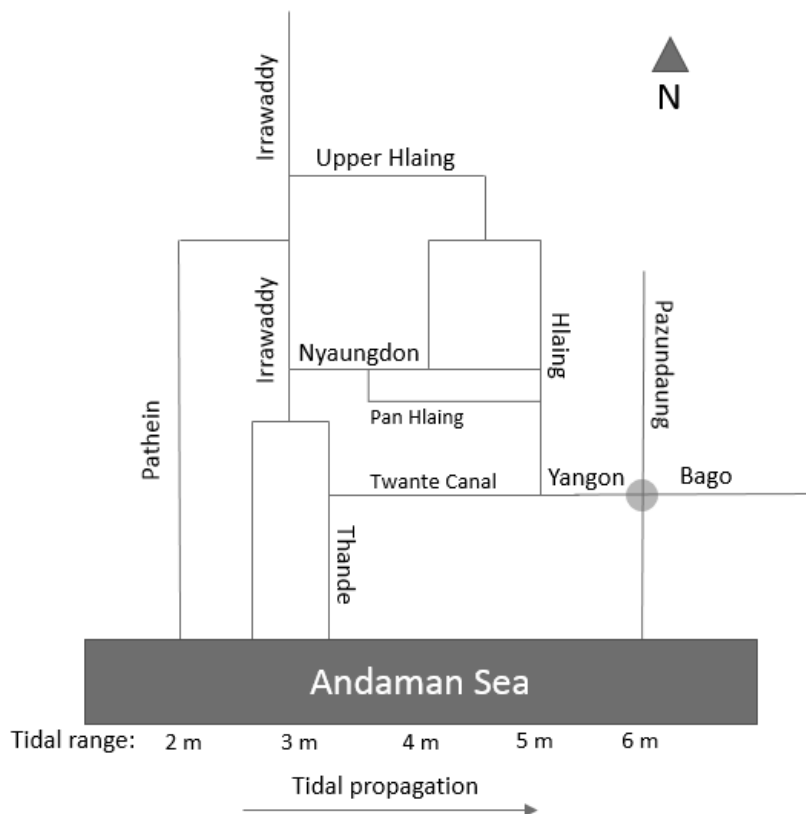
Figure 2.1: River network of the Irrawaddy Delta. The numbers show the increasing spring tidal range from West to East.

The blue circle shows the area of interest. The bay head of the estuary is formed by a confluence of the Yangon River and the Bago River. In the middle of the confluence, between the Yangon River and the Bago River, the Pazundaung Creek flows into the estuary.

Figure 2.2 shows the bathymetry of the confluence with the navigation route. The navigation channel follows the natural channels of the estuary which have a natural averaged depth of 13 m below MSL. But at the confluence of the estuary ships have to cross the Inner Bar where the natural depth is 6.5 m below MSL. In order to let ships with a draught up to 9.0 m pass the Inner Bar, Monkey Point Channel has been dredged. Monkey Point channel is designed to have a length of 2000 m, a minimum width of 100 m and a minimum depth of 9.0 m below MSL.
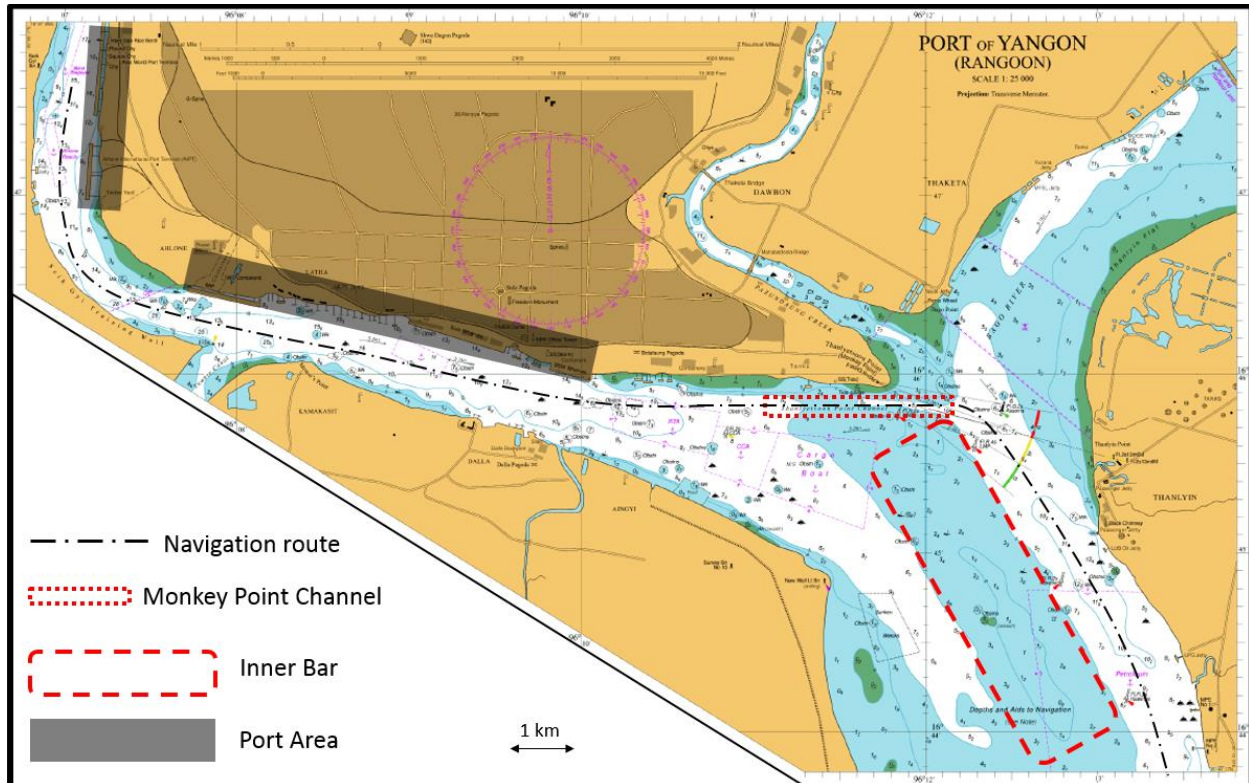
Figure 2.2: Bathymetry of he confluence of the Bago River and the Yangon River with the navigation channel highlighted by the dashed line. Source: (RHDHV, 2016)

2.1 Hydrodynamic conditions

In this subsection the hydrodynamic conditions are considered which consists of the river discharges, the tide and salt intrusion, and the wave climate.

Myanmar's climate is dominated by two seasons; the dry season and the monsoon season. These seasons are clearly presented by the Irrawaddy discharge curve (see Figure 2.3). The dry season is from December to May and the monsoon season from June to November. How much of the discharge is flowing into the Yangon Estuary is not known for sure because there is no long term data on the discharges of the rivers that connect the estuary with the Irrawaddy River. The only available data is shown in Table 2-1 and Table 2-2. Aung (2013) defined dry season and monsoon season discharges, based on data by Alexander Gibb (1972). In addition discharge data of the same rivers that is defined by a MMU student, is used for comparison.
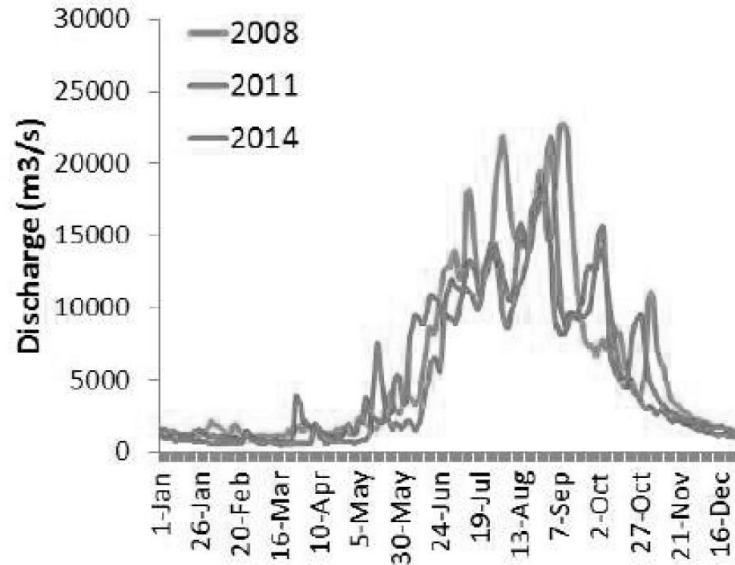
Figure 2.3: Measured discharge of the Irrawaddy River (DMH, 2014).

Table 2-1: Defined river discharges by Aung (2013)

	Dry season [m3/s]	Monsoon season [m3/s]
Yangon River	627	6853
Pazundaung Creek	143	866
Bago River	315	1566

Table 2-2: Defined river discharges by MMU student (RHDHV, 2016)

	Mean monsoon discharge [m3/s]	Maximum discharge [m3/s]
Yangon River	5570	8600
Pazundaung Creek	333	580
Bago River	700	1220

From this data it can be concluded that the monsoon river discharge in the Yangon River is the largest discharge flowing into the estuary origins from the Irrawaddy and flows through the Yangon River into the estuary. This data must be considered carefully and just used as an indication. The discharges are further considered in Chapter 3.

Myanmar has a semi-diurnal tide (Bosboom & Stive, 2015). As shown in Figure 2.1, the tide propagates along the Irrawaddy delta from west to the east during the rising period. This is because the amphidromic point is located near Sri Lanka and the tide propagates in anti-clockwise direction north of the equator (Bosboom, 2016). The water depth of the Andaman Sea reduces gradually in north east direction, causing the tide to shoal towards the north east end of the Andaman sea basin. As a result the tidal range differs along the Irrawaddy Delta as shown in Figure 2.1. Furthermore, the mean water level differs between the dry season and the monsoon season. During the monsoon the wind is blowing dominantly from the South-West, causing for a wind induced set-up of 0.5 m (RHDHV, 2018). The tide table for Yangon Estuary is shown in Table 2-3. The tidal variation is considered in more detail in Chapter 5.

Table 2-3: Tide table for Monkey Point (MP) and Elephant Point (EP)

	MP [m]	Relative to MSL [m]	EP [m]	Relative to MSL [m]
HHW	5.8	2.7	6.6	2.9
LHW	4.4	1.3	4.9	1.2
MSL	3.1	0	3.7	0
HLW	1.6	-1.5	2.5	-1.2
LLW	0.7	-2.4	0.8	-2.9

During the dry season, tidal fluctuations in water level are observed up to the confluence of the Irrawaddy River and the Nyaungdon River. No information has been found on the tidal intrusion difference between dry season and monsoon season. Salt intrusion reaches up to confluence of the Nyaungdon River and the Hlaing River (RHDHV, Pan Hlaing Sluice Project, 2018). During monsoon season the salt intrusion is pushed back to the location of Yangon Port (see Figure 2.4). The salt intrusion in the Bago River reaches up to the limit of the convergence length of the Bago River in the dry season (Attema, 2014). The limit of the salt intrusion monsoon season is not known for the Bago River.
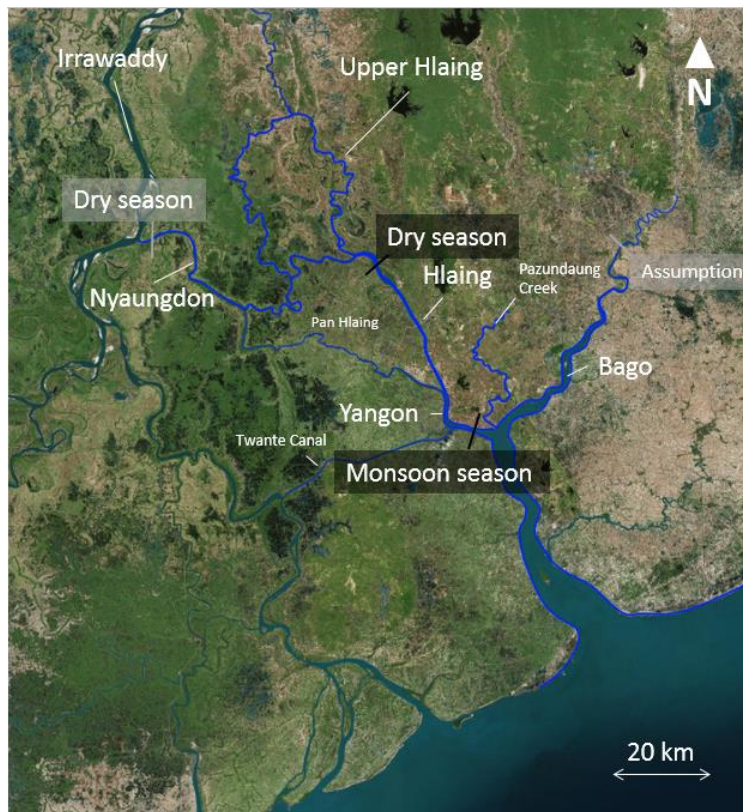
Figure 2.4: Tidal and salt intrusion. In black the salt intrusion limit during dry season and monsoon season. In grey the tidal intrusion limit in dry season. Tidal intrusion limit during monsoon is not known.

Because of the South-East Asian monsoon climate, the wind is dominantly from the North-West during the dry season. Because the wind is blocked by the Himalayas, the wind speeds are very low in this season. During the monsoon season the dominant wind direction is from the South-West. Because of the large fetch over the Indian Ocean, the winds are stronger during this season (see Figure 2.5).

From the data it is noticed that the wave height is strongly correlated to the seasonal wind direction. During the dry season 90% of the waves is smaller than 1.0 m. The wave conditions are represented in Figure 2.5.
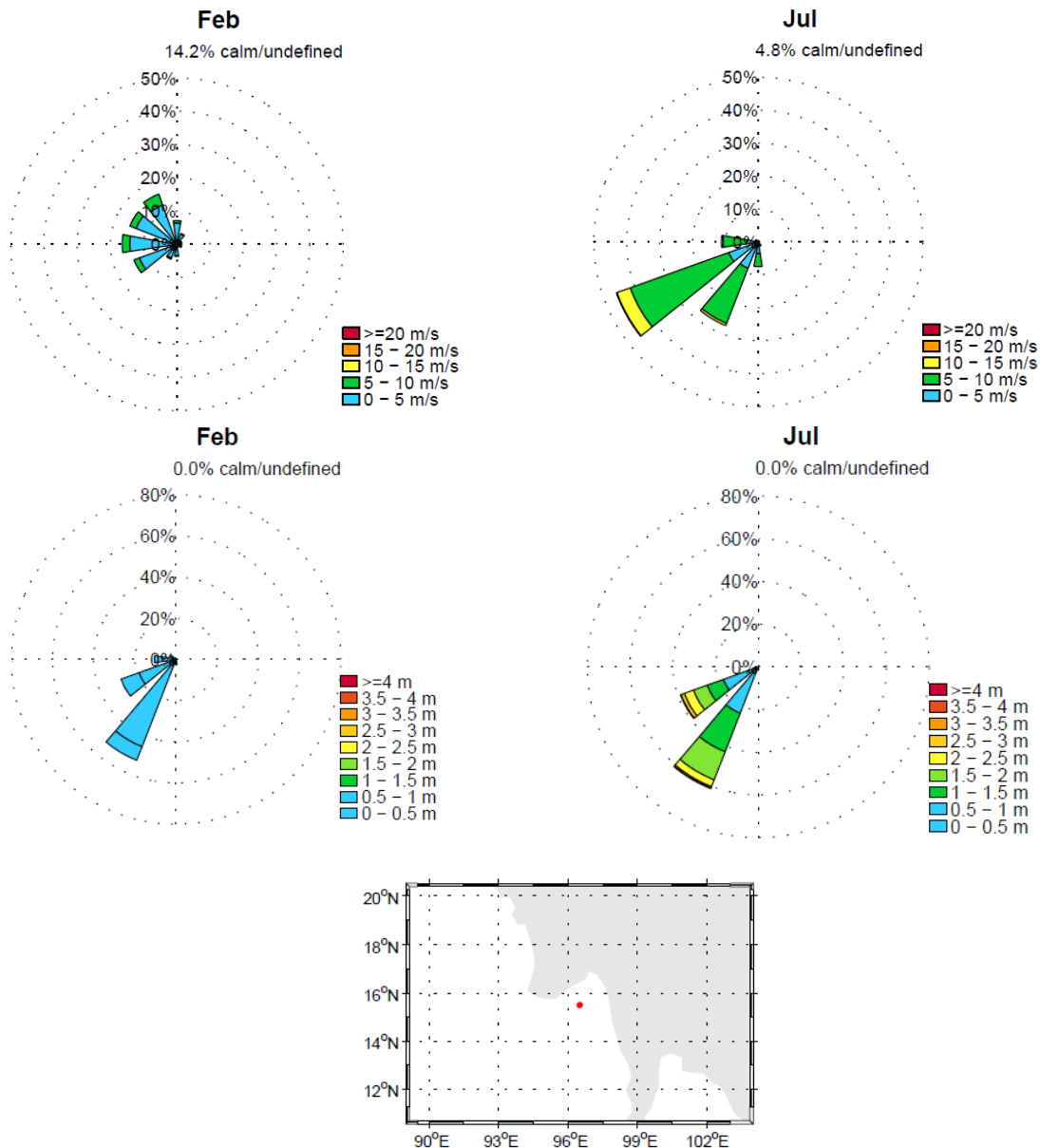
Figure 2.5: Wind and wave roses for February (dry season) and July (monsoon season)
(WorldWaves offshore database, 2015)

Waves could play an important role in the upstream transport if fine sediments by resuspending settled sediments near the estuary mouth, enabling the sediment to be transported upstream by the tide (Bosboom, 2016). But since this study focusses on the sediment dynamics at the confluence/bifurcation where the effect of waves is expected to be negligible, waves are not considered any further.

2.2 Sediment conditions

In this section the distribution of different sediment types along the estuary is shown. Next, the sediment concentrations in the Irrawaddy River, in the Yangon Estuary and in the Gulf of Martaban are considered.

2.2.1 Sediment distribution in the estuary

In Yangon Estuary a mix of sediments can be found. Based on the research by JICA (2016), the following map has been made, showing the distribution of sediment in the estuary.
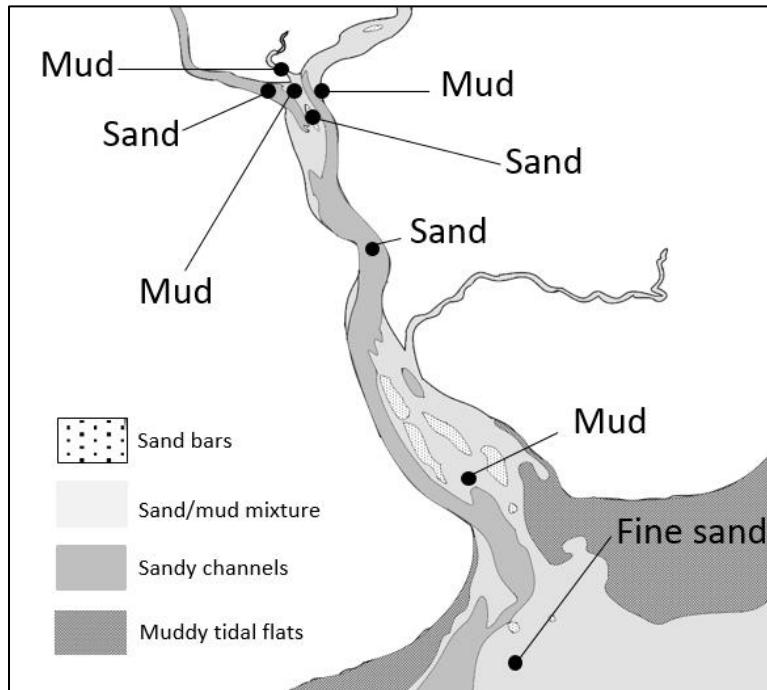
Figure 2.6: Sediment distribution in Yangon Estuary. Bullets represent sediment samples by JICA (2016).

Furthermore, the dredged material of a dredging project in 2016 by Boskalis has been analysed. In the middle of Monkey Point Channel mainly very soft clayey fine sand was found. On the slopes of the channel medium sand with gravel is found (Boskalis, 2016).

Figure 2.7: Dredged sediment by Boskalis (2016). Left: Very soft clayey fine sand from the middle of the channel. Right: medium sand with gravel from the south slope (Inner Bar)

2.2.2 Sediment concentrations

In order to get a better understanding of the sediment dynamics in the estuary it is important to know what the input and output of sediment is. Therefore, the sediment concentrations on the boundaries of the estuary system are analysed. The sediment concentration in the Irrawaddy River is represented by Figure 2.8. From the figure, the correlation between the discharge and the sediment concentration is clearly noticeable. The average monsoon sediment concentration in the Irrawaddy is 1 g/l. During the dry season the average sediment concentration is 0.1 g/l.
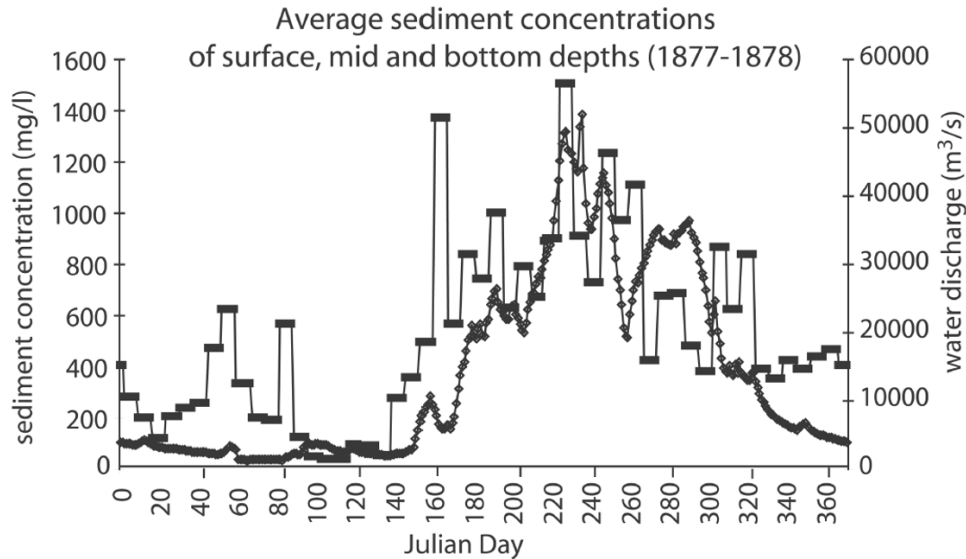
Figure 2.8: Sediment concentration in the Irrawaddy River at Seiktha (Robinson, 2007)

Sediment concentrations in Yangon Estuary are measured by Gibb & Partners (1976) and Nelson (2000). Both measurement data show high peaks in sediment concentration during spring tide in dry season. During the monsoon season the sediment concentrations are about five times lower than during the spring tide in dry season. However, the spring/neap variation is also noticeable in the monsoon season. For neap tide conditions in dry season the measurements give very different values. Gibb & Partners (1976) measured sediment concentrations exceed 2 g/l, while the sediment concentrations measured by Nelson (2000) do not exceed 0.5 g/l. This error can be explained by the fact that the range of the neap tide defined by Gibb & Partners (1976) is 3.9 m while the neap tidal range in Table 2-3 and by Nelson is 2.4 m. Therefore, the concentrations of Nelson (2000) are considered normative.

11

Yangon River

Bago River

Estuary, Thilawa
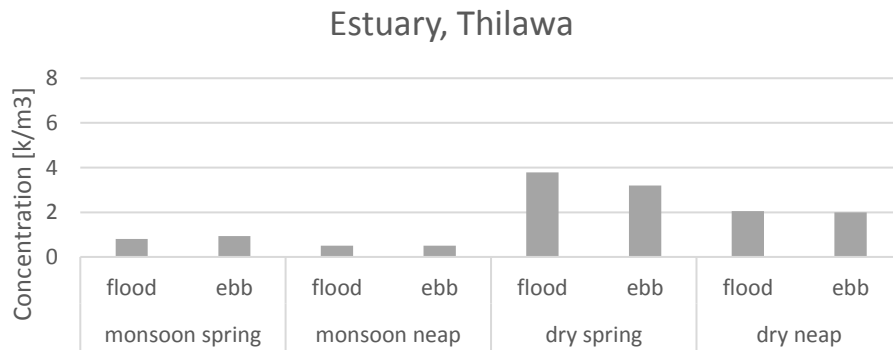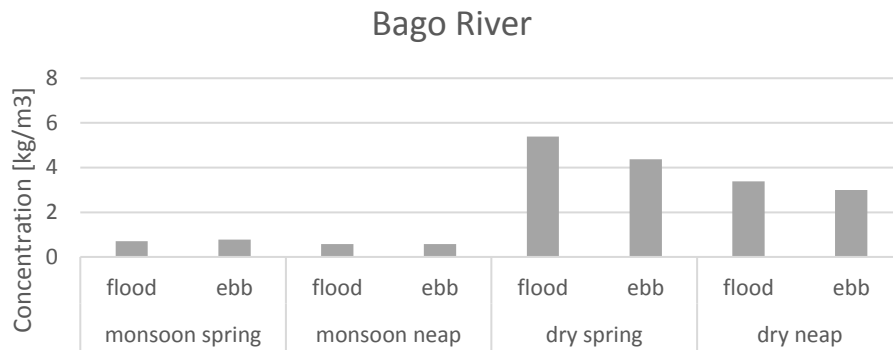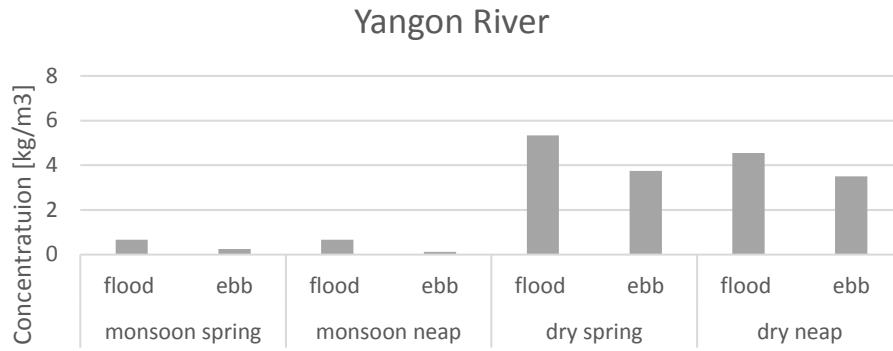
Figure 2.9: Sediment concentrations in the Yangon Estuary (Gibb & Partners, 1976)
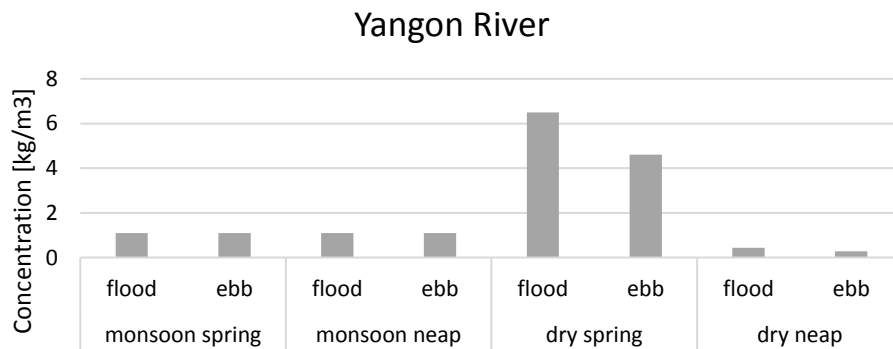
Yangon River

Figure 2.10: Depth averaged suspended sediment concentrations in the Yangon River (Nelson, 2000)

In order to determine where the sediment is going to, research to the sediment concentrations in the Gulf of Martaban is done. Unfortunately, no concentration values in the Gulf of Martaban are known. Instead, satellite pictures of the Gulf of Martaban have been analysed. These pictures show the relative amount of turbulence. From these pictures it can be concluded that the suspended sediment concentration in the sea is fluctuating on a weekly basis. Both in the dry season and the monsoon season the pictures show conditions where the water seems clear and very turbid (see Figure 2.12 and Figure 2.13). Hence, the turbidity of the Gulf of Martaban is not seasonally depended. Because of the weekly fluctuations in turbidity, the turbidity seems more likely to vary with the fortnightly rhythm of the spring/neap cycle. But because there is no measured data on water levels, the satellite pictures cannot be related to a tidal condition. From the pictures it can be concluded that the Gulf of Martaban contains a lot of suspended sediment. Furthermore, it can be noticed that the turbidity is limited to the 20 m depth contour as presented in Figure 2.11.

Figure 2.11: Gulf of Martaban with depth contours. The red dashed line shows the location of Yangon Estuary. Source: (Navionics, 2018)
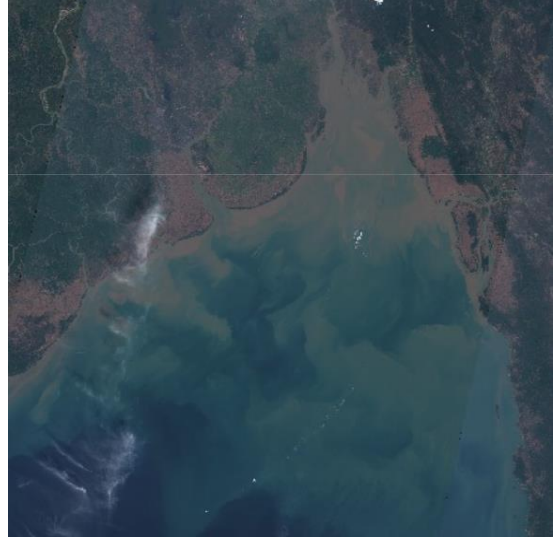
Figure 2.12: Gulf of Martaban at 24-01-2019 (left) and 31-01-2019 (right). Source: (Sentinel, 2019)
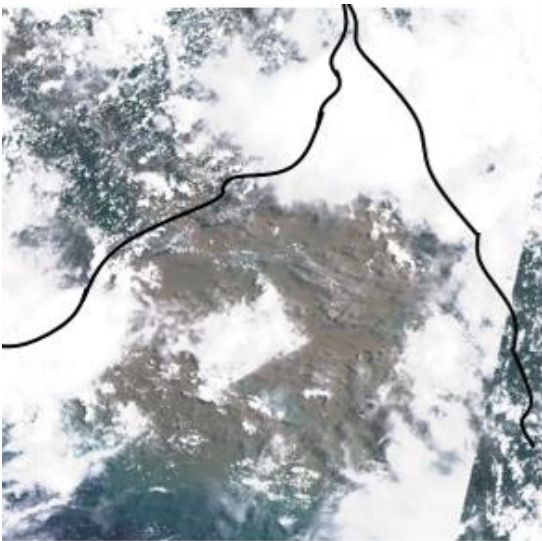
Figure 2.13: Gulf of Martaban at 20-09-2018 (left) and 26-09-2018 (right). Source: (Sentinel, 2019)

2.3 Morphologic conditions

The morphologic conditions are defined by doing an analysis to nautical charts. The old nautical charts from 1798, 1872, 1893, 1930, 2007 and 2017 show how the bathymetry of the estuary has developed in more than 200 years. The charts are analysed in chronological order.

Figure 2.14 shows that the Bago River is in line with the estuary banks while the Yangon River is perpendicular to the estuary. This suggest that the Bago is part of the main estuary system. The Yangon seems an individual river flowing out in the estuary. Furthermore, the bars in the middle of the estuary, just downstream of the confluence are a striking object in the estuary.

Figure 2.14: Yangon Estuary 1798

Figure 2.15 shows that, in comparison with the bathymetry of 1872, the orientation of the Yangon River changed and the angle of the bifurcation has changed to a more equal ratio between the approach angle between the Yangon River and the Bago River. The bars along the estuary axis downstream of the confluence are still present.

Figure 2.15: Yangon Estuary 1872

In Figure 2.16 it can be noticed that the river training wall was not present in the bend of the Yangon River upstream of the confluence and the bend is much larger. Furthermore, it can be seen that the Bago River channel and the estuary channel are connected while the Yangon River channel is separated by a shoal. In addition, the Hoasting's shoal is present in the middle of the confluence.

In order to erode the Hoasting's shoal, the King's Bank Wall was constructed (see Figure 2.17). Furthermore, another wall is constructed in the bend of the Yangon River. Also it can be noticed that the Twante Canal is constructed in these years.

The construction of the King's Bank Wall did however not result in the erosion of the shoal as the shoal is still present in the nautical chart of 2007 (see Figure 2.18). Compared to the bathymetry of 1893, the Yangon River has become deeper around the river mouth. The river channel is expanded downstream of the confluence. It is striking that the channels from the Yangon River and the Bago River are parallel. This suggest that the flow from the Yangon River and Bago River are somehow in balance. This is also a potential explanation why the shoal did not erode, because the flows seems to push each other in a certain direction with parallel channels as a result. Furthermore, the presence of Monkey Point Channel is presented in Figure 2.18. It can be seen that the channel is dredged just north of the Hoasting's shoal.

Figure 2.16: Yangon Estuary 1893.

Figure 2.17: Yangon Estuary 1930 at the estuary split. Construction of the Kings Bank Wall. The goal of the wall was to erode the Hastings Shoal.
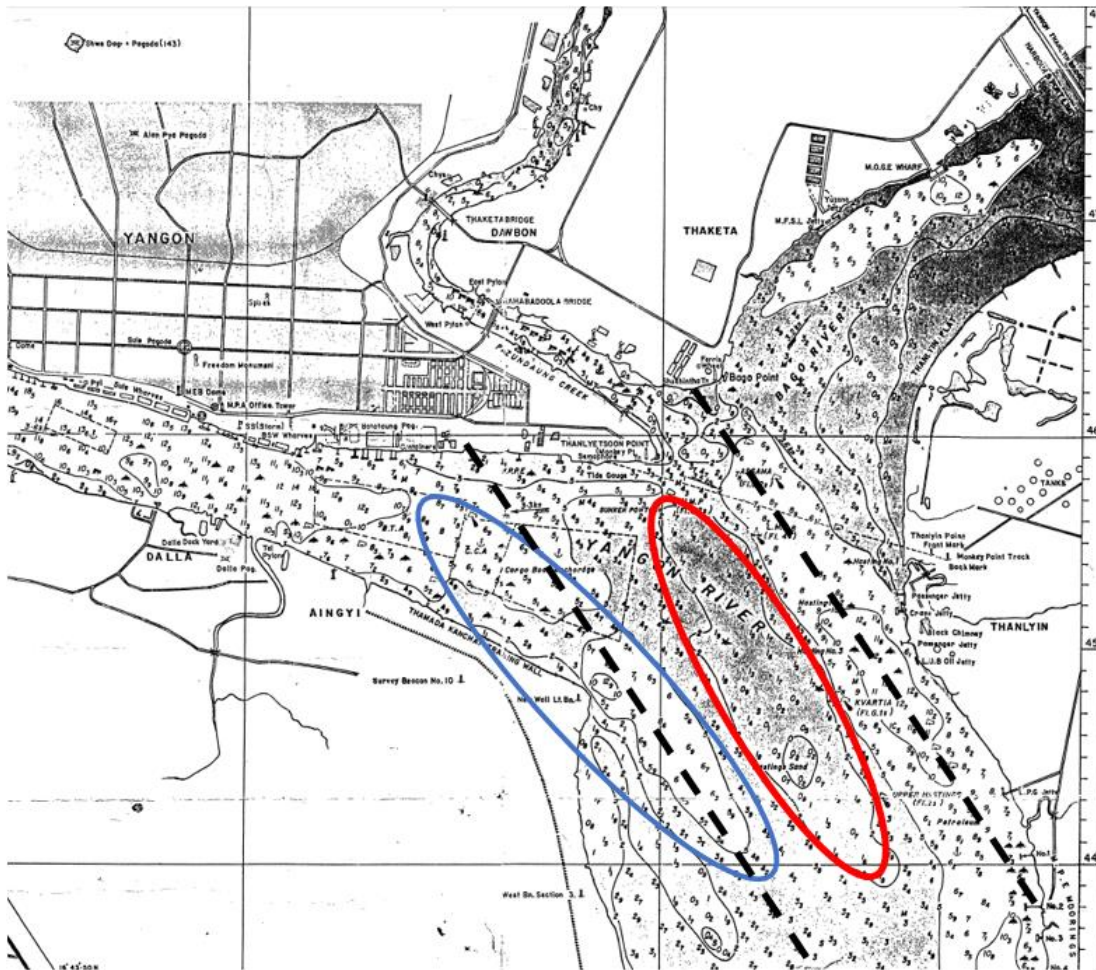
Figure 2.18: Nautical chart 2007; zoom Inner Bar. The blue oval represents the channel evolution. The red oval highlights the Hoasting's shoal. The black dashed lines indicate the parallel channels of the Bago River and Yangon River

Comparing the charts of 2007 and 2017 it can bed noticed that the Yangon River channel further developed. The channel has become deeper with a more uniform bed. In Figure 2.19 the main channel of the estuary is clearly visible in white. The channel has an averaged depth of 14 m below MSL and forms a connection between the offshore and the Bago River. Furthermore, the Yangon River is separated from the estuary channel by the Inner Bar. Since this shoal is located to the western bank and the Yangon is expected to bring in the most sediment because of the dominant monsoon discharge, the shoal is expected to be formed by deposition of sediment coming from the Yangon River.

The three most important findings from the analysis to the nautical charts are:

- The Bago River seems part of the estuary system where the Yangon River is more an individual river.
- Dynamics of the confluence seems dominant over the individual river flow since the Kings Bank Wall did not result in erosion of the Hoastings Shoal.
- The Inner Bar is present in the estuary for more than 200 years. The fact that it is still at the same position shows that the bar is stable
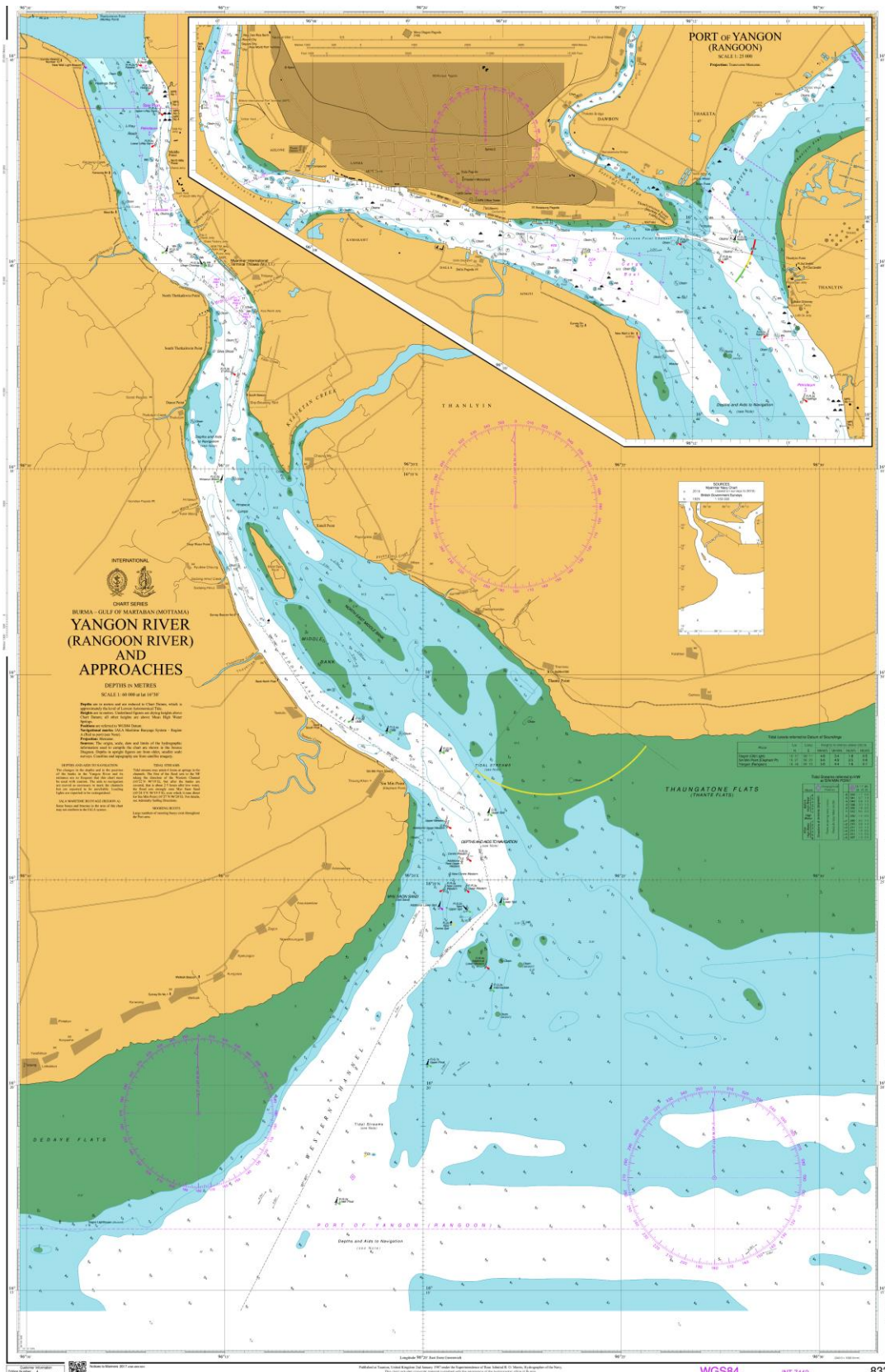
Figure 2.19: Yangon Estuary 2017

2.4 Conceptual model stage 1

The conceptual model of the first stage consists of the boundary conditions defined in this chapter. The size of the framework is limited by the connection with the Irrawaddy and the estuary mouth.
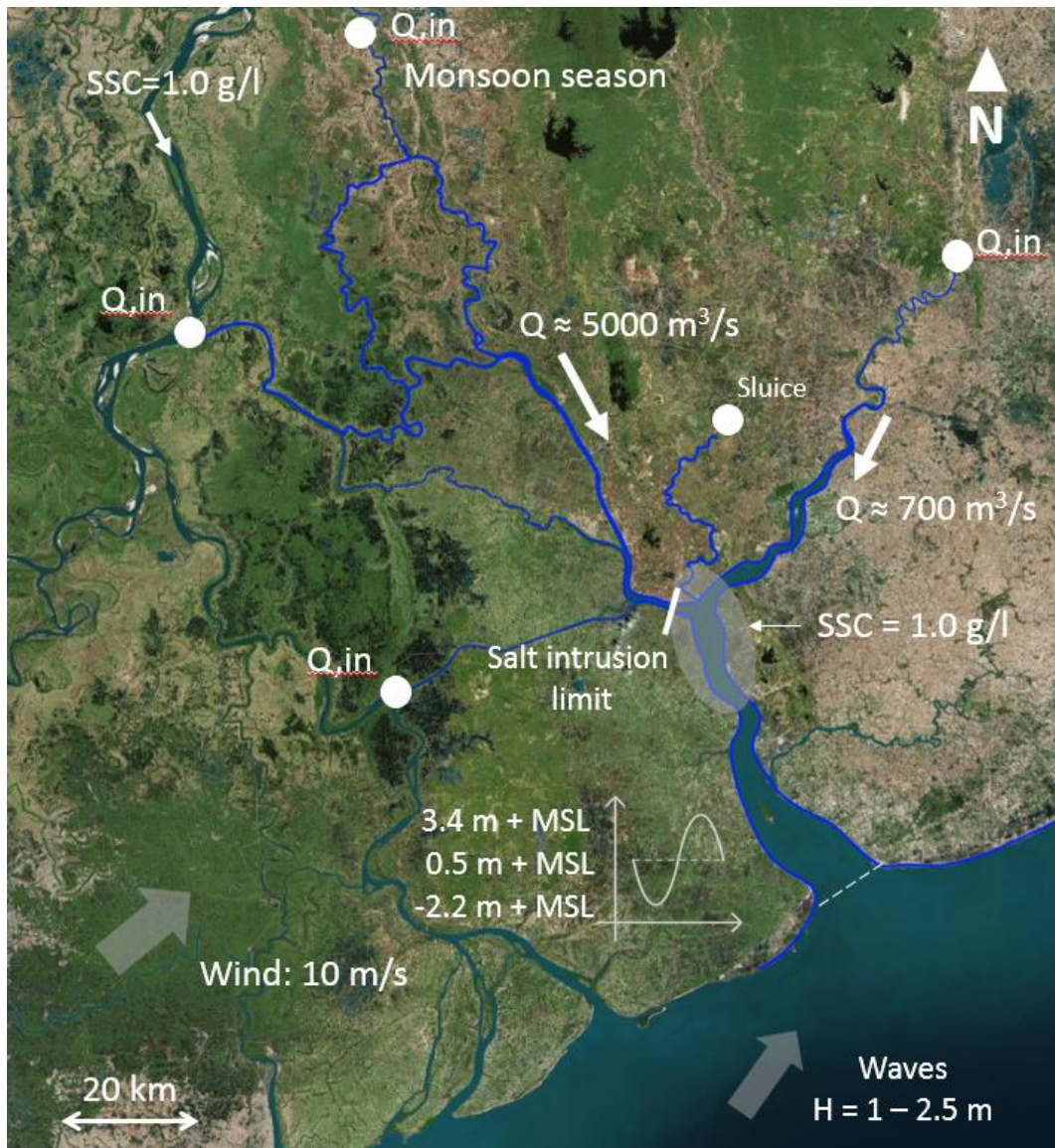
Figure 2.20: Stage 1 conceptual model, monsoon season. Q,in is the symbol for the locations where water enters the system. Q is the average discharge. SSC Is the measured suspended sediment concentration within the oval. H is the wave height.

Figure 2.21: Stage 1 conceptual model, dry season. Q,in is the symbol for the locations where water enters the system. Q is the average discharge. SSC Is the measured suspended sediment concentration within the oval. H is the wave height.

Based on the SSC in the Irrawaddy and in the estuary, it is expected that during the monsoon season lots of fine sediment are transported from the rivers in seaward direction causing for the high turbidity in the Gulf of Martaban. In dry season the SSC in the Irrawaddy is too low in order to explain the SSC values in the estuary. It is therefore expected that the high SSC values in the estuary during dry season are caused by the tide. Furthermore, because the water level in the monsoon season is 0.5 m higher, the shear stress on the shoals can be lower and less erosion will occur and therefore less sediment will be brought in suspension.

Because the dominant wind directions are SW and NE, the wind is perpendicular to the estuary axis. Therefore the potential fetch is expected to be small and hence the effect of wind on the estuary hydrodynamics is also expected to be small. It has been decided not to consider the effect of wind any further.

3 Estuary classification

Classification of an estuary can be very helpful in composing a conceptual model because estuary classification gives a first indication on which hydrodynamic and morphodynamic processes are important within the estuary. One way to distinguish different types of coasts is by looking at the hydraulic boundary forcing to the system (Bosboom, 2016). This is called process-based classification. Dominance by fluvial, wave or tidal processes can be seen from the morphological characteristics of a delta. Boyd et al (1992) defined typical lay-outs of river-dominated, wave-dominated and tide-dominated coasts. These lay-outs are shown in Figure 3.1.
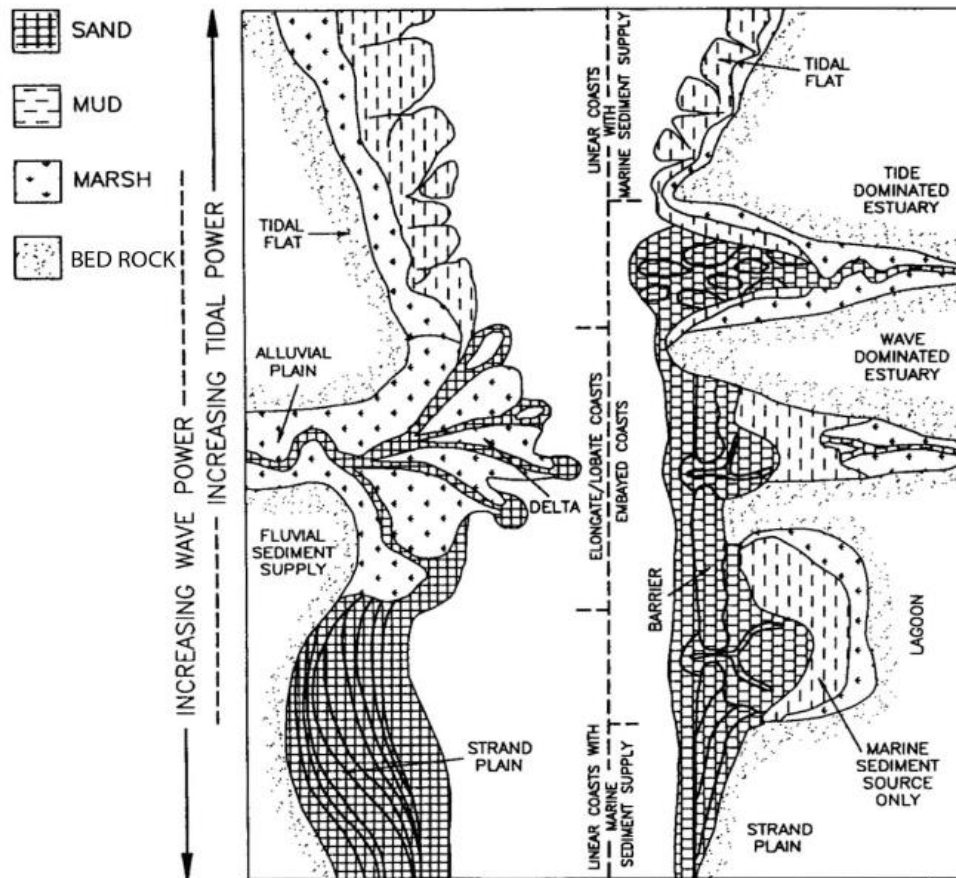
Figure 3.1: Coastal forms for prograding and transgressive coasts (Boyd et al, 1992).

The left side from Figure 3.1 shows a prograding coast, which is typical for a river-dominated coast where an excessive sediment supply is causing the progradation of the coast and the formation of a delta. Delta formation does not occur at the Yangon Estuary so the estuary is not considered as a river-dominated system. The right side of the figure shows a transgressive coast as a result from a rise in sea level or because of insufficient sediment supply with flooding of the river valley as a result. The waves at the delta of Yangon Estuary are low, so wave-dominance is not expected. Yangon Estuary shows a lot of similarities with the tide-dominated estuary from Figure 3.1. Hence, the focus is on the aspects of a tide-dominated estuary.

"In simplest descriptive terms, tide-dominated estuaries are those in which tidal currents play the dominant role in determining the fate of the river-borne sediments" (Wells, 1995). Tide-dominated estuaries are usually funnel-shaped as a result from the complex balance between tide-driven processes, river flow and the amount of sediment in the system. The funnel-shape (indicated by 4) and other characteristic morphologic features of a tide dominated-estuary are shown in Figure 3.2.
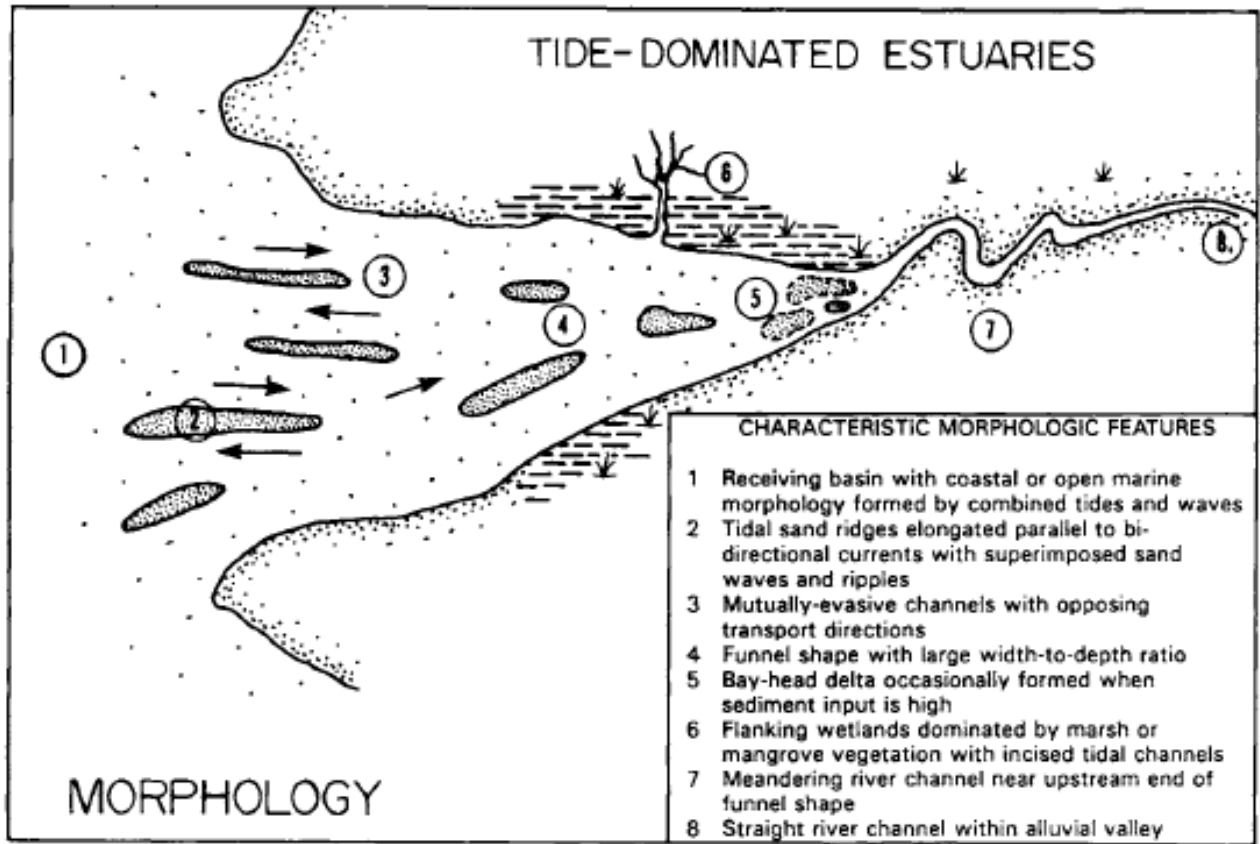
Figure 3.2: Characteristic morphologic features of a tide-dominated estuary (Wells, 1995)

Yangon Estuary shows a lot of similarities with the typical morphology of a tide-dominated estuary, defined by Wells. The most characteristic features (the tidal sand ridges, bay head delta and flanking wetlands) are clearly visible in the Yangon Estuary (Figure 3.3). As Wells (1995) mentions, bay head deltas are occasionally formed when the river related sediment input is high. Because the sediment input during the monsoon is also high, the bay head delta is expected to be formed by sediment depositions originating from the rivers.

23
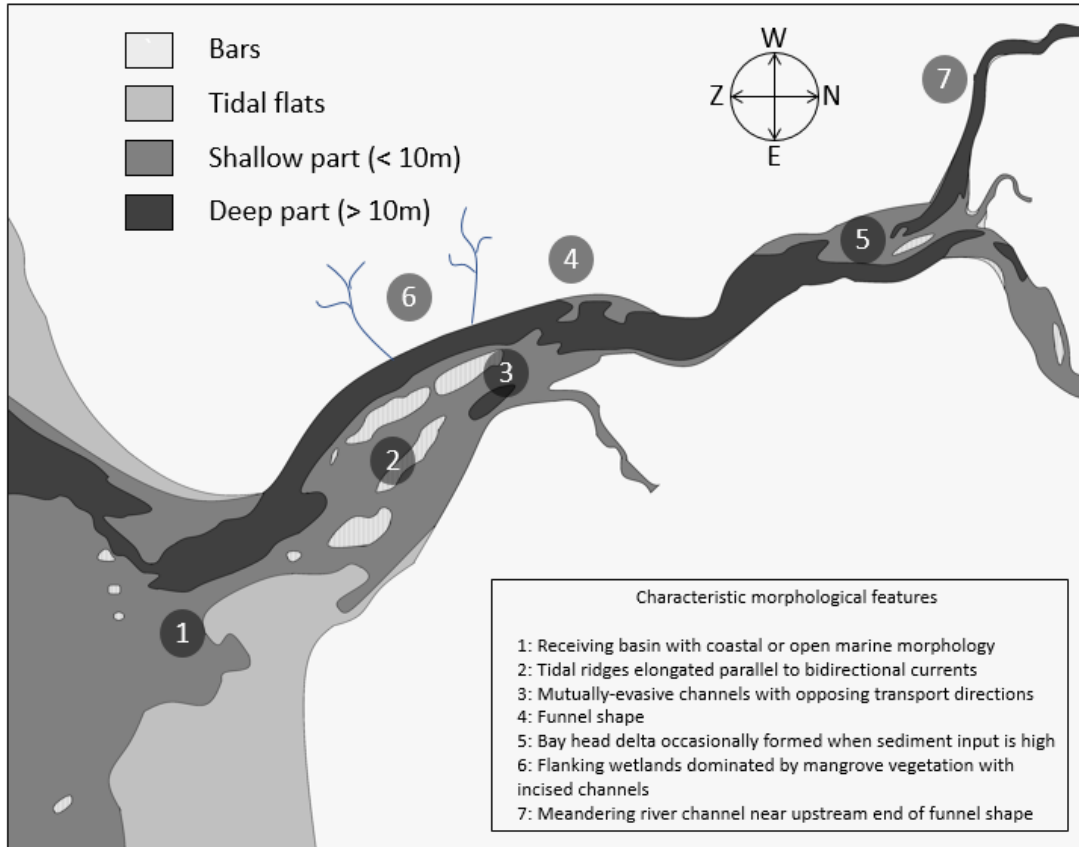
Figure 3.3: Characteristic morphologic features of the Yangon Estuary

Based on the process-based classification and the combination of these morphologic similarities, Yangon Estuary is assumed to be a tide-dominated estuary. Tide-dominated estuaries are expected to be flood dominant, resulting in import of sediments from the delta. To get a better understanding of flood-dominance, tidal asymmetry in estuaries is further considered in Section 4.1.1. Because the formation of an estuarine bay head delta is important in relation with the sedimentation at the confluence, the confluence and bifurcation dynamics are analysed in Section 4.2**Error! Reference source not found.**. A tide-dominated estuary has typical a tidal prism which is 10 times larger than the river discharge. To support the assumption that Yangon Estuary is a tide-dominated estuary, the ratio between the tidal prism and the river discharge is investigated with the hydrodynamic model in Chapter 5**Error! Reference source not found.**. Tide-dominated estuaries are commonly well-mixed (Wells, 1995).

4 Estuarine, riverine and sediment processes

In this section processes are analysed that, based on the first stage conceptual model, may be important in relation with the sedimentation of Monkey Point Channel. First, typical estuarine processes are considered. Next, the riverine processes are analysed and subsequently the sediment processes are investigated. In the last section of this chapter consists of case studies to reference estuaries.

4.1 Estuarine processes

In this section the processes tidal asymmetry and Estuary Turbidity Maximum (ETM) are analysed. Also the processes lag effects and estuarine circulation have been analysed but their contribution to the sediment dynamics in the Yangon Estuary was not determined. Therefore, the process analysis of lag effects and estuarine circulation is shifted to Appendix 13.3C.

4.1.1 Tidal asymmetry

As mentioned in Chapter 3, the tide is expected to play a dominant role in the sediment dynamics of the estuary. In this section, attention is payed to the potential residual sediment transport caused by tidal asymmetry. When a tidal wave propagates in deep water, the wave has a progressive character; velocity and water level are in phase. In the absence of friction, the tidal wave propagation can be written as :

$$c = \sqrt{g(h \pm \eta)}$$

When the tidal wave enters the Gulf of Martaban, the wave will be slowed down due to friction which results in shoaling of the tidal wave. The shoaling is presented in Figure 2.1; the tidal range increases along the coast of the Irrawaddy delta from west to east. As the amplitude increases, the wave celerity of the tidal wave crest will increase as well, causing the high tide to propagate faster. As a result the rising period of the tide will be shorter than the falling tide. This phenomenon is often referred to as tidal asymmetry. The shorter rising period causes for higher flood flow velocities. When the peak velocities between flood and ebb differ, one speak of peak flow asymmetry. Since the sediment transport is related to sediment transport to the power 4, peak flow velocities can cause for a net sediment transport in the direction of the higher peak flow velocities. In addition, higher peak flow velocities can cause for more erosion causing for higher sediment concentrations that can be transported. When the net sediment transport is in the flood direction, the tide is flood-dominant. When the net sediment is in the ebb-direction the tide is ebb dominant. Based on the shoaling of the tide, the tide at the inlet of Yangon Estuary is expected to be flood dominant.

In the estuary the tidal wave will deform due to a combination of friction and shoaling due to the convergence of the funnel-shaped estuary. Because the estuary cross-section gets progressively smaller in upstream direction , the tidal energy is converged causing for an increase of tidal amplitude. The balance between energy loss due to friction an energy convergence due to width restriction determines whether the tidal amplitudes increase or decrease along the estuary channel. Flood dominance in estuaries in enhanced by a large tidal amplitude, shallow channels and the absence of large intertidal areas (Bosboom & Stive, 2015). Because the tidal amplitude in Yangon Estuary is large and large intertidal areas are not present in the estuary, the tide is expected to be flood-dominant. Consequently higher flood velocities and import of sediment can be expected during the dry season. During the monsoon season the river discharge will cause for a residual transport in seaward direction. In combination with the fact that Yangon Estuary is not

filling, Yangon Estuary is expected to be ebb-dominant during the monsoon season. Besides asymmetry around the horizontal axis (peak flow asymmetry), the horizontal tide can also be asymmetric around the vertical; acceleration asymmetry. Acceleration asymmetry refers to the change in flow velocity during the falling and rising period. Acceleration asymmetry is important when considering fine sediments. Due to the small settling velocity, fine sediment needs more time too settle. Basically, this occurs during slack water when the flow velocities are low. When the slack duration around high water (HW) is longer than during low water (LW), one speaks of acceleration asymmetry. The asymmetry can be caused by the fact that around HW slack the surface area is larger than during LW. Assuming the same amount of discharge goes in and out, the velocity change during HW is smaller than during LW. Hence, sediment has more time to settle which causes for a net sediment transport in the food direction. The peak flow asymmetry and the acceleration asymmetry are further investigated in Chapter 5.

4.1.2 Estuarine Turbidity Maximum

An important feature of estuaries is the Estuarine Turbidity Maxmimum (ETM). An ETM is an area of very high suspended sediment concentrations which is caused by the balance between the flushing river flow, estuarine circulation and tidal asymmetry (Winterwerp & Van Prooijen, 2016). Around the limit of salinity intrusion, sediments are trapped between the saline and freshwater front. As the salinity front is moving up- and downstream with the tide, the ETM is spread over a certain range. At the salinity intrusion limit the upstream sediment transport from the seaside and the downstream sediment transport from the riverside causes for the convergence of sediment. In addition to the trapping of sediment, also flocculation occurs. Flocculation leads to increasing settling velocities, thereby strengthening the ETM. As a result large amount of fine sediments deposit in the ETM zone causing for the formation of mud layers. During high river discharge events the balance between the saline flow and the fresh water flow may be disturbed leading to flushing of the estuary. Erosion of the formed mud layer depends on the strength of the layer related to the consolidation time and on the shear stress induced by the river flow. Tide induced resuspension and transport is the cause most commonly considered for turbidity maxima in well-mixed estuaries (Postma, 1967; Allen et al., 1980; Dronkers, 1986), while density driven circulation is important in partially mixed estuaries (Schubel, 1960). This is indicated by Figure 4.1.
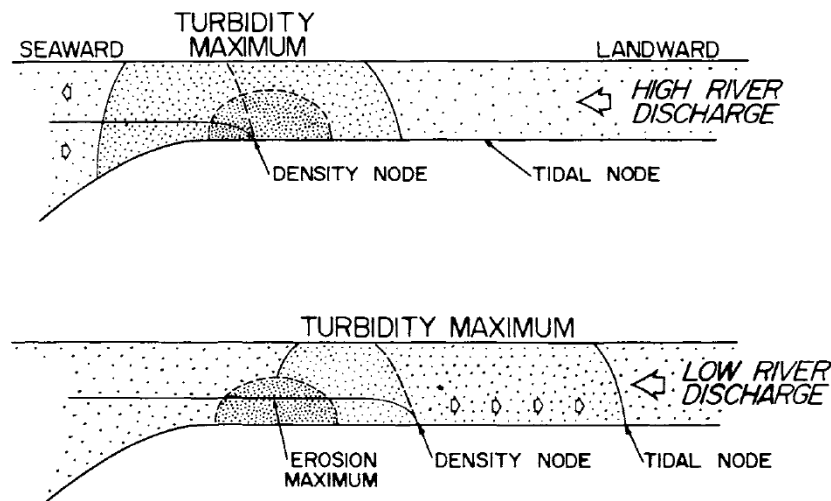
Figure 4.1: Conceptual diagram showing the seasonal displacement of an estuary turbidity maximum. Density processes dominate the trapping of fine sediment during high river discharge, tidal processes dominate during low river discharge. The density node represents the salt intrusion limit and the tidal node represents the tidal intrusion limit. Source: (Wells, 1995)

In order to get a better understanding of the formation of an ETM, research to ETM's in other estuaries has been done. Because Yangon Estuary is a tide-dominated estuary, ETM formation in the following tide dominated estuaries has been analysed; Ems Estuary, Gironde Estuary and the Severn Estuary.

In the Ems Estuary, the extreme high sediment concentrations, which exceed 6 g/l, are related to the increased import of fine sediment and the landward shift of the ETM due to tidal amplification (Maren, 2015). The sediment is trapped around the tidal node. A same kind of process cannot be related to the high sediment concentrations in the Yangon Estuary during dry season because the tidal node is 80 km more upstream than the location of the measured sediment concentrations (see Figure 2.4).

In the Gironde Estuary, basically two dominant forms of an ETM occur. During high river discharge the ETM is caused by the trapping of sediment around the salinity intrusion limit. During the period of low river discharge the ETM shifts upward the estuary beyond the salinity limit towards the tidal current limit (see Figure 4.2).
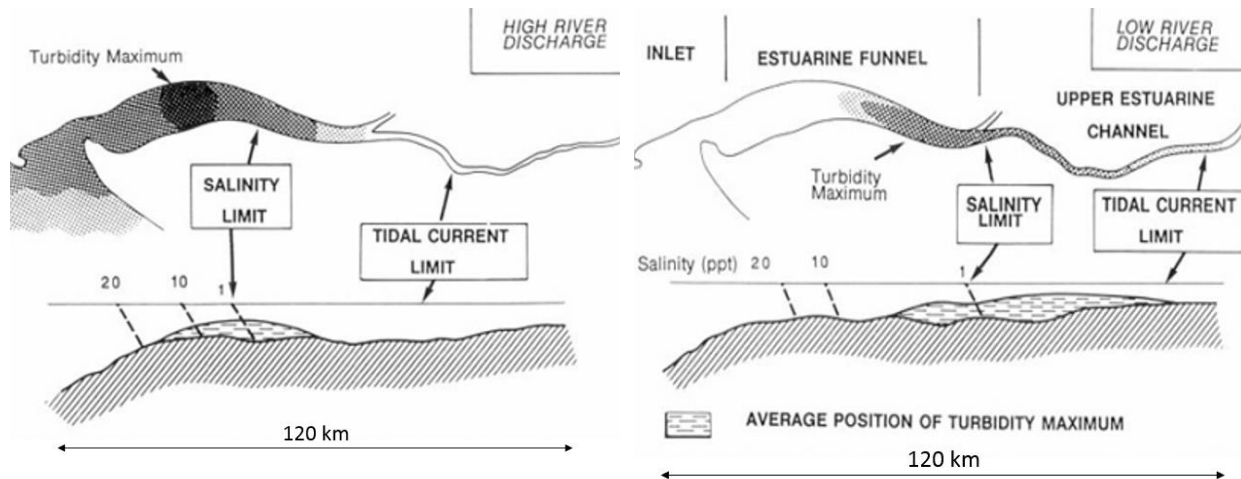
Figure 4.2: Location of the ETM in the Gironde Estuary for high and low river discharge. Source: (Allen G. , 1991)

The mud distribution is clearly related to the ETM location. The mud that is deposited in the area presented by Figure 4.3, is able to stay at the shallow area (0-5 m), but is eroded from the estuary channel (5-10 m) (Allen G. , 1977). A same kind of distribution is expected in the Yangon Estuary based on the sediment samples that have been taken (see Figure 2.6). The location of the ETM during the period of low river discharge (dry season), is expected to differ from the situation in the Gironde Estuary. Because there is no information on SSC along the longitudinal estuary axis, the location of an ETM in Yangon Estuary is unknown. Therefore, the potential ETM location is related to the limit of salt and tidal intrusion (see Figure 4.4). Since the salt intrusion limit in the dry season is about 40 km away from the measured SSC of 5 g/l, it is unlikely that the high sediment concentrations are caused by this ETM. Therefore, it can be concluded that there must be another type of ETM which is causing for the high SSC around the confluence of Yangon Estuary.
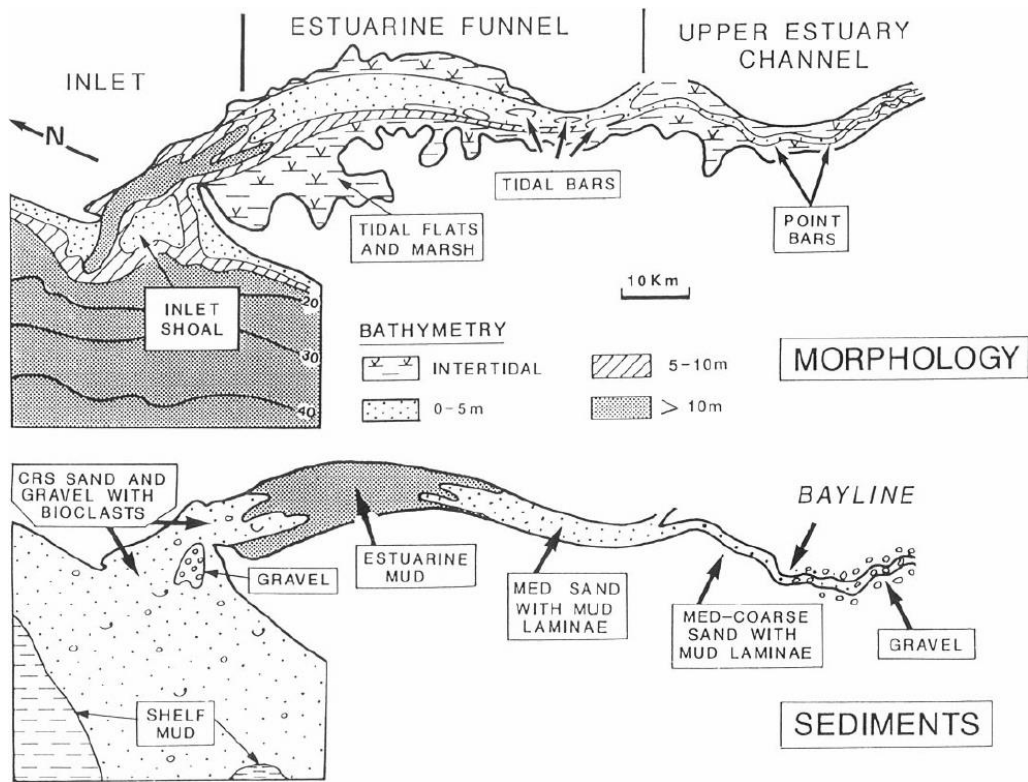
Figure 4.3: Morphologic and sediment conditions of the Gironde Estuary. Source: (Allen G. , 1991).
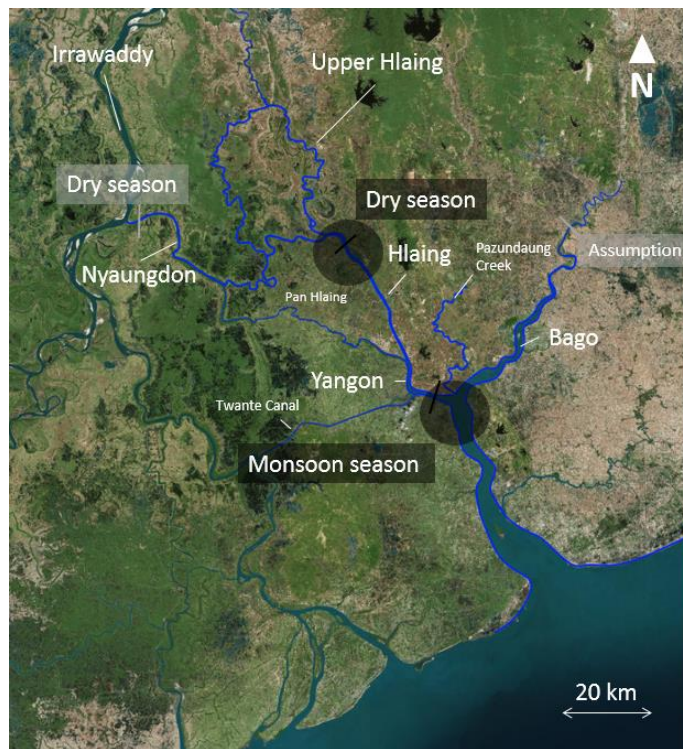
Figure 4.4: Potential locations of ETM based on the salt intrusion.
The black circles indicate the potential ETM location per season.

The ETM in the Severn Estuary shows comparable conditions as the Yangon Estuary (Nelson, 2000). The ETM formation in the lower Severn Estuary is located 40 km downstream of the salt intrusion limit and is the second ETM in the estuary (with an ETM un the upper estuary beyond the salt intrusion limit) (Manning, 2010). The ETM in the lower estuary is caused by the erosion of stationary mud layers during spring tide events (Kirby & Parker, 1983). During spring tides there is increased mixing and settling of suspended sediment, with all but a background concentration (of the order <0.5 g/l) reaching the estuary bed (Kirby & Parker, 1983). As the tidal range gradually diminishes towards neap conditions, the static suspensions formed at slack water survive progressively longer into each successive tide, until they eventually resist erosion and remain throughout the complete tidal cycle. The suspension then has several tidal cycles in which to consolidate gradually. If, on the succeeding neap-to-spring cycle, re-erosion of this layer is not complete, a small increment of deposited sediment may remain to become part of the estuary bed on a longer timescale (Dyer, 1994). Consequently, the SSC shows a fortnightly rhythm, forced by the spring/neap tidal cycle (see).The process of erosion during spring tides and deposition during neap tides is also expected in the Yangon Estuary because:

- Import of sediment cannot result in such locally high SSC because the salt intrusion limit is too far away in order to provide for a trapping function which concentrates the suspended sediment to SSC values of 5 g/l
- The local erosion of stationary and settled mud layers provides an explanation for the local high SSC.
- The estuary shows the same spring/neap rhythm of SSC as in the Severn Estuary.

Figure 4.5 and Figure 4.6 show the concept of the SSC variations during dry season. Just like in the Gironde Estuary, the mud is expected to be eroded from the estuary channel and deposited on the shoals next to the channel. Because the middle part of Yangon Estuary consists only of the estuary channel without shoals, no mud is expected in this region.
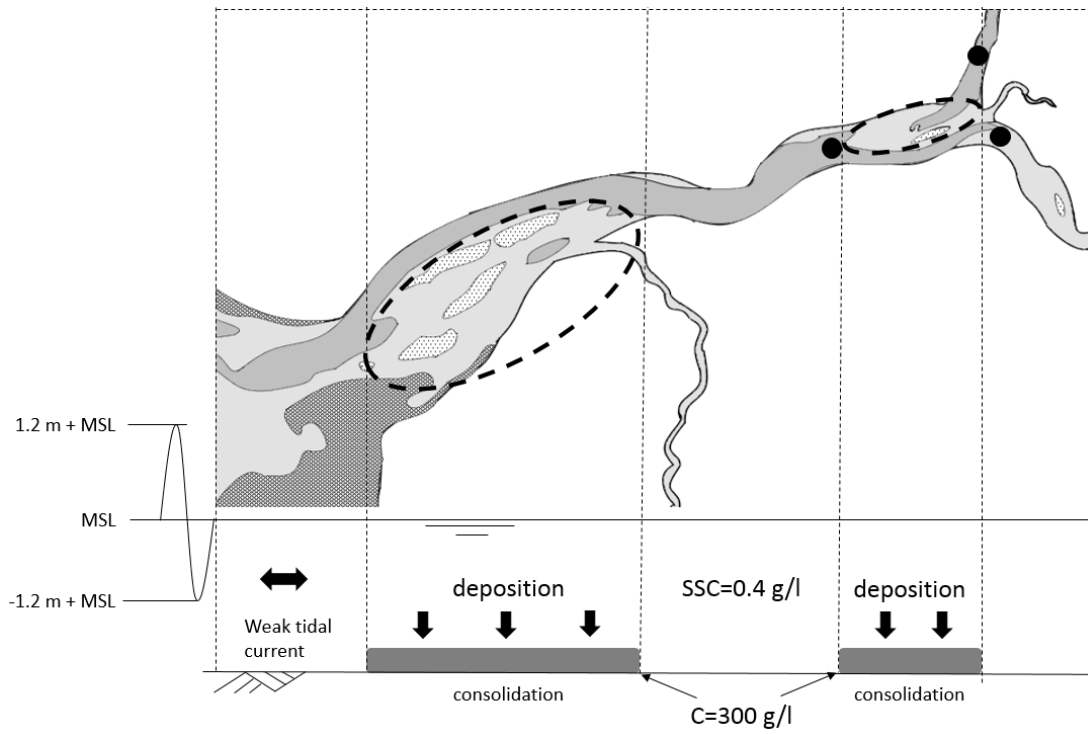
Figure 4.5: Conceptual diagram of deposition and consolidation of fine sediments on the shoals during neap tide. The black dots represent the locations where the SSC is measured.
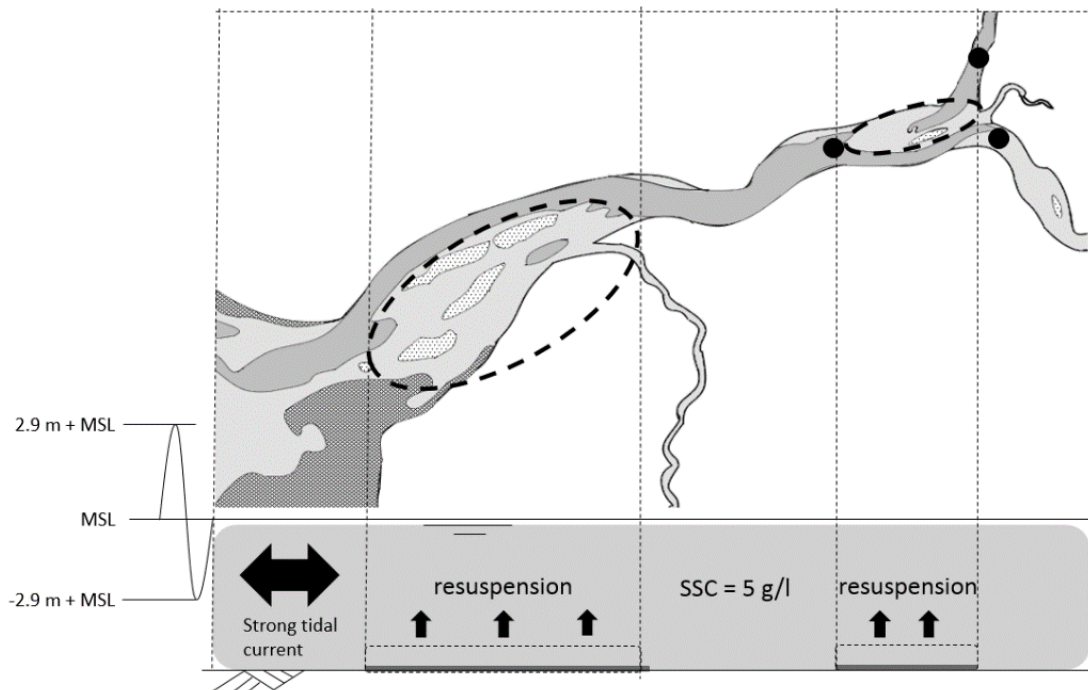
Figure 4.6: Conceptual diagram of resuspension of stationary and settled mud during spring tide. The black dots represent the locations where the SSC is measured.

4.2 Riverine processes

In this section the flow at the estuary head is dealt with. Because the tidal range at the split between the Yangon River, the Pazundaung Creek and the Bago River can be 5 m, strong currents flow in both landward and seaward direction. When the water in the estuary is flowing in seaward direction the split is considered as a confluence and when the water is flowing in landward direction the split is considered as a bifurcation. Hence, research to the flow at a confluence and bifurcation are part of this thesis.

4.2.1 Confluences

To get e better understanding of the dynamics at a confluence, a study is done to confluences in general. A good description of a confluence is given by Best (1997). Best describes six characteristic confluence zones (see Figure 4.7).
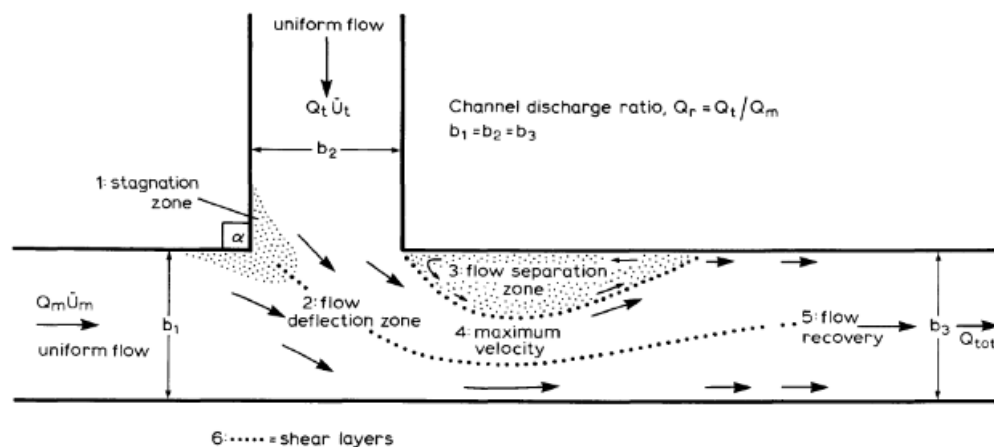
Figure 4.7: Confluence zones (Best, 1987)

There are two zones in which sedimentation is likely to occur; the stagnation zone and the flow separation zone. In the stagnation zone, the flow from the different branches conflict, causing for a reduction of the flow velocity. Because of the lower flow velocities at the stagnation zone, sediment is deposited. Due to the sharp corner at the flow separation zone, the flow is not able to follow the bank and the flow gets separated from the river bank. In this zone a low pressure area is created which results in an eddy. This eddy causes for sediment deposition in the flow separation zone due to the "tea cup effect" (Mosselman, 2016).

A second process that needs to be taken into account is mid channel bar growth (Ashworth, 1996). When two branches meet at a confluence, the flow from the branches do not immediately combine to one flow. This gradually process is visualised by means of Figure 4.8. There are two situations in which mid-channel bar growth occurs. First, when the combination of the cross-section of the two branches is larger than the downstream branch, scour will occur at the confluence. Because of the low flow velocities in the middle of the channel, the transport capacity is low and sediment is deposited. When the flow recovers the deposition of sediment decreases. As a result a mid-channel bar is formed (see Figure 2.16). The second situation is when the cross-section of the channel downstream of the confluence is larger than the combination of the upstream branches, sediment originated from upstream can be deposited downstream of the confluence, causing for mid-channel bar formation.

As a result the flow is small in the middle of the channel just after the junction. Due to low flow velocities, the sediment transport capacity of the flow is low in the middle of the channel and sediment deposition in the middle of the channel occurs.
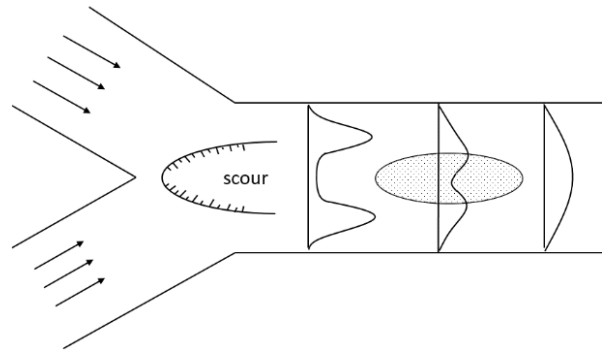
Figure 4.8: Principle of mid-channel bar growth (Ashworth, 1996)

In order to transfer this knowledge to Yangon Estuary, the same zones are defined for the confluence in Yangon Estuary. This is shown in Figure 4.9. Between the Yangon River and the Bago River a stagnation zone is expected. This stagnation zone will be located just downstream of the mouth of the Pazundaung Creek. Based on the bathymetry, the deflection zone is expected in the middle of the Yangon River channel and the Bago River channel downstream of the confluence (indicated by 2 in Figure 2.17). At the corner of the Yangon River mouth, the flow is not able to follow the western bank and eddy formation will occur in the flow separation zone (indicated by 3 in the figure). At the flood and ebb flow channels indicated by number 5 in the figure, the flow recovery is expected and the maximum flow velocity is reached at location 4 where the estuary width has decreased. Furthermore, the mid-channel bar growth between the flows of the Yangon River and the Bago River is clearly visible.
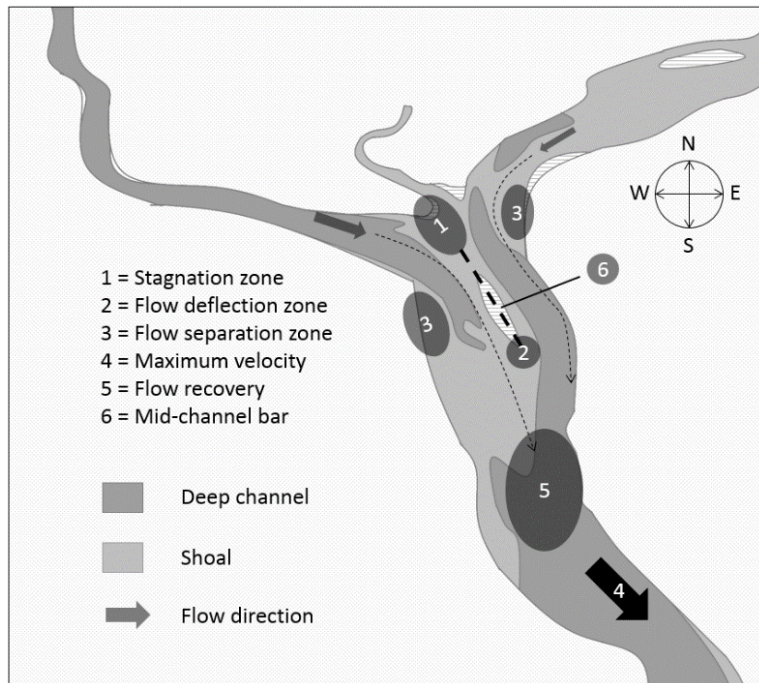
Figure 4.9: Conceptual diagram of the confluence zones in Yangon Estuary

4.2.2 Bifurcations

A bifurcation is a junction in a river where the flow separates from one branch in two other branches. How the discharge and sediment are distributed between the two branches, depends on the following features; the bifurcation angle, asymmetrical approach, Bulle effect and gravitational pull (Mosselman, 2017). First consider a bifurcation with symmetrical approach and bathymetry with a large bifurcation angel (see Figure 4.10; schematisation 1). When flow is approaching a bifurcation, the flow has to change its direction by 90 degrees. The rotation of the flow is caused by pressure build-up in the drive-up zone. The pressure from the drive-up zone results in a force that drives the flow around the corner. The flow velocities are reduced in the drive-up zone causing for settling and deposition of sediment. The amount of sedimentation can be reduced by creating a smaller bifurcation angle. Due to a smaller bifurcation angle, the flow is separated more fluently and the area of the drive-up zone decreases.
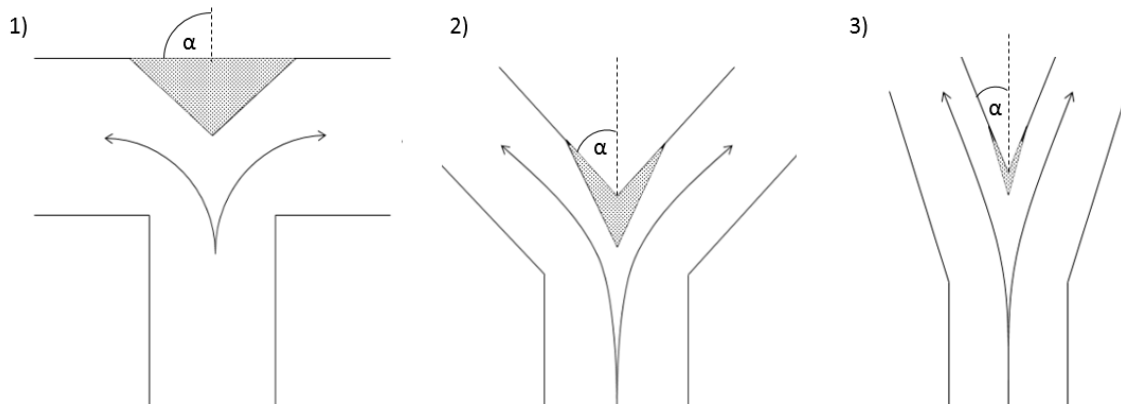
Figure 4.10: Schematisation of flow at a bifurcation with decreasing bifurcation angle from left to right: 1) α = 90°, 2) α = 45°, 3) α = 20°. The grey area is referring to the sedimentation area in dive-up zone.

Figure 4.10 shows that a smaller bifurcation angle can reduce the amount of sedimentation at the head of the split. Looking at bifurcations at rivers in The Netherlands, for instance the Pannerdensche Kop, it can be noticed that minimisation of the bifurcation angle results in minimum sedimentation at the split.

In the bifurcation in Yangon Estuary, asymmetrical approach occurs because the largest amount of discharge is expected to flow along the eastern bank. As a result, most of the flood discharge will flow into the Bago River. Due to flow separation at the corner of the Bago river mouth, eddy formation occurs that causes for sedimentation at the inner band of the Bago River. In addition, the Bulle effect is causing for bed-load transport towards the inner bend due to the effect of helical flow. Just downstream where the outer bend is on the eastern bank, the bed load transport will be directed towards the Inner Bar. Gravity pull causes bed load material to stay in the deeper Bago channel instead of being transported in towards the Yangon River.
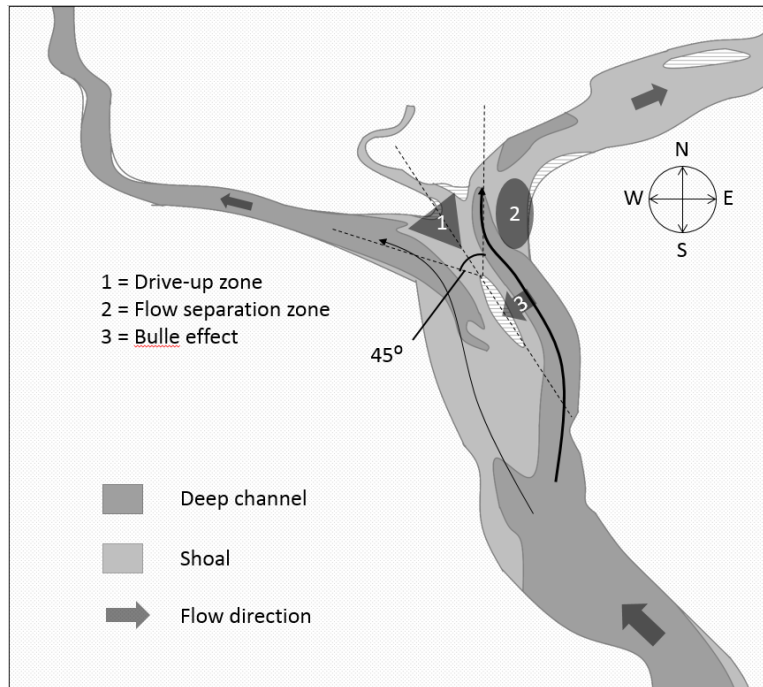
Figure 4.11: Conceptual diagram of the bifurcation zones in Yangon Estuary

4.3 Sediment processes

In estuaries multiple soil types can be found such as clay, silt and sand. One way to distinguish these different soil types is by particle size. Table 4-1 gives an overview of the different soil types and their particle sizes.

Table 4-1: Soil types with grain sizes (Verruijt, 2010)

Soil type	Grain size
Clay	< 4 µm
Silt	4 µm – 64 µm
Fine sand	64 µm – 125 µm
Sand	125 µm – 2 mm
Gravel	> 2mm

Another way to distinguish soil types is by chemical composition. Sandy materials consist most of quartz and clay consists of small plates. These small plates are slightly negatively charged and therefor capable of binding with positive hydrogen ions (Coulomb force). Because the clay particles are so small, Van der Waals force also starts playing a role. The balance of Van der Waal's force and Coulomb force makes clay a cohesive soil. Besides hydrogen, clay can also bind with positively charged organic matter. When clay is mixed with silt, organic matter and water, it is called mud (Winterwerp & Van Prooijen, 2016). The quartz of sandy materials are not charged and are therefore non-cohesive sediments. Because of cohesion, the behaviour of clay and mud sand in comparison with is very different. The effect of cohesion plays an important role in the erosion, transport and settlement of the sediment. For instance, the amount of energy required for erosion of mud is much larger than the energy required to keep the fine sediments in

suspension and when the mud is in suspension, it takes much more time to settle than for sand because of the smaller settling velocity.

Traditionally, sediment transport is divided in bed load transport, suspended load transport and wash load transport as shown in Figure 4.12.
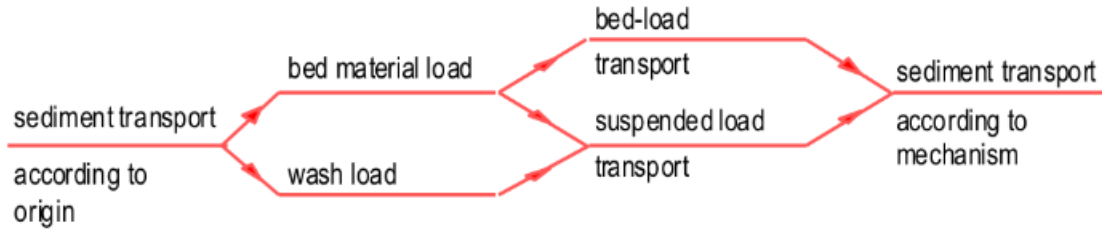
Figure 4.12: Types of sediment transport (Blom, 2016)

Bed load transport is defined as the transport of bed material by rolling and sliding along the bed (Blom, 2016). Suspended transport is the transport of sediments which have less weight and are therefore in suspension for some time, after which they deposit on the bed. The settling velocity of sand is in the order of cm/s while the settling velocity of silt is in the order of mm/s (Winterwerp & Van Prooijen, 2016). When the sediment particles are very small, the particles can stay in suspension at all times. This is called wash load. Combining the type of transport with the type of sediment the next main sediment transport modes are defined:

Sediment	Transport	Cohesiveness
Mud	Suspended load	Cohesive
Fine sand	Suspended load	Non-cohesive
Sand	Bed load + suspended load	Non-cohesive

In the transport cycle of sediment there are three main phases of particle motion; settling, deposition and erosion. In the next sections these phases are discussed for non-cohesive sediment and cohesive sediment.

4.3.1 Non-cohesive sediment transport

In Section 2.2**Error! Reference source not found.** it is presented that the bed of the estuary channels mainly consists of medium sand with a mean particle size of 300 µm and silty material (D50 = 90 µm) can be found at the estuary mouth. Based on section 2.2, both bed-load transport and suspended-load transport are considered. In order to analyse the sediment transport of non-cohesive sediments Van Rijn's empirical relations are used. Van Rijn distinguishes bed-load transport from suspended-load transport by means of a reference height a (see Figure 4.13).
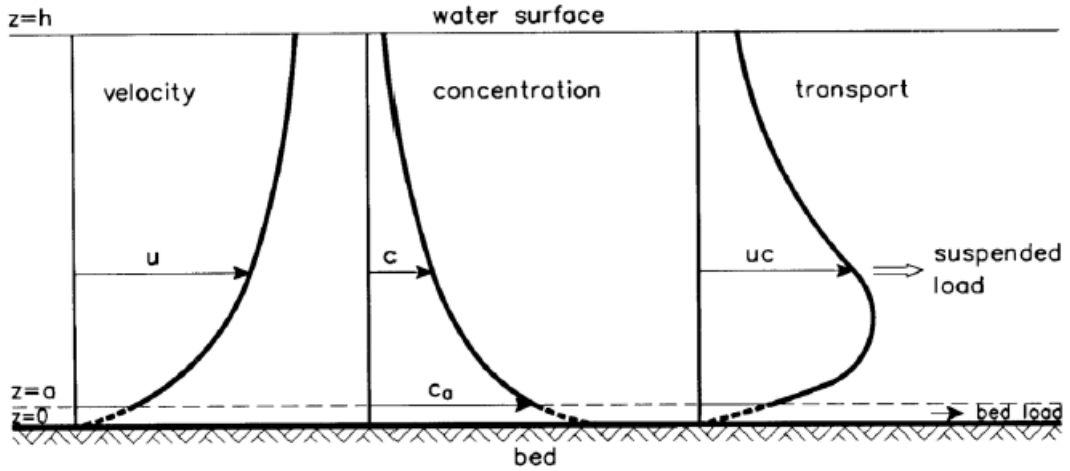
For this conceptual model, a Rouse profile is created to define the ratio between bed-load transport and suspended-load transport.

The Rouse profile for τ = 0.5 N/m2 shows that fine sand is concentrated in the layer to 1 m above the bed. When the bed shear stress increases to τ = 1.0 N/m2, the fine sand will be distributed all over the water column. Concentrations 1 m above the bed start exceeding 2 g/l when the be shear stress becomes larger than 2.0 N/m2.

Next, the Rouse profiles for medium sand ($D_{50}= 300$ µm) are presented by Figure 4.15.
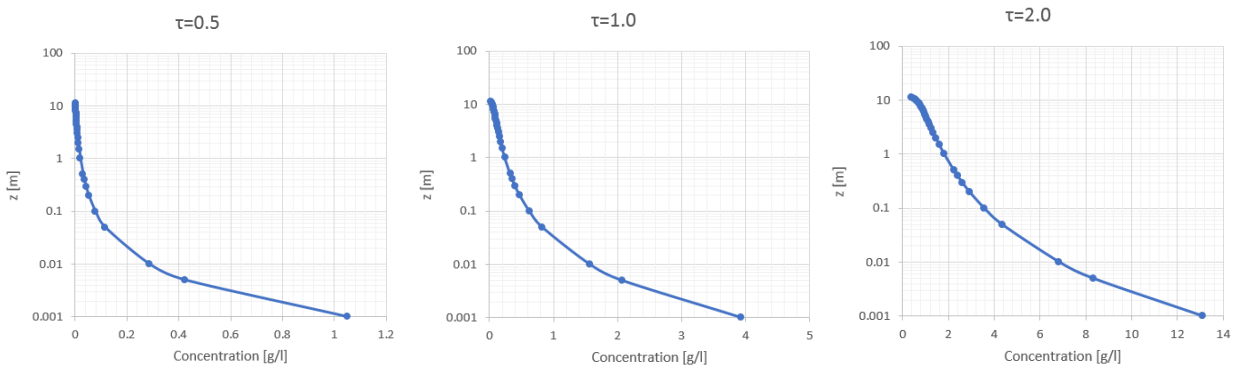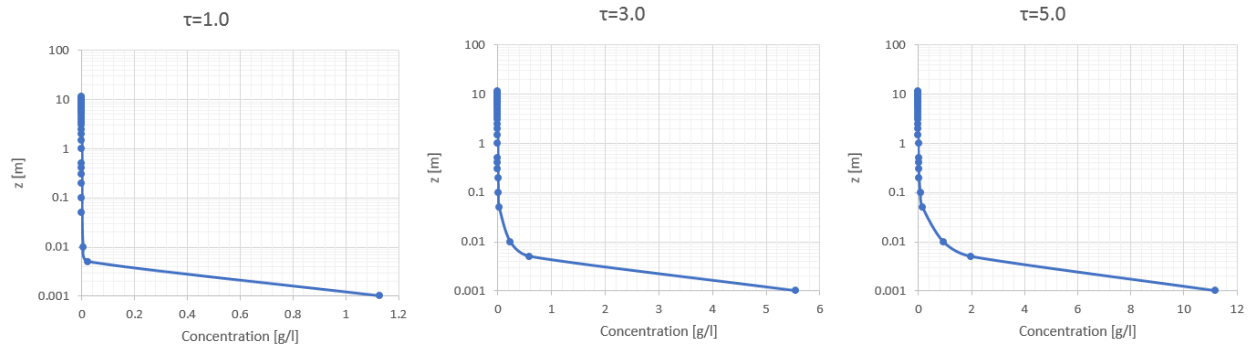
Figure 4.15: Rouse profiles for medium sand ($D_{50} = 90\ \mu m$) for different bed shear stresses (τ) [N/m2]. Note: changing x-axis values

The Rouse profiles for medium sand show that despite of high shear stresses the sediments stay concentrated near the bed. Consequently, the sand is expected to be transported close to the bed causing the sand to stay concentrated in the channels and less on the shoals.

4.3.2 Cohesive sediment transport processes

Due to the cohesiveness the transport processes of fine sediments are more complex than the sediment dynamics of non-cohesive material. Where the morphological response is still a balance between erosion and deposition, the processes that influence the erosion and deposition are different. The important cohesive sediment transport processes are presented in Figure 4.16.
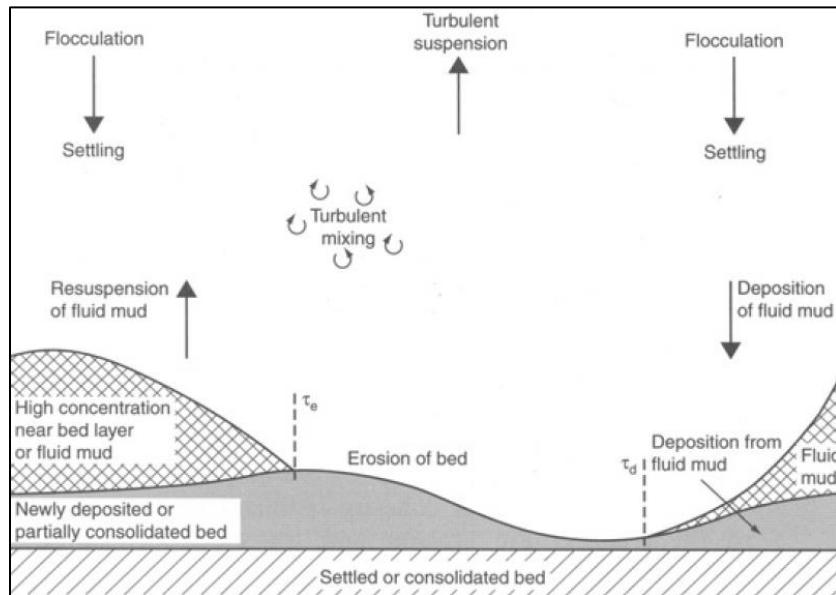
Figure 4.16: Cohesive sediment processes (Whitehouse, 2000)

In this section settling is considered in combination with flocculation. And the critical bed shear stress for erosion is considered in combination with consolidation. The cohesive sediment is referred to as mud. Mud can be found in multiple stages. Mud may occur as a mobile suspension, fluid mud or settled mud (Ross & Mehta, 1989). Mobile fluid mud layers can move freely through the tidal cycle, whereas stationary fluid mud layers are most likely to be re-entrained only during spring tides. Incomplete re-entrainment of stationary fluid muds enables longer consolidation

37

times with stronger settled mud layers, which might not erode during the next spring tide as a result.
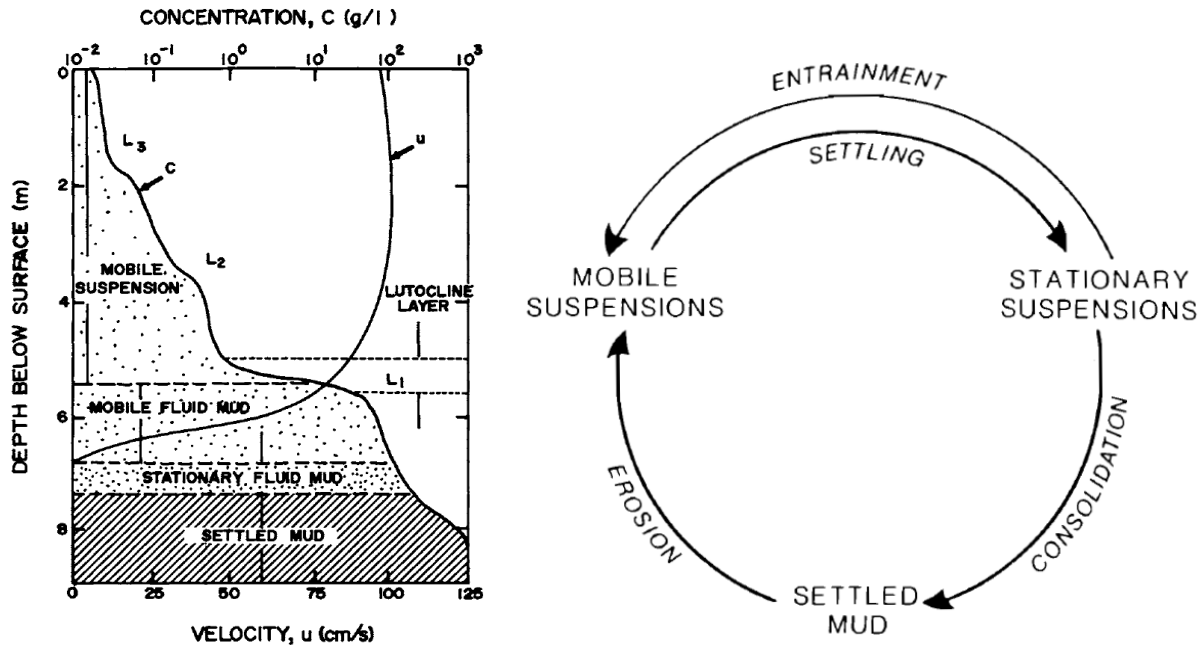
Figure 4.17: Cohesive sediment processes (Wells, 1995), (Kirby & Parker, 1983)

Settling

The settling velocity of non-cohesive material can roughly be estimated by using Stoke's law. The settling velocity for fine sediments depends on the specific weight of the soil and the grain size. Because the specific weight of the quartz and plates is constant, the settling velocity is mainly determined by the particle size. The size of the cohesive sediment particles depends on the rate of flocculation. Flocculation is aggradation of cohesive particles due to the electrostatic forces that bond particles. During the flocculation process, polymers from organic matter bond to the clay particles and form larger flocs. The size of the flocs depend on the suspended sediment concentration, turbulence, salinity, temperature and the amount of organic matter (Winterwerp & Van Prooijen, 2016). Due to turbulence, flocs can grow but also break. Higher turbulence causes for a higher probability of collision of particles, just like the sediment concentration. But when the turbulence is too high, shear stress on the flocs causes them to break. Salinity causes for a reduction of the double layer around the spherical particle which lowers the repulsion Coulomb force enabling the particles to approach each other and Van der Waals force starts to dominate. A thinner double layer results in a stronger bonding. Because an estuary forms the transition between fresh and saline water, flocculation can be of large importance to the sediment dynamics within the estuary. Larger flocs will basically have a larger settling velocity. But when the flocs become too big and start feeling each other, hindered settling can occur which lowers the settling velocity. This process is presented by Figure 4.18. The concentration when the flocs start to form is indicated by c_{Floc} and the concentration when flocs start to hinder each other is indicated by c_{Hinder}. The concentration at which the settling velocity becomes negligible is indicated by c_{gel}. From this point consolidation starts.
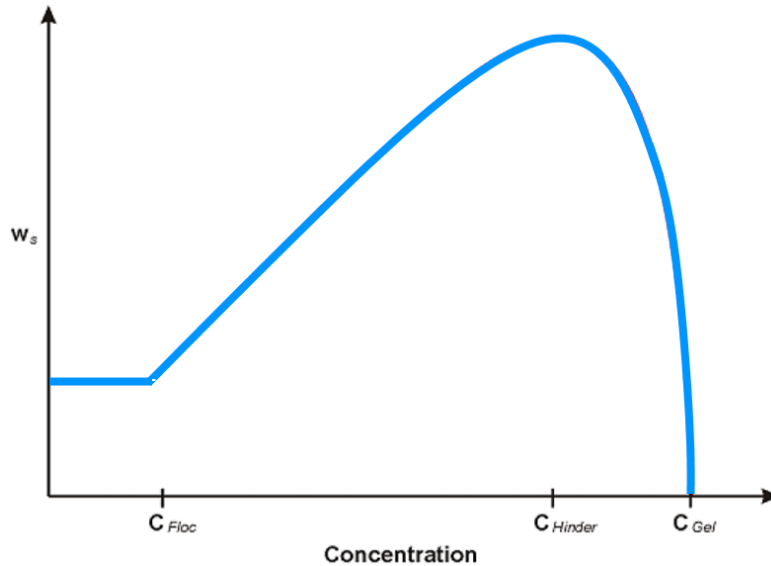
Figure 4.18: Hindered settling.

Important to this research is the location where flocculation might occur because the flocculation process can cause for sedimentation. The largest effect of flocculation is expected at the transition from fresh to saline water. As presented in , the salt intrusion is assumed to be too far away from the area of interest to have impact on the sedimentation in Monkey Point Channel. However, during monsoon season, when the river discharge is expected to carry a lot of sediment, the fresh/saline transition is expected to be close to the Yangon River mouth where flocculation can have direct impact on the sediment dynamics at the confluence.

Nelson (2000) analysed the settling and hindered settling behaviour of a sediment sample from the Yangon River. The suspension had an initial concentration of approximately 3 g/l. In less than 5 min, flocculation and particle settling occurred, and the concentration of sediment decreased. In less than 30 min, approximately the duration of slack water at the change in tides, all of the sediment settled out. In addition a fluid mud sample was taken at 1 m above the bed. The sample had an initial concentration of 41.3 g/l. The settling was rapid at first; the volume decreased by one third in 15 min. After 1 hour the volume had decreased by two third of its original volume. After 24 h the volume of the fluid mud had decreased to 12% of its original volume. So the density of the fluid mud layer increased from 41.3 g/l to approximately 124 g/l in 1 h and to 344.2 g/l in 24 h (see Figure 4.19a).
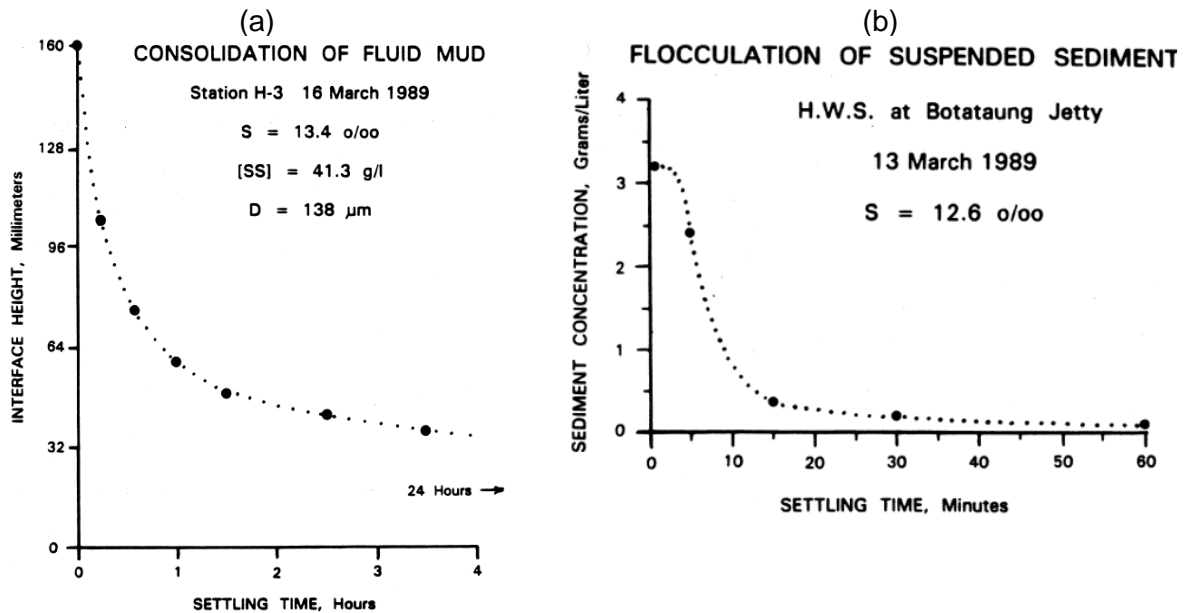
Figure 4.19: (a) Hindered settling of fluid mud taken from the Yangon River (Nelson, 2000).
(b) Settling behaviour of suspended sediment sample taken from the Yangon River (Nelson, 2000).

Deposition

The result of settling is the deposition of particles on the bed. Deposition is defined as the gross flux of cohesive sediment flocs on the bed. Sedimentation occurs when the gross flux of deposition exceeds the flux of erosion. The deposition flux only depends only on the concentration and settling velocity of the sediment and does not depend on a critical bed shear stress for deposition (Winterwerp & Prooijen, 2017). In other words; deposition will always occur if the settling velocity is larger than zero. Sedimentation depends therefore on the critical bed shear stress for erosion only.

Consolidation and erosion

When the critical bed shear stress for erosion of the deposited flocs is not exceeded, the flocs are able to stay on the bed. During the deposited period, consolidation of the bed will occur. Consolidation is defined as the process in which the bed volume decreases due to the gravitational force on the bed that causes water to be pressed out of the pore volumes. Due to the compression the density of the bed and the internal strength of the bed increases (Verruijt, 2010). Three stages of consolidation can be distinguished (Van Rijn, 1993):

- Initial stage (days): hindered settling and consolidation occur at the same time. Flocs are grouped in an open structure with high pore volumes.
- Secondary stage (weeks): Pore volumes are reduced and water is pressed out of the pores through the drains in the layer. Strength of layer increases
- Final stage (years): Flocs break down, pore volumes reach minimum limit and the density of the layer reaches its maximum.

Table 4-2: Density ranges for several consolidation stages (Van Rijn, 1993)

Consolidation stage	Rheological behaviour	Wet sediment density [kg/m^3]	Dry sediment density [kg/m^3]
Freshly consolidated (1 day)	Dilute fluid mud	1000 – 1050	0 -100
Weakly consolidated (1 week)	Fluid mud	1050 – 1150	100 – 250
Medium consolidated (1 month)	Dense fluid mud	1150 – 1250	250 – 400
Highly consolidated (1 year)	Fluid – solid	1250 – 1350	400 – 550
Stiff mud (10 years)	Solid	1350 – 1400	550 – 650
Hard mud (100 years)	Solid	> 1400	> 650

Van Rijn (1993) has defined critical bed shear ranges for different bed concentrations in multiple estuaries. From these values the

Table 4-3: Critical bed shear stresses for erosion in the (Van Rijn, 1993)

	τ_e critical bed-shear stress for erosion [N/m²]				
Location	$c = 100$ kg/m³	$c = 150$ kg/m³	$c = 200$ kg/m³	$c = 250$ kg/m³	c = 300 kg/m3
Delfzijl harbour (Eems)	0.05 – 0.15	0.15 – 0.20	0.20 – 0.25	0.40 – 0.60	-
Cardiff Bay (Severn)	0.20 – 0.30	0.40 – 0.50	0.60 – 0.70	0.70 – 0.90	-
Loire	0.10 – 0.15	0.15 – 0.20	0.20 – 0.30	0.30 – 0.40	0.80 – 1.20
Belawan	0.20 – 0.30	0.40 – 0.60	0.80 – 1.00	-	-

Previously in this section (see **settling**), the hindered settling process of the fluid mud, taken from the Yangon Estuary, was analysed. Relating the sediment information to the density stages of Table 4-2, the sediment consolidates much faster than the values of Van Rijn (1993). Based on the measurements by Nelson (2000) the sediment concentration after 1 h exceed 100 kg/m³. Hence the critical erosion after 1 h is assumed to be in the range of 0.15-0.30 N/m² (see Table 4-3). After 24 hours the deposited fine sediment is consolidated to a concentration of >300 kg/m³ and therefore the critical bed-shear stress for erosion is defined in the range of 0.40 – 0.70 N/m². Furthermore, Nelson (2000) observed mobilisation of stationary mud when flow velocities exceed 0.5 m/s which agrees which a bed shear stress of 0.25 N/m². The fluid mud gets dispersed when the velocities exceed 1.0 m/s which agrees with a bed shear stress of 1.0 N/m². As indicated by Figure 4.17, under the mobile layer a stationary layer.is expected which is less exposed to shear as long as the mobile layer is not dispersed. Hence, the stationary layer has more time to consolidate and settled mud layers develop. Whether this consolidated layer erodes depends on the consolidation time.

4.4 Conceptual model stage 2

In this conceptual model stage the conceptual diagrams of Chapter 4 are combined in order to investigate how these processes interact. In 4.1 the conceptual diagrams shows the spring/neap cycle of SSC in the estuary. When this is combined with the flow dynamics at a confluence and bifurcation, as presented in Figure 4.9 and Figure 4.11, one can notice that every tidal cycle new suspended sediment is brought into the stagnation-zone. Because in the stagnation-zone the flow velocities and the bed-shear stresses are expected to be low, the mud may be able to stay longer on the bed than just during slack water, enabling the layer to consolidate which causes for higher critical bed shear stresses for erosion as mentioned in 4.3. When the critical bed shear for erosion stress exceeds the induced bed shear stress during spring tides the mud is not eroded from the bed, as expected for the shoals, which enables the layer to consolidate further. Finally, the concentration becomes problematic for the ships.

The flood dominant tide causes for the import of sediment and the transport of eroded sediment from the shoal towards the estuary bay head.

During the monsoon the suspended sediment is expected to be transported seaward due to the high river discharge. During the dry season the suspended sediment is expected to be transported landward by the flood dominant tide. Hence the SSC is higher in dry season since the suspended sediment stays in the estuary.

As shown in the graphic visualisations the stagnation zone is located within the zone of high SSC. Because in the stagnation zone the expected bed-shear stresses are low both during flood and ebb, the suspended sediment has a lot of time to settle. As the sediment is able to consolidate, the critical bed shear stress for erosion increases. When the critical bed-shear stress for erosion exceeds the bed shear stress during spring tide, the sediment is able to stay on the bed of Monkey Point Channel. When the concentration of the mud layer exceeds 1250 kg/m^3, it becomes problematic for the ships. The combination of the high SSC with the low bed-shear stresses that are expected in the stagnation zone.

5 Hydrodynamic model

Based on the processes considered in the previous chapter, numerical models are used to do a quantitative research to discharges, water levels and flow velocities in order to analyse the discharge distribution, tidal asymmetry and the confluence dynamics.

5.1 Present numerical models of Yangon Estuary

During this research, two available numerical models have been used; a Sobek model and a MIKE21 model. This paragraph gives a brief description of these models.

5.1.1 SOBEK

In 2015, RHDHV was involved in a project to design a sluice in the Pan Hlaing River to control the amount of water flowing through the Pan Hlaing River. To get a better understanding of the flow in the Pan Hlaing River, a SOBEK model has been created which is able to calculate the discharge distribution over the Irrawaddy Delta and hence the discharge through the Pan Hlaing River. A schematisation of the SOBEK model is shown in Figure 2.1, the model domain is shown in Figure 13.7. The SOBEK model is basically a 1DH model with multiple boundaries at the Andaman Sea and landward boundaries in the Irrawaddy River, Upper Hlaing River and Bago River. The Pazundaung Creek is not included in the model. The tidal boundary conditions of the SOBEK model are calculated based on tidal constituents and tide tables of the area (RHDHV, 2016). The boundary conditions at the river boundaries consist of discharge time-series. Discharge data from a measurement station at Pyay is used to define the discharge time-series for the in the Irrawaddy. The time-series that are used in the model consist of average values for the discharge over one year. The boundary conditions at the Upper Hlaing River and Bago River are based on single discharge data values and the same yearly pattern of discharge as the Irrawaddy River. The model was calibrated on water levels at the Hlaing River and the Mezali. The calibration results are shown in Appendix D.

5.1.2 MIKE21

In 2016 RHDHV created a 2DH model with the MIKE21 software (DHI, 2018). The model was made in order to analyse flood events within the Yangon Estuary (RHDHV, 2017). Figure 13.8 shows the model domain. The tidal signal at the estuary mouth is the only dynamic boundary condition of the model. The tidal signal is based on measured time series at Elephant Point and is relative to MSL. The boundaries at the landward end of the rivers are defined as land. It is assumed that dry season can be represented by the situation without river discharges. To define the bathymetry, RHDHV has done a bathymetry survey between Monkey Point and the estuary mouth. The bathy data is leveled to MSL. The model is calibrated with measurement data of water levels at Thilawa and current speeds at different locations along the estuary. Roughness is used as calibration parameter which resulted in varying values for the bottom roughness over the estuary. The calibration results are shown in Appendix D.

5.2 Model set-up

During this research it is decided to use the RHDHV's MIKE21 model of the Yangon Estuary in combination with the RHDHV's SOBEK model of the Irrawaddy delta. First it was decided to work further with the MIKE21 model because the reliable results for the hydrodynamics in dry season. By using the proper bathymetry, fairly accurate grid and roughness field based on validation, time is saved and duplicated prevented.

The interaction between the tide and the river discharge in the Irrawaddy Delta is expected to influence the amount of discharge that flows into the Yangon Estuary. In order to implement the interaction between Yangon Estuary and the Irrawaddy delta it was decided to combine the MIKE21 model with the SOBEK model. Besides, no bathymetry data is available for the Bago River and Hlaing River which results in uncertainties during high discharges through these branches. Therefore it is decided to limit the landward boundaries of the MIKE model to the limit of detailed bathymetry. The resulting model domain is shown in Figure 5.1.
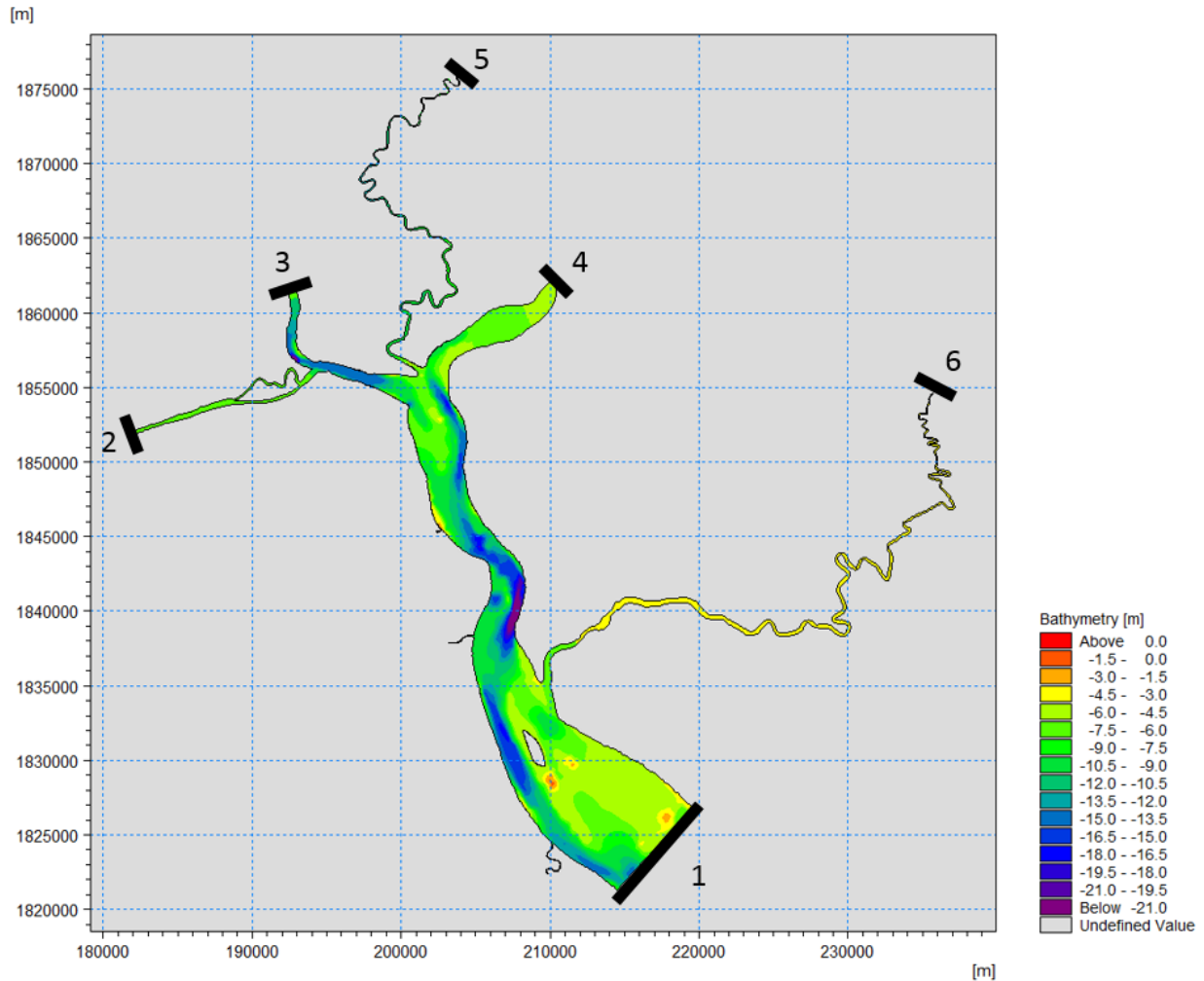
Figure 5.1: Model domain with boundary conditions. 1: Water level time-series. 2: Discharge time-series Twante Canal. 3: Discharge time-series Hlaing River. 4: Discharge time-series Bago River. 5: Land boundary. 6: Land boundary

5.2.1 Grid

The model has a 2D grid created with MIKE flexible mesh. The size of the arm of the triangle grid cells varies between 50 m and 150 m. The first 8 km upstream from the estuary mouth in upstream consists of larger cells with a grid size of 150 m. Upstream from this location the size of the grid cells is reduced to 50 m. Since Monkey Point Channel has a width of about 100 m, the grid size is a bit large. However, the grid size of 50 m is thought to be sufficient to give reliable results for the hydrodynamics at the confluence.

Based on the available data and the scope of this research, it was decided to continue with the 2DH model and not to make a 3D model. The consideration for creating and using a 3D model follows from the estuary processes as described in Appendix B and Appendix C. To properly calculate the transport of fine sediment, processes such as estuary circulation, ETM formation and lag effects must be included in the model because these processes can have a major influence on the residual transport of fine sediment. These processes are a result depth varying flows and therefore a 3D grid is necessary to include these processes in the model. However, by expanding the model over the vertical, the computation time increases drastically. In combination with the increasing complexity of the model, which makes it more difficult to conclude which combinations of processes are related to the result in hydrodynamic and morphodynamic changes, it is decided to make a 2DH model. As a consequence, the model is inappropriate to determine the residual transport of fine sediment. Since sand is mainly transported as bed-load, the 2DH schematisation of the Yangon Estuary is thought to produce reliable results for sand transport calculations (Van Maren, 2019).

5.2.2 Boundary conditions

The 2DH schematisation of the Yangon Estuary has six boundaries (See Figure 5.1). Boundaries 5 and 6 are defined as land-boundaries because the landward end of the Pazundaung Creek consists of a sluice and is therefore defined as a land-boundary. Boundary condition 6 is chosen as a land-boundary because the tidal influence is expected to be limited to this length. This branch functions as tidal storage. Boundary condition 1 consists of the same water level signal as used in the SOBEK model. Boundary conditions 2,3 and 4 are discharge time-series that are extracted from the SOBEK model. Figure 5.2 shows the output locations of the time-series in the SOBEK model which agree with the boundaries of the MIKE model.
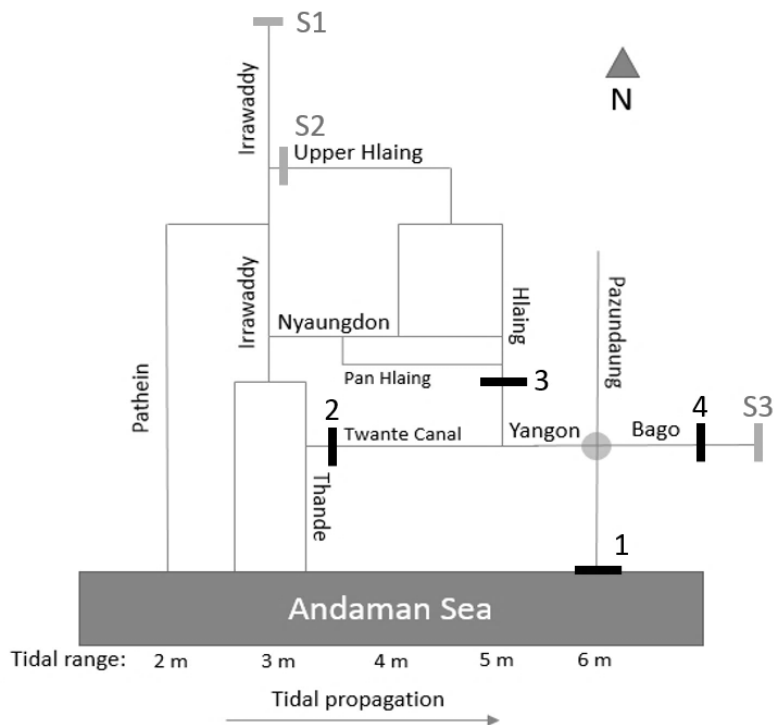
Figure 5.2: Output locations of discharge time series in SOBEK model. S1: Discharge time-series of Irrawaddy River. S2: Discharge time-series of Upper Hlaing River. S3: Discharge time-series of Bago River. 1: Water level time-series. 2+3+4: Output locations in SOBEK for discharge time-series as boundary conditions in MIKE.

The SOBEK boundary conditions are defined for a year, so the model can be run for a year as well. In this way, a year of output is generated at locations 2,3 and 4. The SOBEK output that is used as input for the boundary conditions of the MIKE model are shown in Figure 3.3 till 3.6.
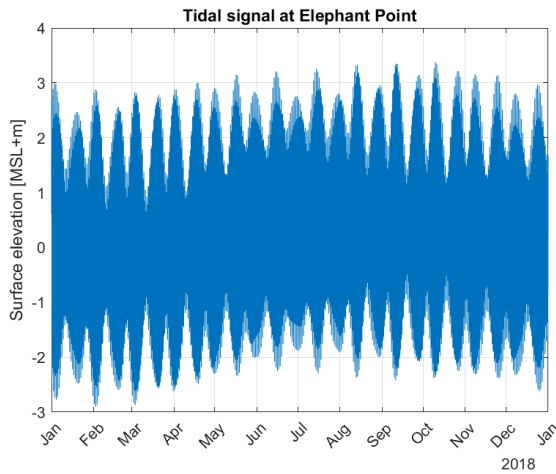
Figure 5.3: Boundary condition at location 1
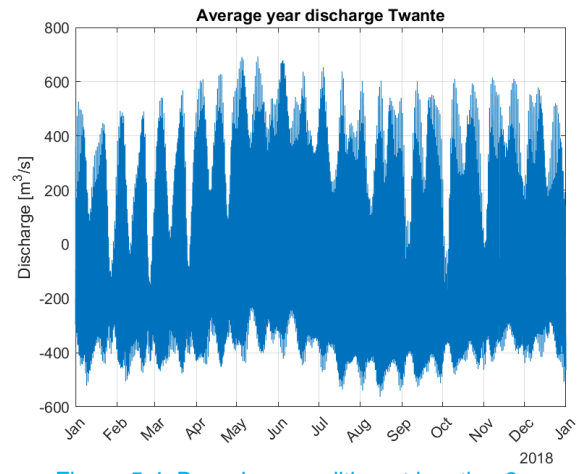
Figure 5.4: Boundary condition at location 2
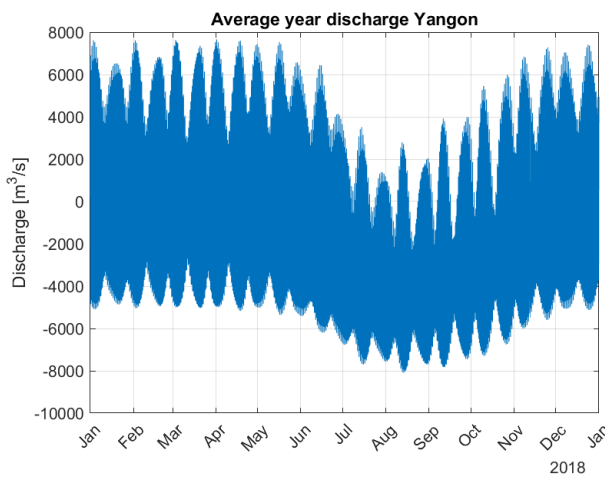
Figure 5.5: Boundary condition at location 3
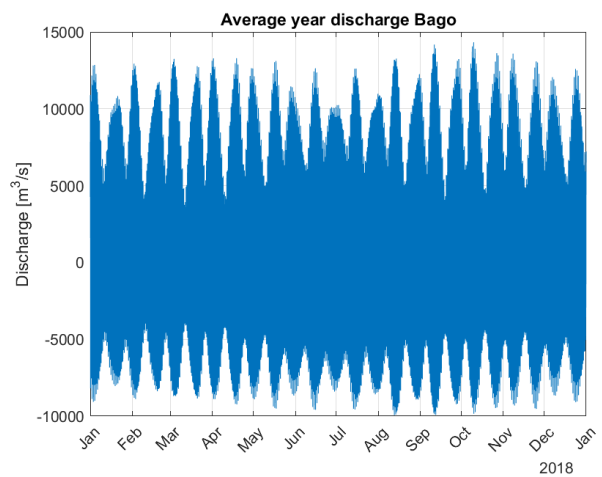
Figure 5.6: Boundary condition at location 4

5.3 Model results

With the hydrodynamic model discharges, water levels and current speeds in the estuary are calculated, which will be analysed in this section. In order to reduce the computational time, it is decided to run the model for the month January and August which represent dry season and monsoon season.

5.3.1 Discharges

In the conceptual model the estuary is classified as a tide-dominated system with well-mixed conditions. In this subsection the calculated discharges within the estuary are used to check the correctness of this classification. Furthermore, the discharge values are used to investigate the discharge distribution over the split at the head of the estuary and the distribution of discharge in the channels and over the shoals. Figure 5.7 shows the output locations for the generated discharge time-series that are used to do the analysis. First, the discharge in cross-section d1 is considered, secondly the discharges in cross-sections d3, d5 and d6 are analysed and finally the ratio between the discharges in cross-sections d1/d2 and d3/d4.
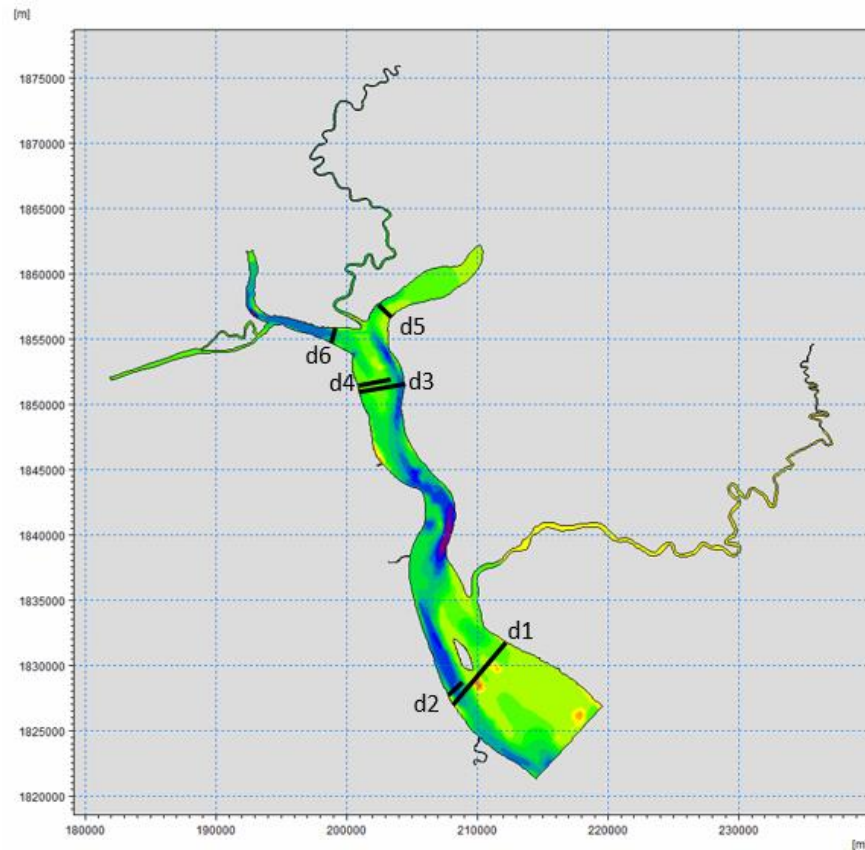
Figure 5.7: Cross-sections for calculating the discharges along the estuary

In chapter 2, process-based and stratification-based estuary classification are introduced. Because of the morphological similarities between tide-dominated estuaries in general and Yangon Estuary, it is hypothesised that Yangon Estuary is a tide-dominated system. This section attempts to substantiate this hypothesis by analysing the ratio of tidal discharge and river discharge. In this section the calculated discharges are shown. A positive value represents landward flow (flood) and a negative value represents seaward flow (ebb).

Figure 5.8: Discharge in cross-section d1 in dry season

Figure 5.9: Discharge in cross-section d1 in monsoon season

Figure 5.10: Discharge in cross-section d3 in dry season

Figure 5.11: Discharge in cross-section d3 in monsoon season

Based on the model results on discharges (see Figure 5.8 and Figure 5.9), the average flood and ebb discharges and the duration are calculated which are shown in the next table.

Table 5-1: Average discharges and duration in cross-section d1

Cross section	Season	Flood		Ebb	
		Q [m3/s]	Duration [h]	Q [m3/s]	Duration [h]
D1	Dry	34.500	5.2	27.500	6.8
	Monsoon	33.000	4.9	31.000	7.1
D3	Dry	19.000	5.0	14.500	7.0
	Monsoon	17.000	4.4	18.000	7.6

Wells (1995) stated that an estuary is tide-dominated when the tidal prism is ten times larger than the river discharge. Likewise, Simpson (1955) used the ratio between tidal discharge and river discharge as an empirical relation to define the amount of stratification. This relation is called the flood number and is defined as:

$$\alpha = Q_f/Q_t$$

Where:

Q_f	River discharge
Q_T	Tidal discharge
α<0.1	well-mixed conditions
α>1.0	stratified conditions

During the dry season, when the river discharge is very low, the tidal discharge is a factor 10 larger than the river discharge and the estuary can be considered as a tide-dominated system with well-mixed conditions. During the monsoon season the river discharge increases and stratification may become important. Because the time-series of the incoming discharge is within the tidal intrusion length, the contribution by the river discharge cannot be determined at once. Hence, the average river discharge is estimated by using the following volume balance.

$$Q_{r,avg} = \frac{Q_{ebb,avg} * T_{ebb} - Q_{flood,avg} * T_{flood}}{T_{ebb} + T_{flood}}$$

The average river discharge in August is about 5000 m3/s. Taking into account the yearly discharge distribution of Figure 5.5, the average monsoon discharge is estimated to be 4000 m3/s. Around the mouth of the estuary (d1) the tidal discharge is between 33.000 m3/s and 34.000 m3/s (see Table 5-1) which halves towards the head of the estuary (d3) where the tidal discharge is between 17.000 m3/s and 19.000 m3/s. Because of the reduction in tidal discharge, more stratification can be expected upwards the estuary. To conclude; the estuary can basically be considered as a tide-dominated system with well-mixed conditions during dry season and partly-stratified conditions in monsoon season.
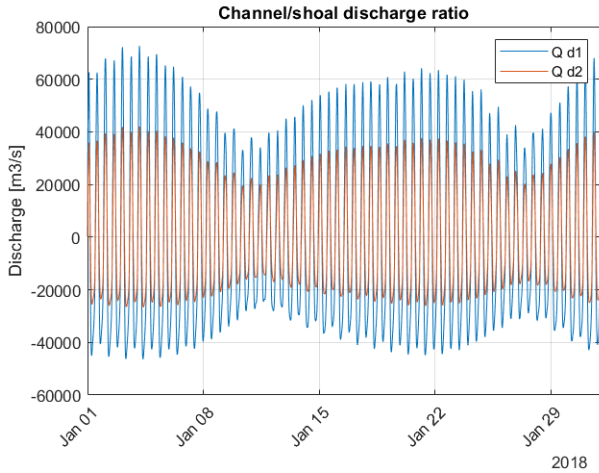
Figure 5.12: Discharge ratio between the channel and the shoal at cross-section d1 in dry season
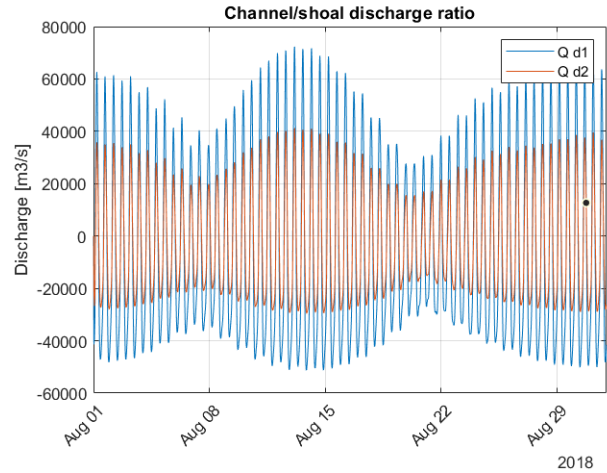
Figure 5.13: Discharge ratio between the channel and the shoal at cross-section d1 in monsoon season
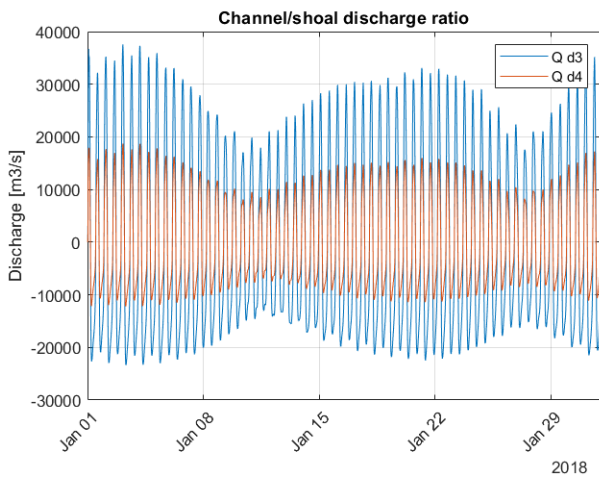
Figure 5.14: Discharge ratio between the channel and the shoal at cross-section d3 in dry season
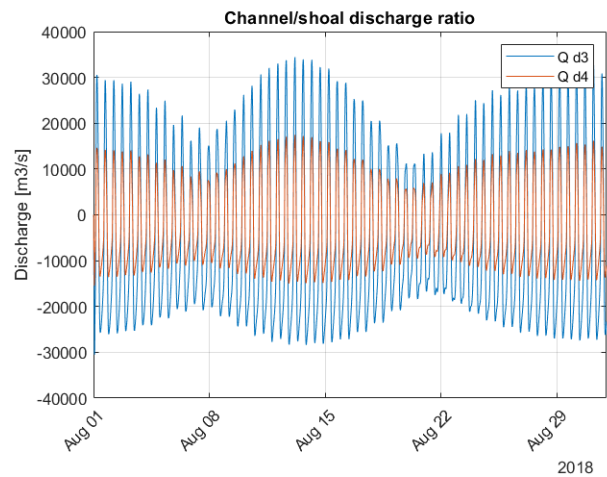
Figure 5.15: Discharge ratio between the channel and the shoal at cross-section d3 in monsoon season

Half of the discharge flows through the channels, while the channels are a third of the flow cross-section (Figure 5.12 - Figure 5.15). The velocities are therefore expected to be higher in the channel than over the shoals.

Because the Bago River is connected to the main channel of the estuary and the river shows the characteristic funnel shape of an estuary, the Bago River is assumed to be part of the major estuary system while the Yangon River is a river-dominated branch that flows into the estuary like a tap. In order to check this assumption, the discharge signals for the Bago River and the Yangon River are analysed. The model results for the discharges in cross-section d5 and d6 are presented in Figure 5.16 to Figure 5.19.
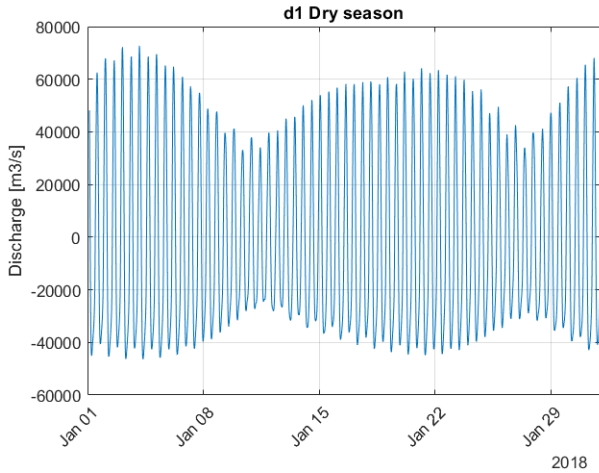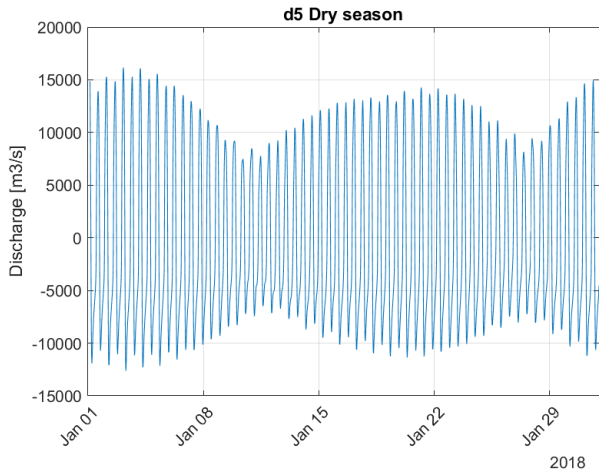
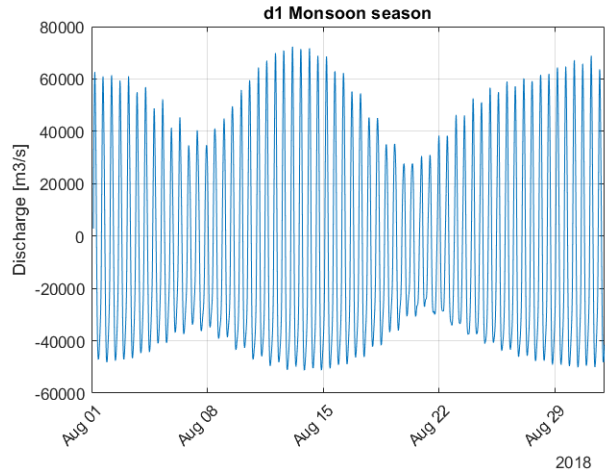Figure 5.16: Discharge in cross-section d5 in dry season
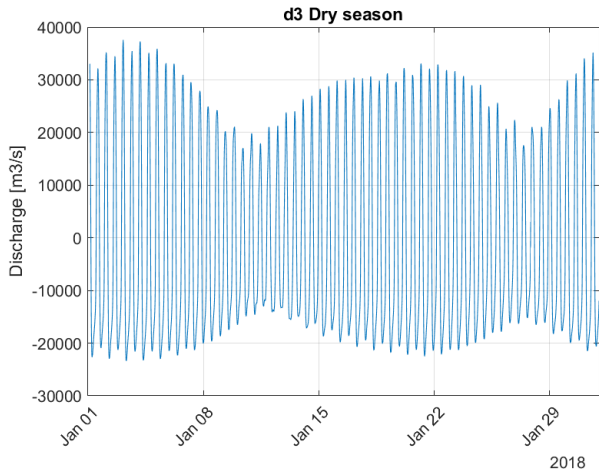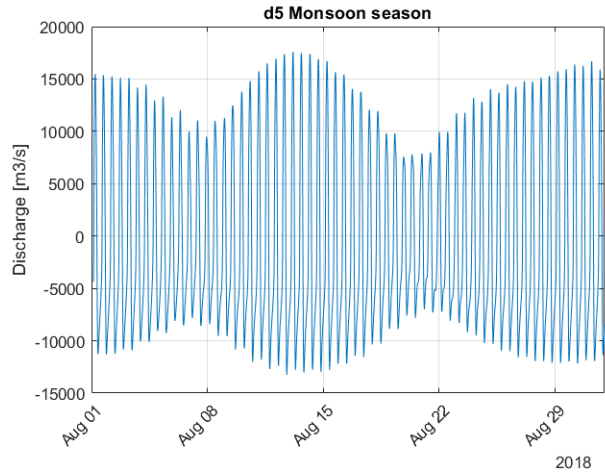

Figure 5.17: Discharge in cross-section d5 in monsoon season

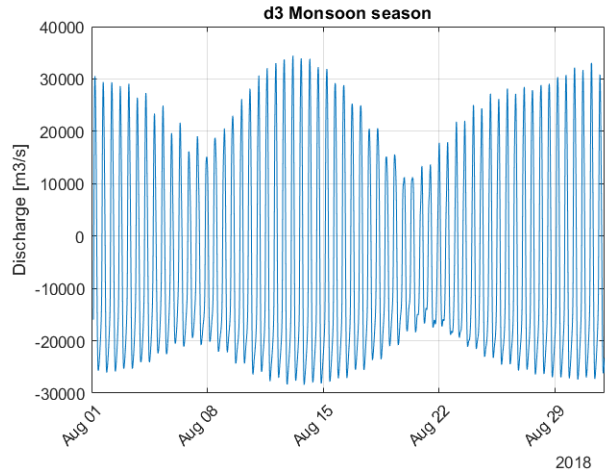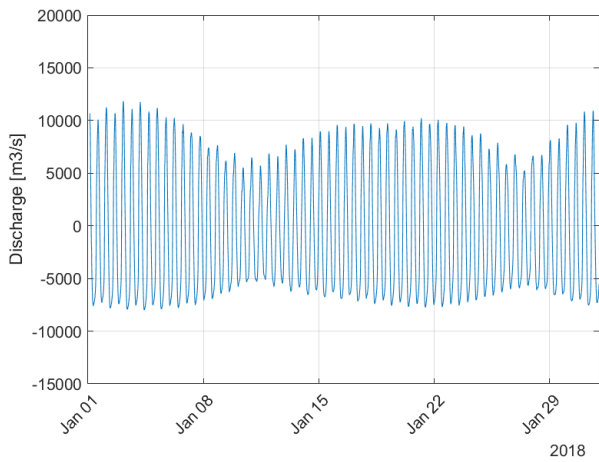Figure 5.18: Discharge in cross-section d6 in dry season
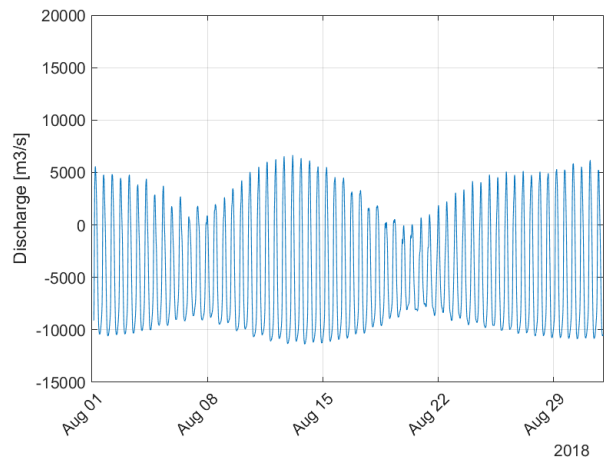
Figure 5.19: Discharge in cross-section d6 in monsoon season

From the plotted discharges, the average discharges with the duration are calculated and presented in Table 5-2.

Table 5-2: Rounded average discharges and duration in d3, d5 and d6 in m3/s

Cross section	Season	Flood		Ebb	
		Q [m3/s]	Duration [h]	Q [m3/s]	Duration [h]
D5 (Bago)	Dry	8.500	4.9	6.300	7.1
	Monsoon	9.100	4.6	6.800	7.4
D6 (Yangon)	Dry	5.600	5.3	5.200	6.7
	Monsoon	2.800	3.1	7.300	8.9

From the model results, the differences between the discharge in the Bago River and the Yangon River are immediately noticeable. The discharge in the Bago is about 1.5 times larger than the

51

discharge in the Yangon River. In addition, the character of the flow is completely different between the two rivers. The discharge that enters the Yangon River during spring flood in monsoon season has been halved in comparison with dry season conditions. The flood discharge in the Bago River increases in monsoon season relative to dry season. This is remarkable, since the discharge in both d3 and d6, decreases. An explanation for this could be the blocking of the flood discharge towards Yangon River by the monsoon river discharge. Because the flood discharge cannot enter the Yangon River, it flows into the Bago River where the river discharge is much less, resulting in an increase of discharge flowing into the Bago River branch. However, one must be aware that in such a situation, density effects can become important. Considering Simpson's flood number for the situation at Yangon River mouth in monsoon season, it can be noticed that the river discharge is larger than the tidal discharge and stratification can be expected.

5.3.2 Tidal asymmetry

As discussed in chapter 2, tidal asymmetry can be of large importance to the net sediment transport within the estuary. In this subsection, tidal asymmetry within Yangon Estuary is considered by analysing the water levels and current speeds that are calculated by the hydrodynamic model. In the conceptual is mentioned that the funnel shape causes for a flood-dominant tide. This is checked within this subsection, by analysing peak flow asymmetry and acceleration asymmetry.

Within the model domain, eight output locations are defined to generate time-series of water level variations and current speeds (see Figure 5.20).
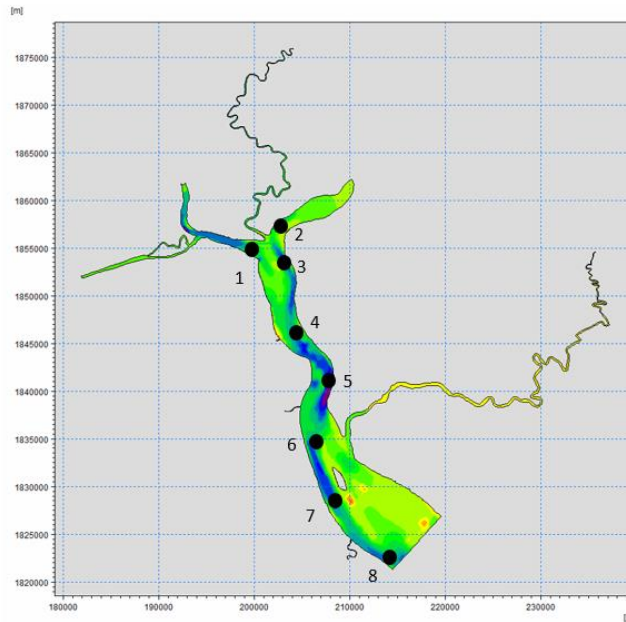
Figure 5.20: Locations to calculate the water levels and current speeds along the estuary

Peak flow asymmetry

First the water levels and current speeds at location 3 and 7 are considered. The tidal range varies between 3.0 m during neap tide and 5.5 m during spring tide.

The seasonal variation on current speeds is clearly visible from the current speeds at location 7 and 3. During dry season the maximum flow velocities occur during flood while in monsoon season the maximum flow velocities become more equal for flood and ebb conditions. But the duration of the ebb is longer than the flood so during monsoon season the residual current is directed in ebb direction. As a consequence, it is expected that during dry season the estuary imports sediment while during the monsoon season the net transport is expected to be in seaward direction.

The hydrodynamic model results show strong tidal asymmetry during the dry season with flood peak flow velocities 1.2 times larger than the ebb peak flow velocities, indicating the flood dominant character of the tide during spring tide in dry season. During neap tides the tidal asymmetry decreases and the peak flow velocities during flood and ebb become more similar. During the monsoon season the peak flow velocities at the inlet of the estuary and at the bay head the peak flow velocities during flood and ebb are equal. In the Bago River the peak flow velocity during flood remains dominant.
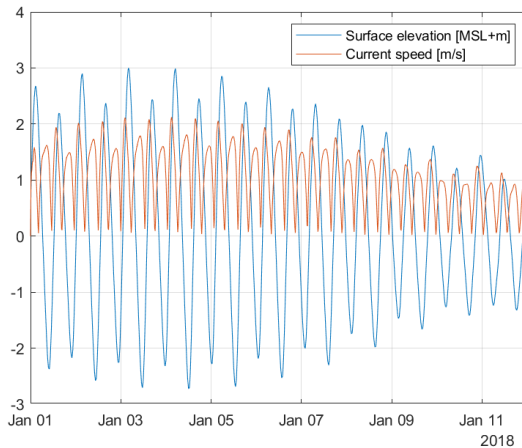
Figure 5.21: Surface elevation and current speed at location 7 during dry season
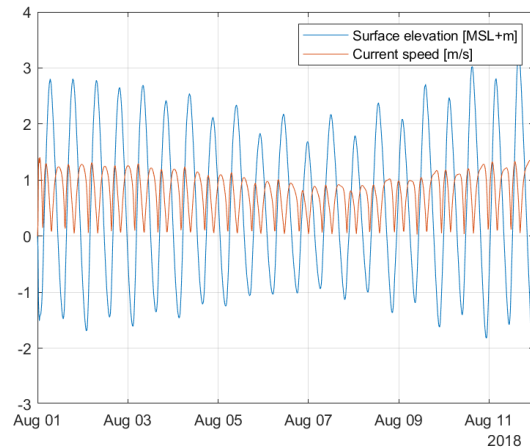
Figure 5.22: Surface elevation and current speed at location 7 during monsoon season
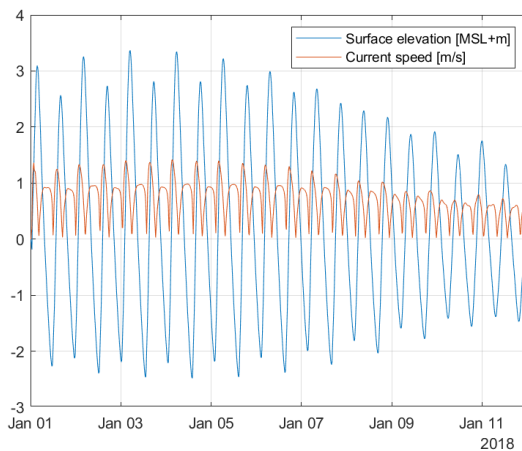
Figure 5.23: Surface elevation and current speed at location 3 during dry season
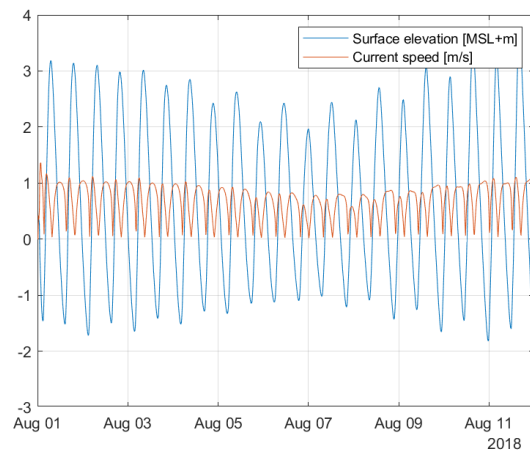
Figure 5.24: Surface elevation and current speed at location 3 during monsoon season

Striking is that the current speeds in the Bago River and the Yangon River differ a lot from the current speeds calculated for location 3 and 7 (see Figure 5.25 till Figure 5.28). From these figures it can be seen that the maximum flow velocities in the Bago River occur during spring flood. Besides it can be seen that the flow velocity profile of the Bago River does not differ much between the dry season and the monsoon season. Therefore the Bago River seems to be a tide-dominated river. The maximum flow velocities in the Yangon River occur during ebb in the monsoon season. The tide seems to have a minor influence on the maximum flow velocity since the difference between the neap and spring situation is small (see Figure 5.28). The flow velocities in the Yangon during dry season are almost equal in flood and ebb direction. In combination with the flow conditions in the monsoon season it can be concluded that the Yangon River is a river dominated branch.
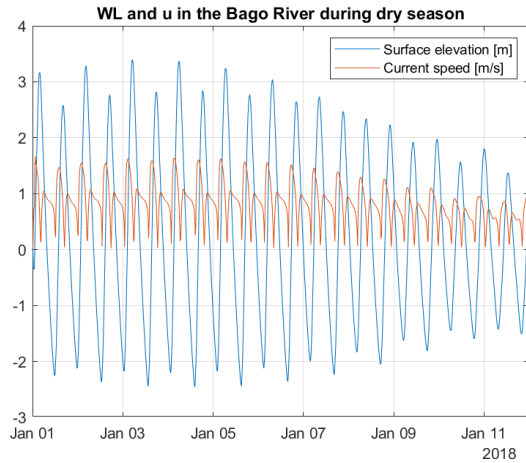
Figure 5.25: Surface elevation (WL) and current speed (u) in the Bago River during dry season
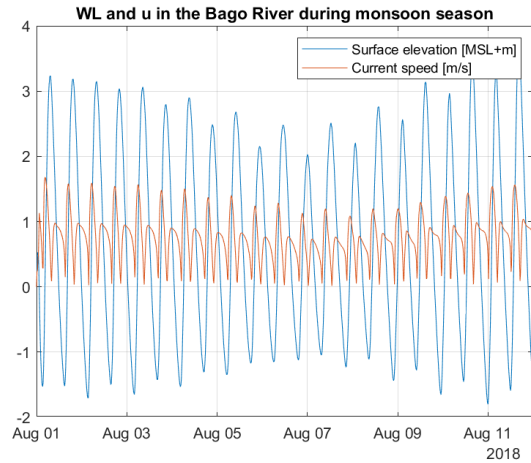
Figure 5.26: Surface elevation (WL) and current speed (u) in the Bago River during monsoon season
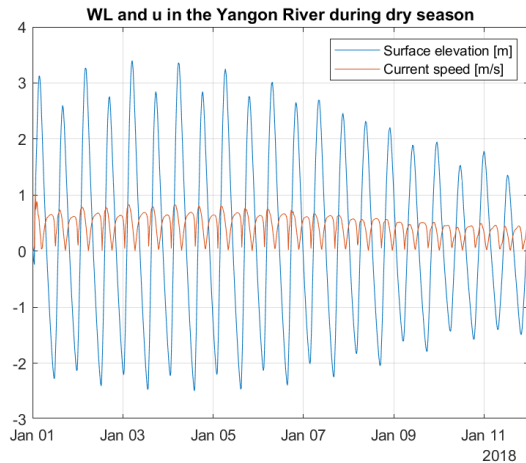
Figure 5.27: Surface elevation (WL) and current speed (u) in the Yangon River during dry season
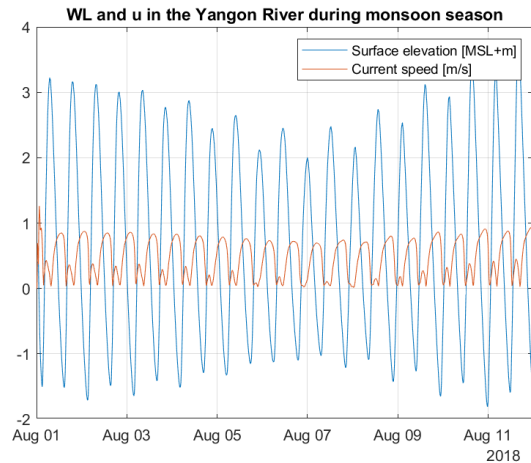
Figure 5.28: Surface elevation (WL) and current speed (u) in the Yangon River during monsoon season

Acceleration asymmetry

Next, acceleration asymmetry in the estuary is analysed. Because the model gives always positive values to the current speeds, the graphs show a nod at slack water. The rate of acceleration can be derived from the angle size at the nod of the graph. A smaller angle relates to higher acceleration. The acceleration asymmetry varies with the season, the moment in the tidal cycle and on the location within the estuary. First the seasonal variation is considered.
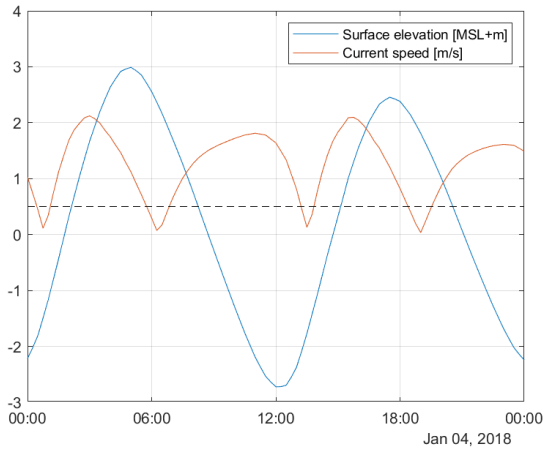
Figure 5.29: Water level and current velocities at location 7 during spring tide in dry season.
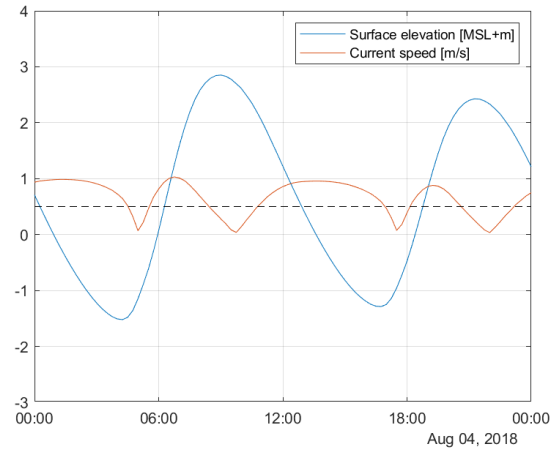
Figure 5.30: Water level and current velocities at location 7 during spring tide in monsoon season.

During spring tide in dry season the acceleration during HW is less than during LW. In the monsoon season the asymmetry increases. The slack time during LW becomes shorter and the slack time during HW becomes longer. During neap tides the difference between the acceleration rate during HW and LW is less, indicating that the acceleration asymmetry decreases when the tidal range decreases.

It is chosen to consider the most extreme conditions so it can be demonstrated between which extremes the hydraulic conditions are varying. Because Monkey Point Channel is located at the head of the estuary, it is chosen to show the results for location 3. Based on the observations by Nelson (2000) it is assumed that the fine sediment is able to settle when the flow velocities are below 0.5 m/s. Therefor the black dashed line is plotted in the figures to define the time when fines are able to settle.
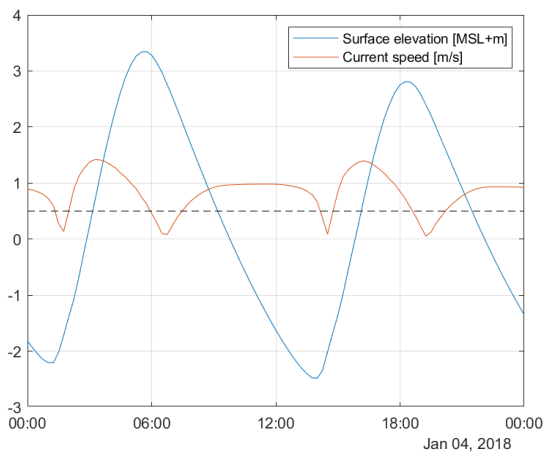
Figure 5.31: Water level and current velocities at location 3 during spring tide in dry season.
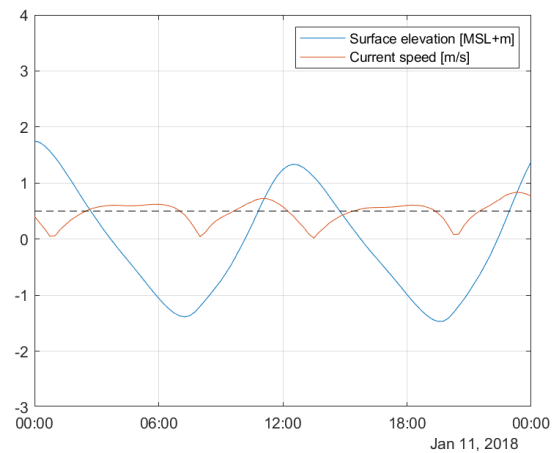
Figure 5.32: Water level and current velocities at location 3 during neap tide in dry season.

From Figure 5.31 it can be seen that the acceleration at HW is much lower than during LW. The black dashed line shows that the fines have twice as much time to settle during HW than during LW. During neap tide the difference in acceleration asymmetry decreases since slack duration during HW and LW are more equal. During spring tide in monsoon season the acceleration asymmetry increases and HW slack takes about twice as long as LW slack. At location 8 at the mouth of the estuary the acceleration asymmetry is less compared to location 3.

5.3.3 Hydrodynamics at the confluence

From the literature study for the conceptual model, the expectation rose that in the stagnation zone for ebb conditions and the stow zone for flood conditions the flow velocities will be low. This expectation is checked by using the hydrodynamic model to calculate the flow velocities at the estuary head in a 2D flow field for different moments in time. In the previous section it became clear that the highest flow velocities occur during spring flood. Hence the flow conditions at the estuary head during spring flood are considered first (see Figure 5.33).
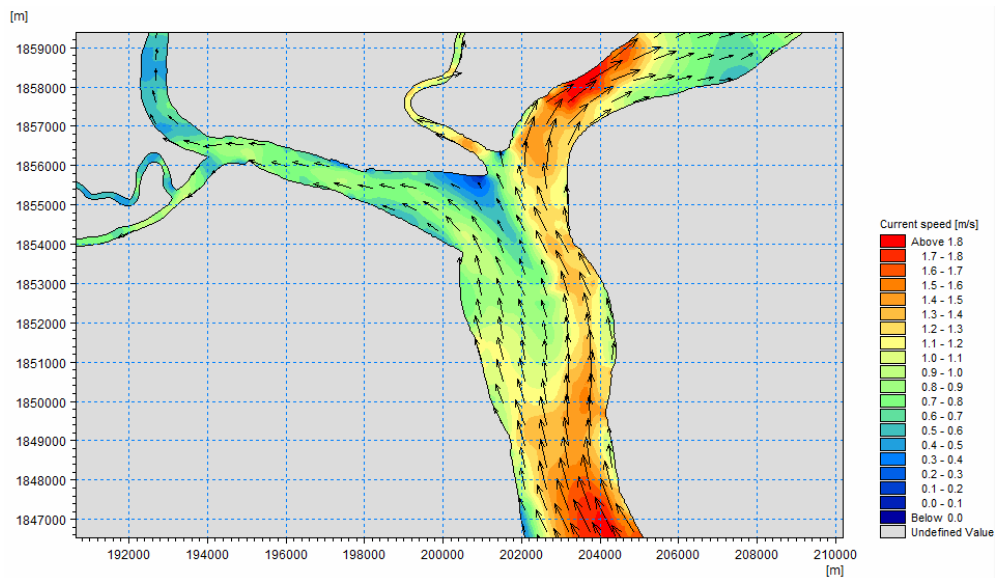
Figure 5.33: Current speed during spring flood in dry season

In the figure it can be clearly seen that however the current velocities exceed 1.5 m/s in the channel, the flow velocities in the stow zone are below 0.5 m/s. Considering the situation during neap tide (see Figure 5.34), the current speed drops even more. Though the current speeds are lower around the whole estuary head, the shape of the stow-zone stays the same.
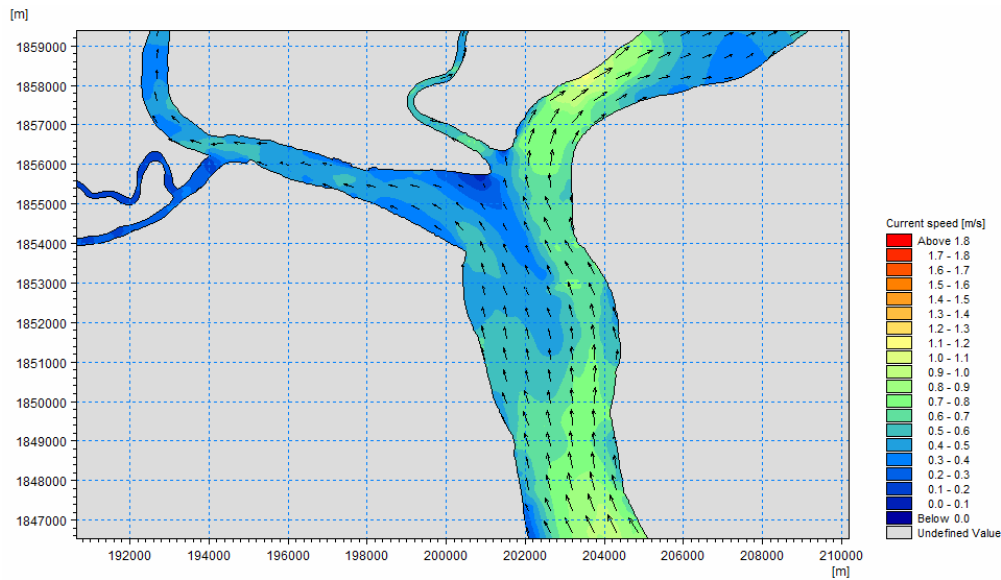
Figure 5.34: Current speed during neap flood in dry season

Considering the flow conditions during ebb (see Figure 5.35), the stagnation zone is clearly visible. While the current speeds in the estuary channels are around 1 m/s, the flow velocities in the stagnation zone are below 0.5 m/s.
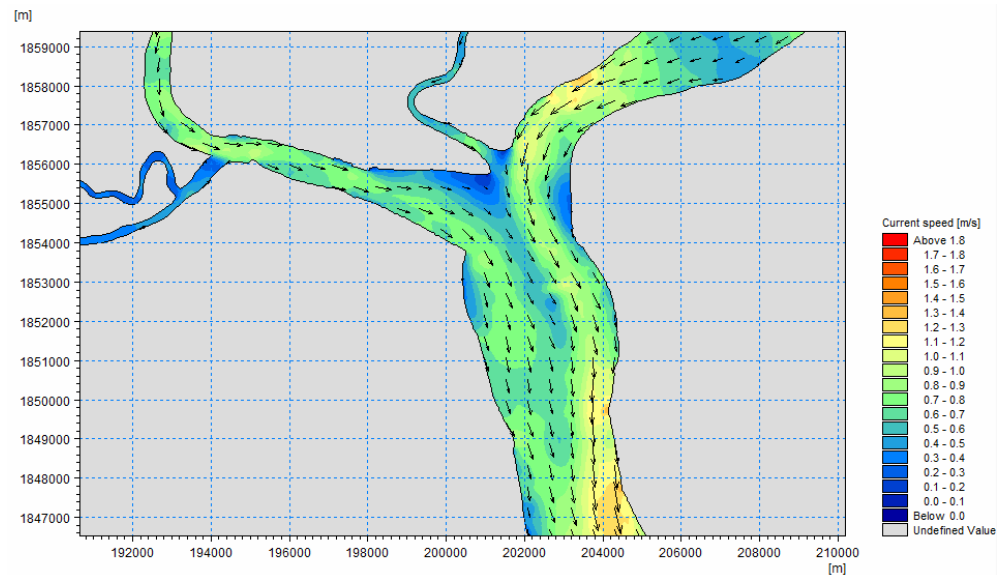
Figure 5.35: Current speed during spring ebb in monsoon season

From these figures it can be confirmed that the hydrodynamic conditions in the stagnation-zone and the drive-up-zone are very mild with very low flow velocities. Due to these low flow velocities, the presumption rises that sediment is easy deposited in this area. To check the possibility of sediments to be deposited in Monkey Point Channel, the bed shear stresses are analysed in the next chapter.

6 Sediment model

With the MIKE sediment model, one is able to calculate the transport of sand and the bed shear stresses in the estuary. Based on the previous two stages of the conceptual model, the following is investigated:

- The morphologic development of the Inner Bar
- The distribution of sand in the estuary
- Bed shear stress in the channels and on the shoals
- Bed shear stress in Monkey Point Channel

6.1 Estuary morphologic development

From the hydrodynamic model results it became clear that the channel formation in the estuary has a lot of influence on the discharge distribution over the split at the estuary head. The sediment model is used to do research to the cause of the current bathymetry. Because mud does not have an angle of internal friction, it is assumed that the development of channels within the estuary is caused by transport of sand. It is assumed that the sand-module is appropriate to give more insight in channel formation. Based on the current bathymetry and the discharge distribution between the Yangon River and the Bago River, it is hypothesised that sand originating from the Hlaing River deposits in front of the Yangon River mouth where the flow cross-section increases due to widening of the river. As a result, the deposited sediment provides resistance to the flood current in the direction of the Yangon River. Keeping in mind that water will always flow through the path with the least resistance, the dominant part of the tidal discharge will flow into the Bago River. Consequently, the larger discharge towards the Yangon will cause for erosion and hence to formation of the channel on the east bank of the estuary head.

In order to investigate this hypothesis, research is done to the morphological response of the estuary when the initial bathymetry consist of a uniform bed. The model domain that is used origins from the available model by RHDHV (RHDHV, 2016). The initial depth of the uniform bed is 8 m below MSL. The bed material is defined as sand with a median grainsize of 0.3 mm, based on the findings by JICA (JICA, 2014). The roughness across the estuary is set to a uniform value in the estuary of 45 m^(1/3)/s which represents a sandy bed. The seaward hydrodynamic boundary condition consist of the same tidal signal as used in the hydrodynamic model of chapter 3, the hydrodynamic boundary conditions for the rivers consist of defined discharge timeseries. These timeseries are based on the Sobek results. Both hydrodynamic boundary conditions consist of a timeseries of 1 year. The boundary conditions are rough estimations but suitable in order to find out what the major effect of a monsoon discharge is on the morphology of the estuary. Because the channel formation is considered as a long-term process, morfac is used. Morfac is a function of MIKE which multiplies the morphologic response per hydrodynamic time step with a user set factor and is reliable when calculating sand transport (MIKE, 2017). The morfac parameter is set to 10 in order to simulate the morphologic response of 10 years. Furthermore, the model is run online to include the morphologic response on the hydrodynamic conditions.
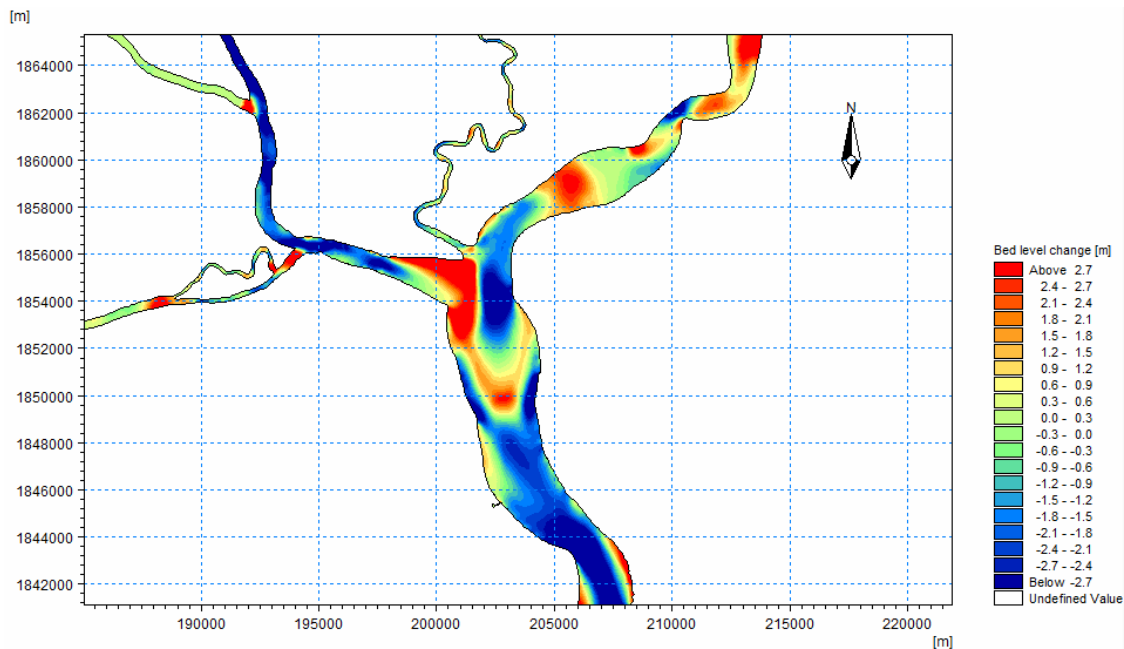
Figure 6.1: Morphologic response after ten years

The model result is presented by Figure 6.1. From the figure a couple of similarities to the current situation can be noticed. First, the model result shows that between the Yangon River and the Bago River a bank is formed. Furthermore, the channel formation on both the eastern bank and the western bank can be noticed. In the current situation also a channel is visible which follows the eastern bank but this channel is shorter. It is expected that due to the depositions in front of the Yangon River mouth, there will be more resistance to the flow in the channel on the western bank than in the channel on the western bank causing for more discharge through the eastern bank channel and less through the channel along the western bank. As a result the channel on the eastern bank will become deeper while the channel on the western bank will become shallower.

6.2 Morphological response of sand

It is expected that sand transport mainly occurs in the deeper channels, since the sand is transported as bed load (see 4.3.1). In this section the model is used to determine if the transport of sand, indicated by erosion and deposition, only occurs in the channels. The sand transport module of MIKE is used to calculate the bed level change to indicate the areas of erosion and deposition within the estuary. It is chosen to do two runs with the model; one in January to represent dry season conditions and one in August to represent monsoon season conditions. The median grainsize is set on 0.3 mm. Sand enters the model from the boundaries. The boundary conditions for sand are defined as "equilibrium conditions" for which the model calculates the equilibrium amount of sand transport for a certain flow at the boundary. The hydrodynamic boundary conditions are equal to those that have been used in chapter 5.

The model results show mainly erosion and deposition of sand in the estuary channel. There is no clear location which shows only deposition or erosion. During the monsoon there is more deposition.
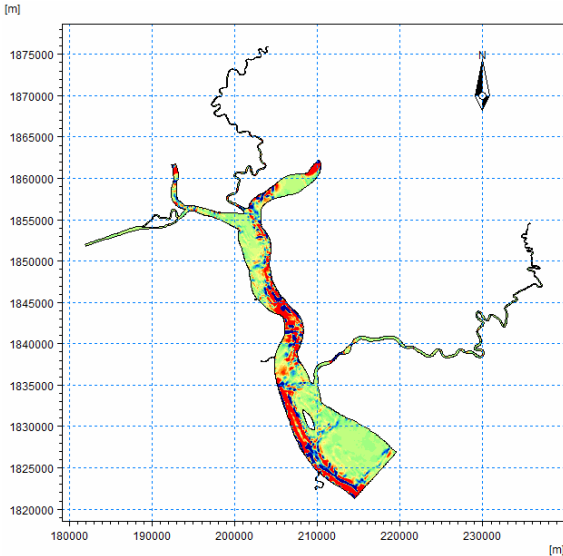
Figure 6.2: Morphological response of sand in Yangon Estuary after one month of dry season conditions.
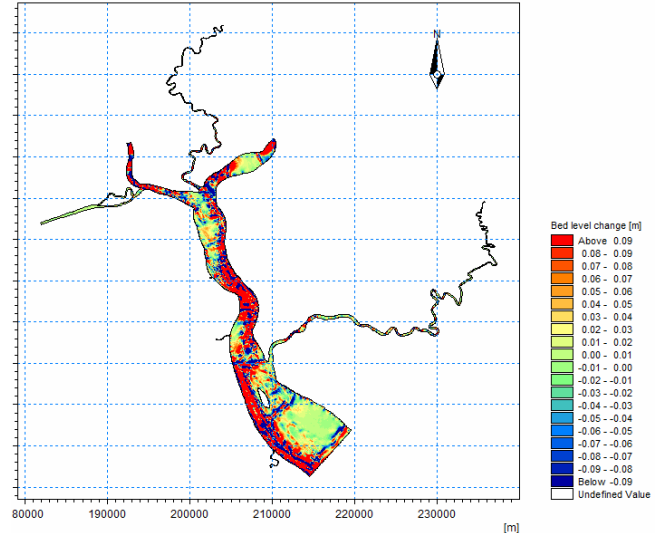
Figure 6.3: Morphological response of sand in Yangon Estuary after one month of monsoon season conditions.

6.3 Bed shear stress

Because the model is not appropriate to calculate the transport of mud, the bed shear stress is used to define potential location for mud deposits. The critical bed shear stresses for the erosion of a mud layer are defined in Table X. The goal of the model is to define the locations at which mud deposits are able to consolidate. Because the goal is to define an area, the model results are shown in a top view. Attention is payed to monsoon season and dry season variations in bed shear stress and to spring/neap variations in bed shear stress. Just like in Chapter **Error! Reference source not found.**, the model is run for the month January to represent dry season conditions and run for the month August to represent monsoon season conditions. The same boundary conditions are used as in Chapter 5. In the MIKE software, bed shear stresses can only be set as output when using the sediment model. However, this model run is only used to determine the bed shear stresses in the estuary, so the sediment transport functions are turned off.
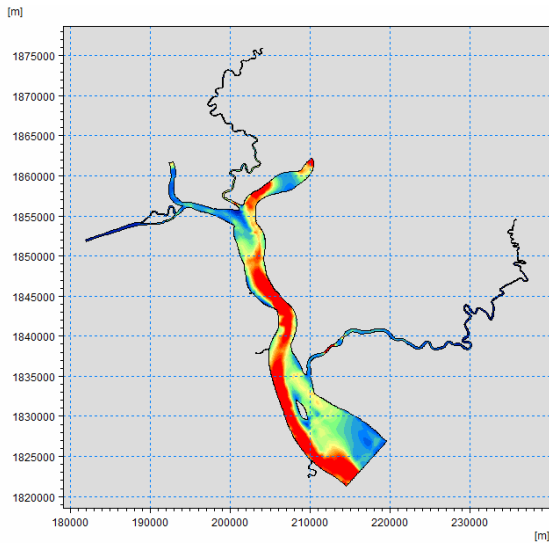
Figure 6.4: Maximum bed shear stress during spring flood in dry season
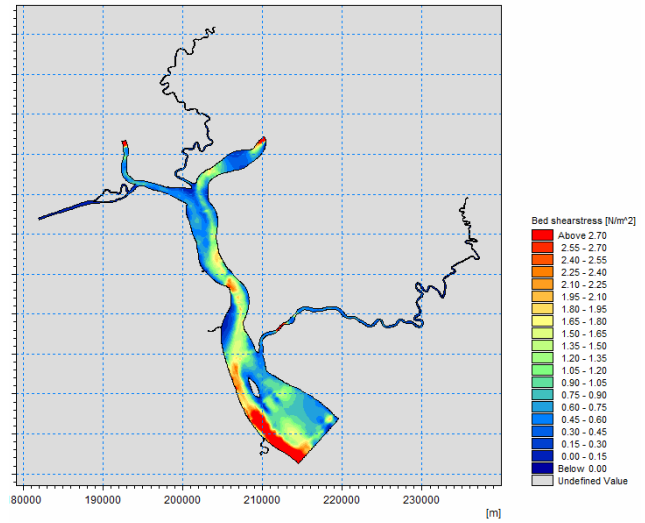
Figure 6.5: Maximum bed shear stress during spring ebb in dry season
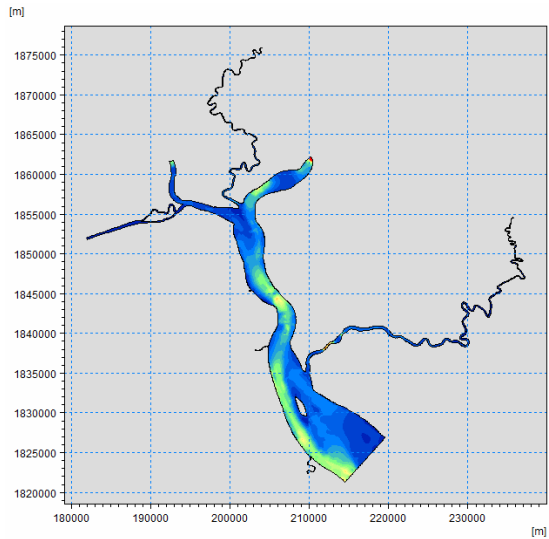
Figure 6.6: Maximum bed shear stress during neap flood in dry season
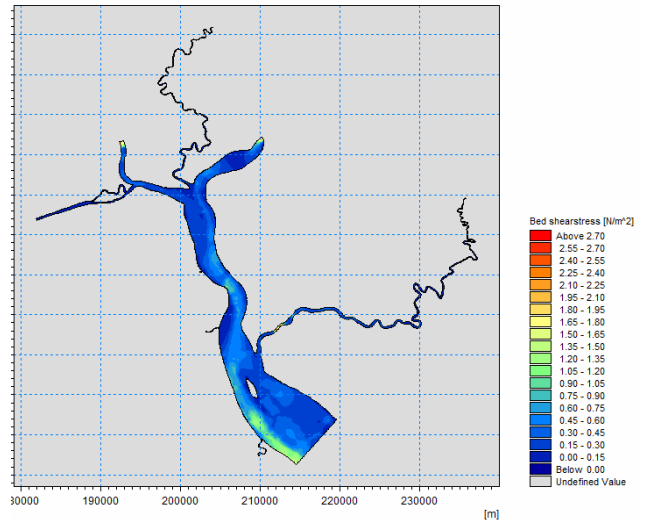
Figure 6.7: Maximum bed shear stress during neap ebb in dry season

In Figure 6.4 to Figure 6.7 the spring/neap and flood/ebb variation in maximum bed shear stress is presented for dry season conditions. The bed shear stress is higher during flood than during ebb, both for spring and neap tidal events. Furthermore, the bed shear stresses are clearly higher in the estuary channel than on the shoals. During neap tides, the bed shear stress outside the channels can drop below 0.3 N/m2.
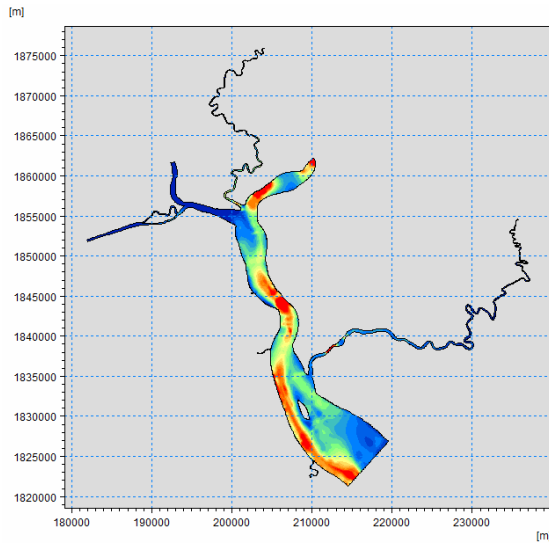
Figure 6.8: Maximum bed shear stress during spring flood in monsoon season
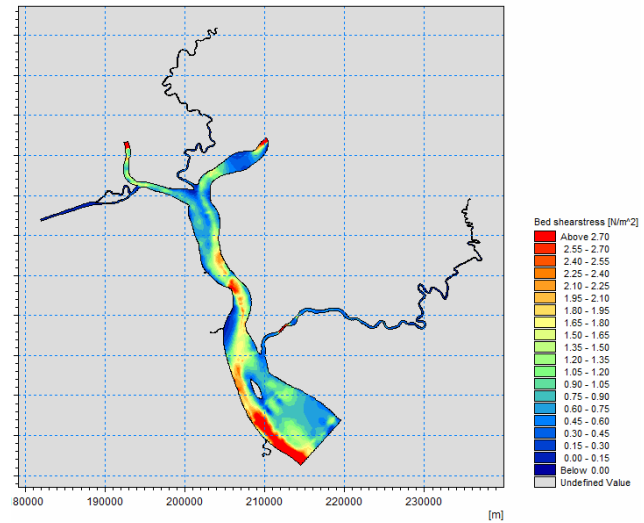
Figure 6.9: Maximum bed shear stress during spring ebb in monsoon season
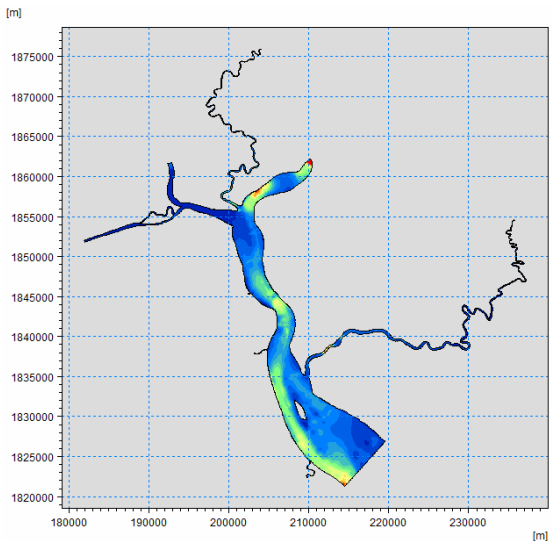
Figure 6.10: Maximum bed shear stress during neap flood in monsoon season
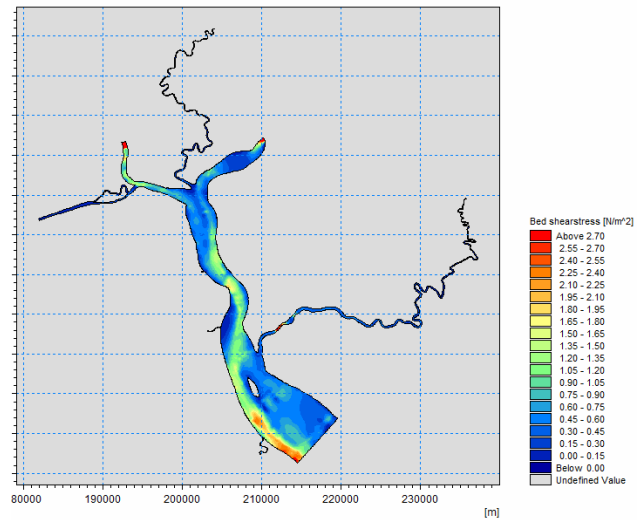
Figure 6.11: Maximum bed shear stress during neap ebb in monsoon season

During monsoon (Figure 6.8 to Figure 6.11) the flood is less dominant and comparable bed shear stresses are found during ebb. During neap tides the bed shear stress is even larger during ebb than during flood. Nevertheless the maximum bed shear stresses still occur during flood, indicating the flood dominant character of the system.

For both dry season as monsoon conditions, the bed shear stresses are highest in the channel. Based on these model results one would not expect mud layers in the channel since the bed shear stresses exceed 0.7 N/m2 which is indicated as the critical bed shear stress for a month consolidated mud. During neap tides the bed shear stress exceeds 0.3 N/m2, the critical bed shear stress for a week consolidated mud layer. Since the bed shear stresses are much lower outside the channel around the estuary mouth and the estuary head, these locations are potential areas for fluid mud depositions. Nelson (2000), reported the presence of fluid mud layers which become mobile during spring tide events due to high bed shear stresses but consolidate during

63

neap tide when the shear stresses are insufficiently strong to mobile the mud layer. Such scenario is possible for the shoal at the estuary mouth and the shoal at the estuary head.

In order to see the variation of the bed shear stress on the shoals, Figure 6.12 Figure 6.13 are generated.
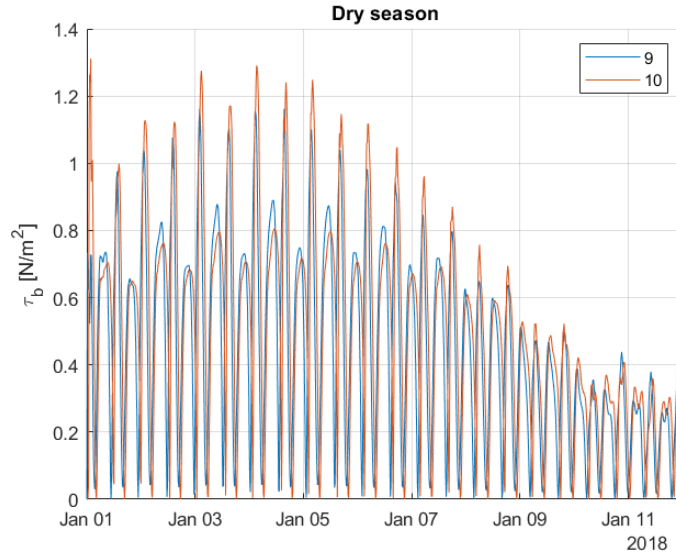
Figure 6.12: Bed shear stress on the northern shoal (9) and southern shoal (10) during the dry season. The maximum shear stress occur during spring tide and the minimum shear stresses occur during neap tide.
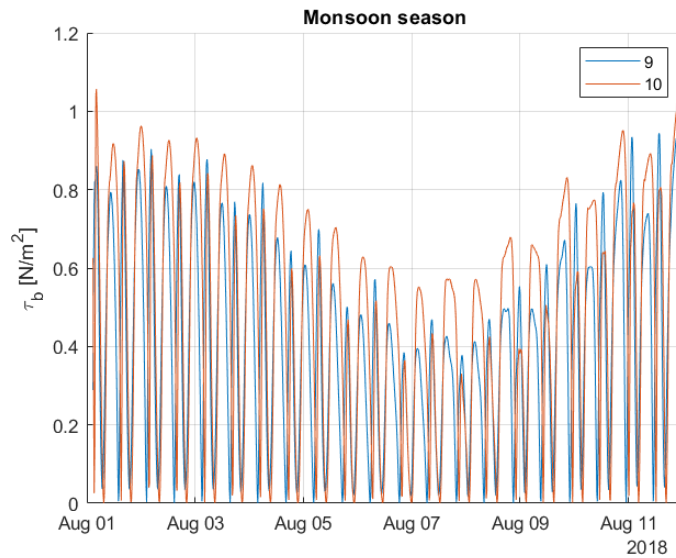
Figure 6.13: Bed shear stress on the northern shoal (9) and southern shoal (10) during the monsoon season. The maximum shear stress occur during spring tide and the minimum shear stresses occur during neap tide.

From these figures it can be noticed that the maximum bed shear stress is higher during dry season.

At the stagnation-zone and stow-zone, the bed shear stress is, just like the current speed, permanently low. In order to get a more accurate results for Monkey Point Channel, output locations have been defined to generate time-series for the bed shear stress in Monkey Point Channel (see Figure 6.14).
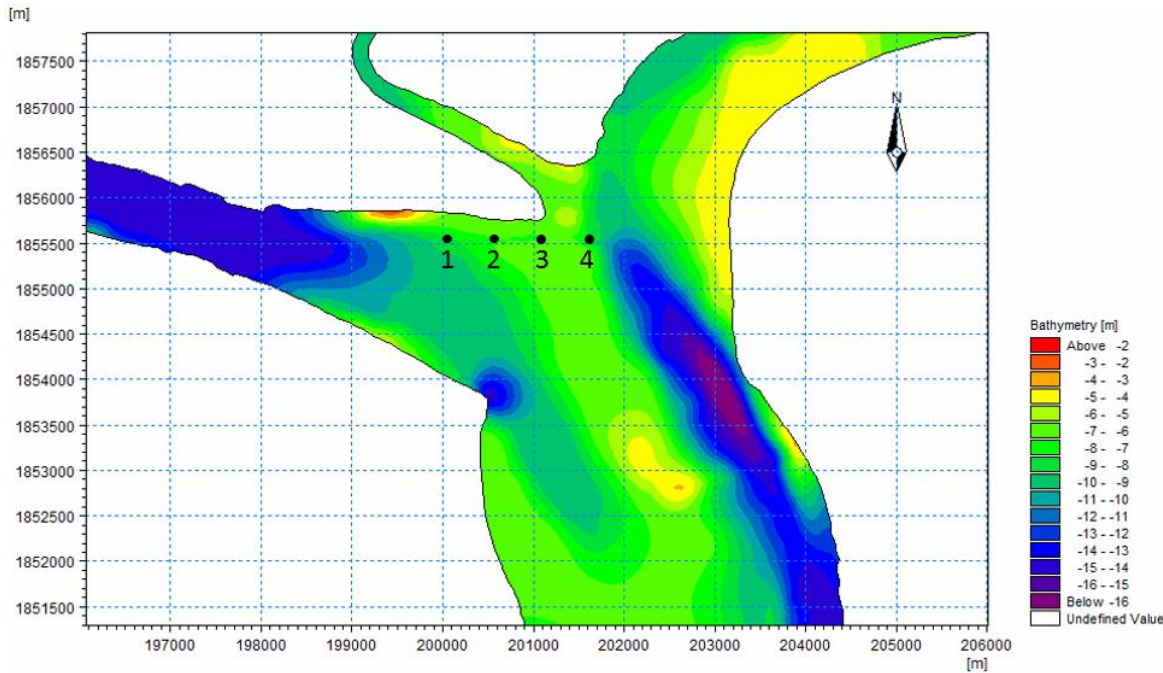
Figure 6.14: Output locations for current velocity and bed shear stress in Monkey Point Channel.
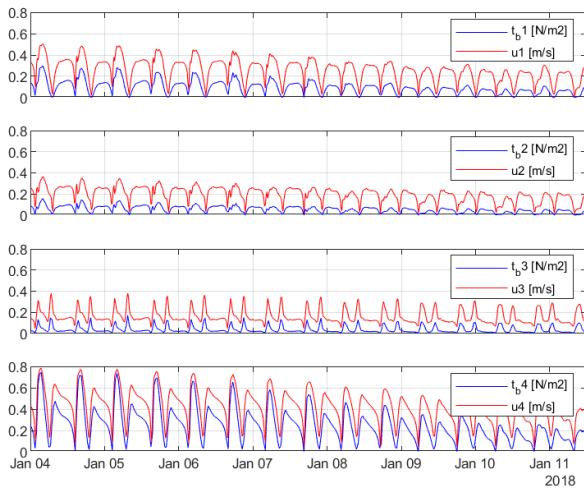
Figure 6.15: Bed shear stress and current velocity in locations 1,2,3 and 4 during spring and neap tide in dry season
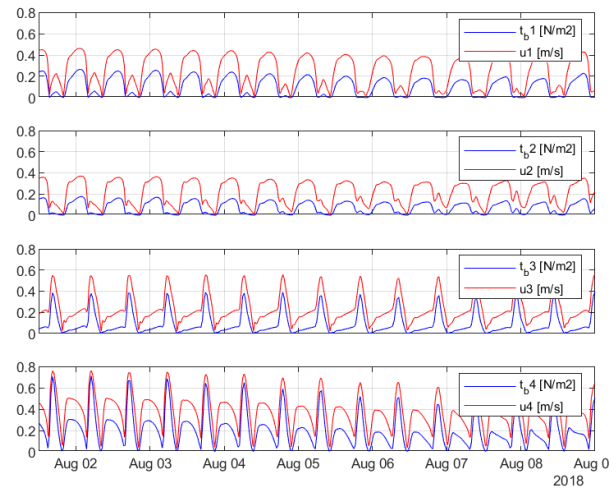
Figure 6.16: Bed shear stress and current velocity in locations 1,2,3 and 4 during spring and neap tide in monsoon season

Figure 6.15 and Figure 6.16 show that during both dry season and monsoon season, the bed shear stresses in the middle of MPC are below 0.2 N/m2, even during spring tide (4th of January and 2nd of August). At location 3 in dry season, two peaks in the flow velocity can be noticed. This caused by the time-lag between the Yangon River and the Bago River (see Appendix). Furthermore, in monsoon season the influence of the ebb dominant Yangon discharge and the flood dominant Bago discharge can be noticed. During flood the bed shear stresses in 3 and 4 (Bago side) increase while at locations 1 and 2 (Yangon side) the bed shear stress decreases. During ebb it is the other way around; bed shear stresses at location 1 and 2 increase while at locations 3 and 4 the bed shear stress is lower than during flood. In both situations this leads to bed shear stresses below the critical bed shear stress for fresh deposit mud (see Chapter 2).

7 Conceptual model stage 3

In the third stage of the conceptual model, attention is payed to the fine sediment dynamics. From the Rouse profiles and numerical model it can be concluded that the transport of sand is mainly limited to the channels. Hence the contribution to the sedimentation in Monkey Point Channel is expected to be small which corresponds to the found sediment in Monkey Point Channel which mainly consist of fine material. Therefore, the sand transport is not further discussed in this section.

The SSC values show two important variations: spring/neap variation and seasonal variation. The reason for these variations to occur has been investigated and is answered by means of the following conceptual diagrams of the SSC in Yangon Estuary.
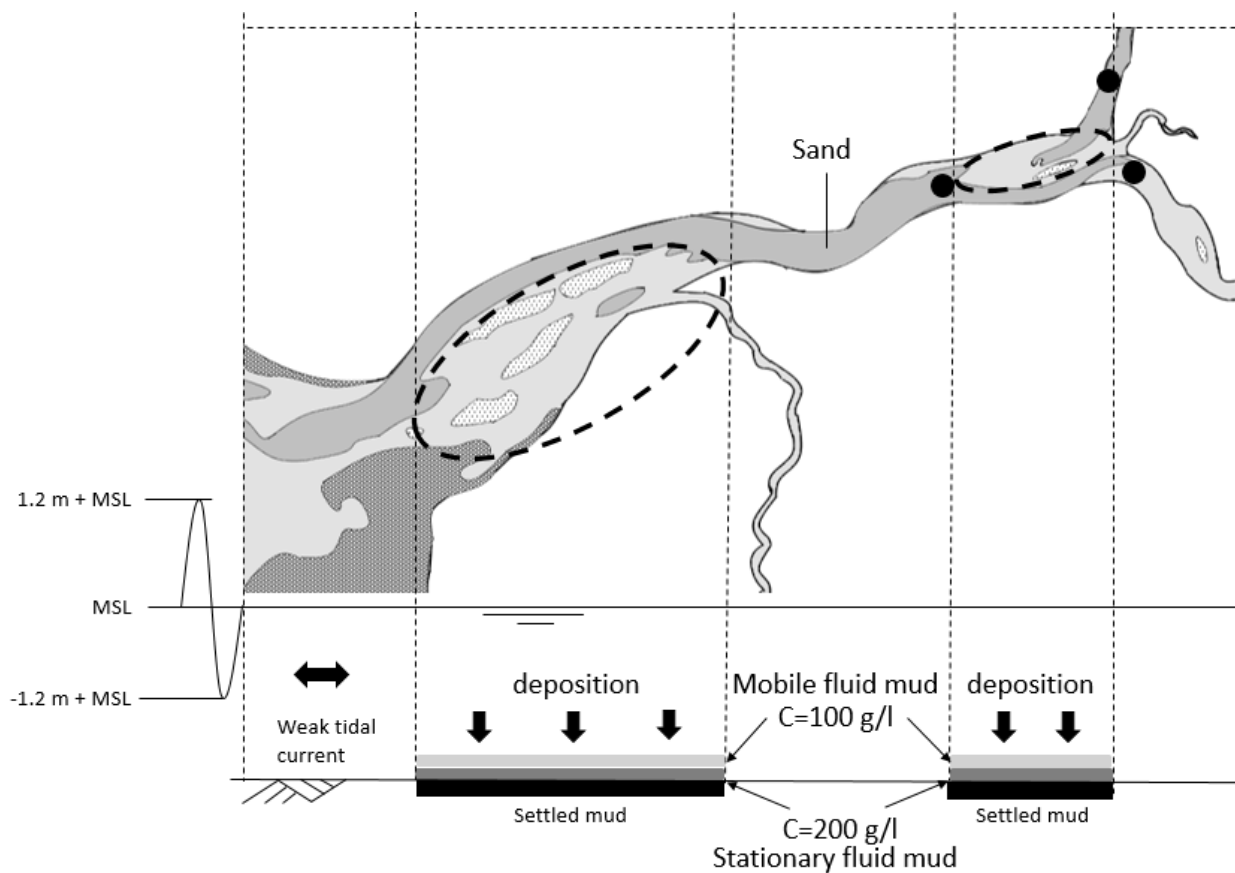
Figure 7.1: Conceptual diagram for the SSC during neap tidal conditions for both the dry season and monsoon season

During neap tide, both in the dry season and the monsoon season, mud is able to deposit on the shoals during slack tide (see Figure 7.1). During slack tide the settled mud strengthens causing for a higher critical bed shear stress for erosion. Hence, the mud is able to stay on the bed when the slack tide is over. During the following peak velocity of the neap tide, not all the mud is resuspended enabling the mobile suspension to settle more and become a stationary fluid mud layer. At the same time, stationary mud layers get more concentrated and become settled mud with a critical erosion shear stress above 1.0 N/m^2.

$\tau_b > 1.0 \; N/m^2$, erosion of stationary fluid mud layer
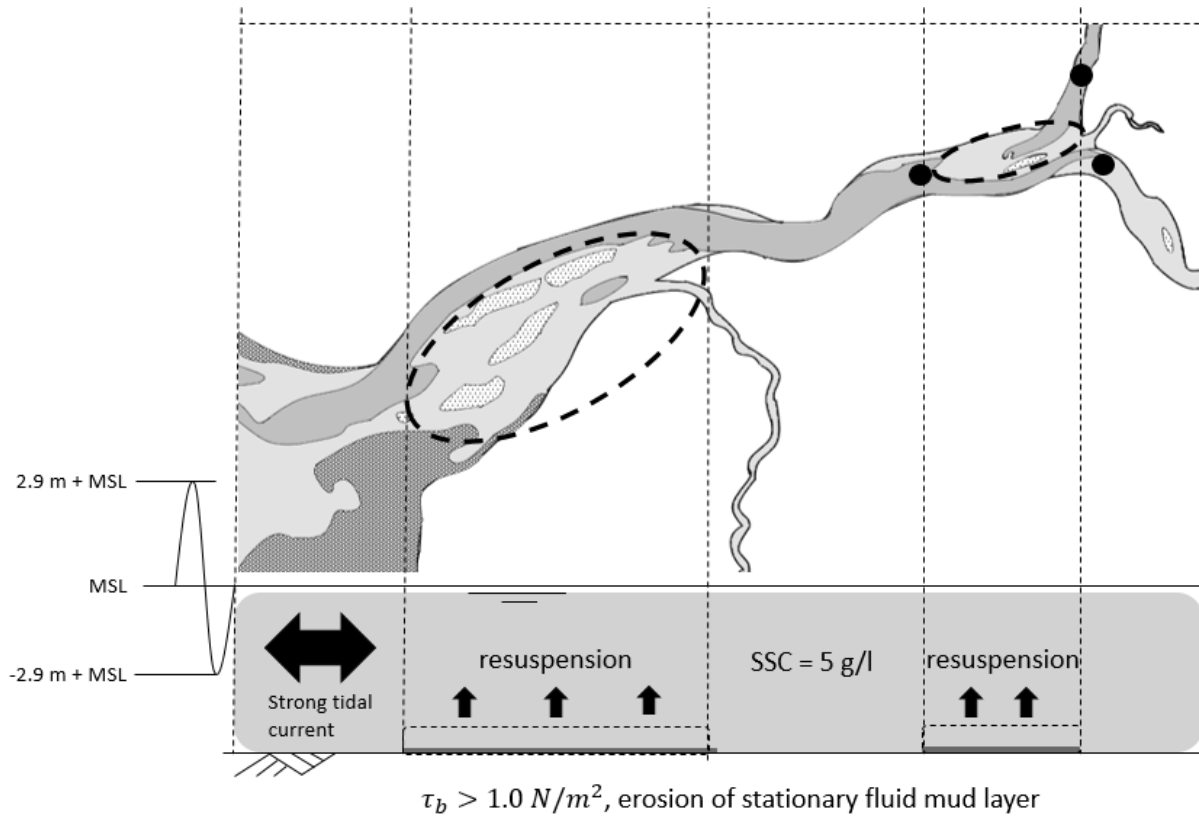
Figure 7.2: Conceptual diagram for the SSC during spring tidal conditions in the dry season

During spring tide in the dry season the flow velocities in the estuary are maximum causing for bed shear stresses up to 1.2 N/m² on the shoals. This bed shear stress causes for the erosion of the mobile fluid mud layer and the stationary fluid mud layer. Due to the erosion the SSC in the estuary reaches values above 5 g/l.

During spring tide in the monsoon season (see Figure 7.3), the maximum flow velocities are less because the river discharge is hindering the tidal flood current from propagating into the estuary. Hence the maximum bed shear stresses are lower too (τ_b<1N/m^2). Consequently, the flow over the shoals is insufficient to erode the stationary fluid mud layers. Therefore, the SSC values are lower during the monsoon season than during the dry season.

Because the average concentration during the monsoon is 1 g/l and the average SSC in dry season is 4 g/l (see 2.2.2), a lot of sediment is available for the sedimentation in Monkey Point Channel. Because the model results show that the bed shear stresses are very low in Monkey Point Channel, much of this sediment will also deposit. In order to check if this hypothesis is right the following test calculation is done:

Based on the measurements by Nelson (2000), the averaged concentration (c) during the year is 1.8 g/l. The settling velocity (w_s) is estimated to be 0.5 mm/s which represents settling flocs (Van Maren, 2015). Based on the calculated bed-shear stresses and the critical bed shear stress for erosion, the sedimentation rate (r) is assumed to be 0.5 (0 = no deposition, 1 = full deposition). After deposition the critical bed-shear stress for erosion increases due to concentration during the hindered settling to 0.3 N/m^2 after 1 h. Based on the calculated bed-shear stresses, erosion does not occur. Because the bed shear stresses at the ends of the channel are quite high less sedimentation is expected at these locations. The area (A) of siltation is estimated to be 1500x100 m. During the year the deposited sediment is expected to consolidate to a concentration (c_{cons}) of 1300 kg/m^3. The amount of sedimentation is calculated with the following formula.

$$V = \frac{c * w_s * r * t * A}{c_{cons}} = 1.8 \; million \; m^3$$

This calculation corresponds to the annual dredging volumes of the local dredging companies. Hence, the hypothesis is supported by this calculation.

8 Mitigation of sedimentation

In this chapter two measures are considered which have to mitigate the sedimentation in the navigation channel. First, the effect of changing the dimensions Monkey Point Channel is investigated. Next, relocation of the navigation channel is considered.

8.1 Adjusting the channel dimensions of Monkey Point Channel

The model results have shown that the bed shear stresses in Monkey Point Channel are too low to prevent deposition and consolidation of fine sediments which eventually results in a reduction of the water depth. It is hypothesised that increasing the channel dimensions of Monkey Point Channel will result in stronger flows through the channel and consequently higher bed shear stresses that prevent consolidation of mud. When the mud is not able to consolidate, the critical bed shear stress for entrainment of the mud layer remains low and the layer will stay mobile. In order to check this hypothesis, the effect of channel deepening and a combination is considered. The effect of the measures is compared to the default scenario without measures.

8.1.1 Deepening

In default scenario the depth of Monkey Point Channel is MSL -7 m and the channel has a width of 100 m and a length of 1500 m. In the last tender of the Myanma Port Authority a desired minimum depth of -5.5 m + C.D. is reported which with a water depth of -8.5 m + MSL. When the waterway is friction dominated, a larger water depth can result in more discharge through the waterway which might result in an increase in bed shear stress (Blom, 2016). Because previous dredging works turned out to be ineffective the water depth in Monkey Point Channel is increased to -10 m + MSL in order to investigate if this results in higher bed shear stresses in Monkey Point Channel. The width is kept at 100 m and the length is increased to 2000 m in order to connect to the natural channel of the Yangon River.
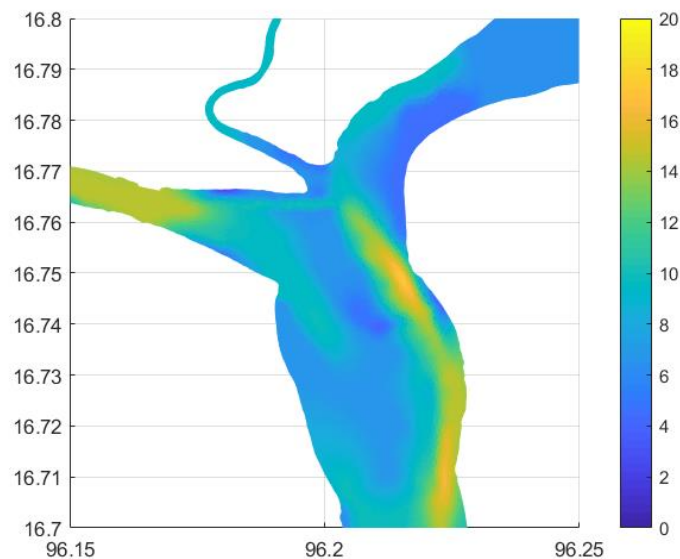
Figure 8.1: Bathymetry after deepening of Monkey Point Channel in m below MSL
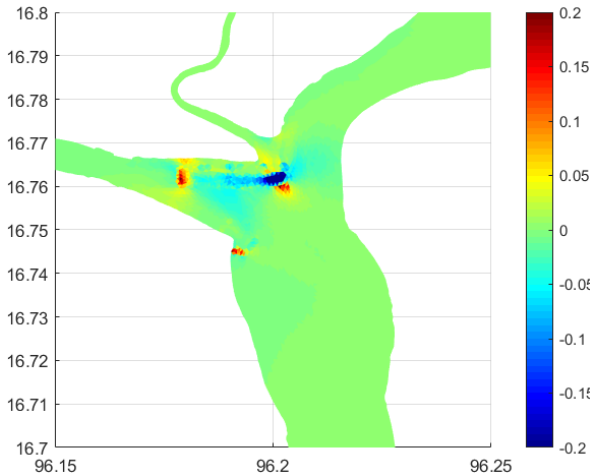
Figure 8.2: Change in bed shear stress [N/m2] after changing the channel dimensions for spring flood condition
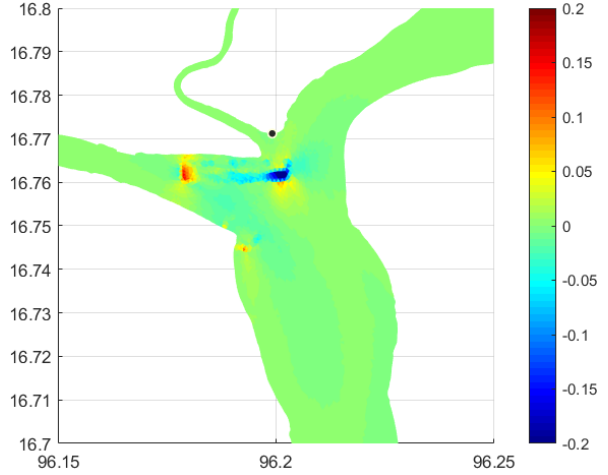
Figure 8.3: Change in bed shear stress [N/m2] after changing the channel dimensions for spring ebb condition

With the model bed shear stresses are computed for the situation with the deepened channel. By subtracting these bed shear stresses with the bed shear stresses of the default situation, the effect of the channel deepening is calculated. Figure 8.2 and Figure 8.3 show that for extreme conditions (maximum flow velocity during spring tide) the bed shear stress in the channel decreases. Based on this result it can be concluded that deepening of the channel results in lower bed shear stresses and the hypothesis does not hold.

8.1.2 Combination of widening and deepening

The effect of deepening turned out to be low. A clarification for this could be the dominance by the Yangon River channel which attracts much more discharge. Hence the flow through Monkey Point channel To check if the widening and deepening of Monkey Point Channel is useful at all, the dimensions of the channel are enlarged to the dimensions of the Yangon River channel. The dredged material is dumped in the Yangon River Channel in order to create more resistance in this channel and increase the discharge towards the enlarged Monkey Point Channel. The resulting bathymetry is presented by Figure 8.4.
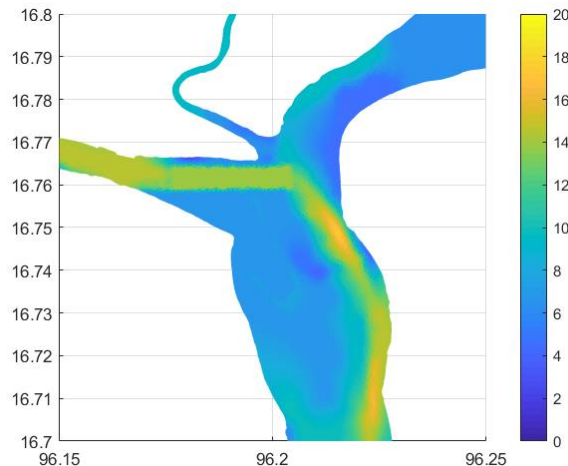
Figure 8.4: Bathymetry after increasing the dimensions of Monkey Point Channel in m below MSL

Figure 8.6 and Figure 8.8 show that the adjustment results in an increase in bed shear stress at the location of Monkey Point Channel. At the formal location of the Yangon channel the bed shear stresses decreased due to the decreased discharge in this area. The bed-shear stresses have mainly increased in the estuary channel on the eastern bank and less in Monkey Point Channel.
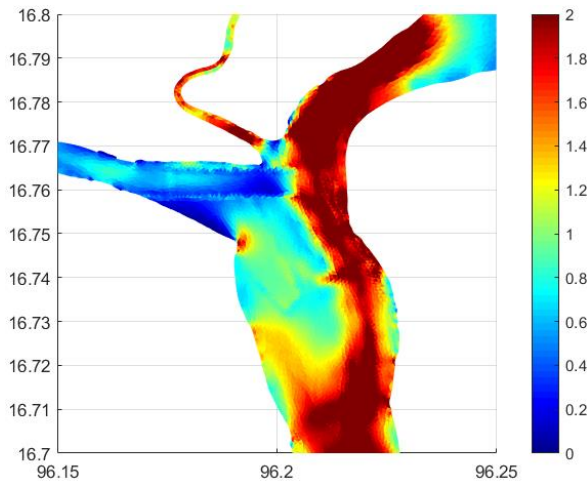
Figure 8.5: Bed shear stress [N/m2] during spring flood
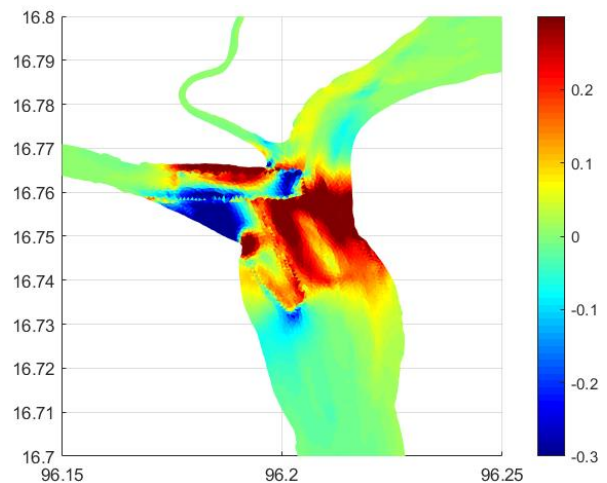
Figure 8.6: Change of bed shear stress [N/m2] after adjustments for spring flood conditions
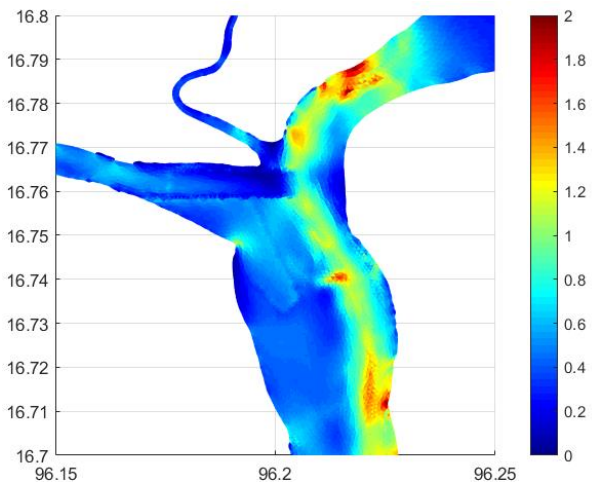
Figure 8.7: Bed shear stress [N/m2] during spring ebb
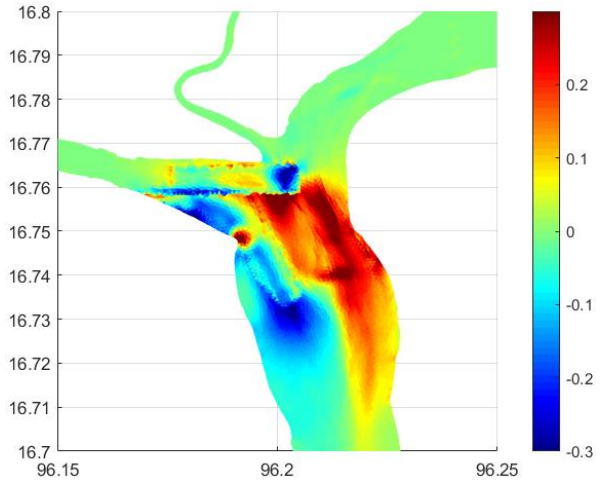
Figure 8.8: Change of bed shear stress [N/m2] after adjustments for spring ebb conditions

In addition, Figure 8.9 and Figure 8.10 show why the bed shear stress did not increase. Despite of the bathymetry changes, the flow at the confluence shows the same pattern as indicated with the red arrow in the figures.
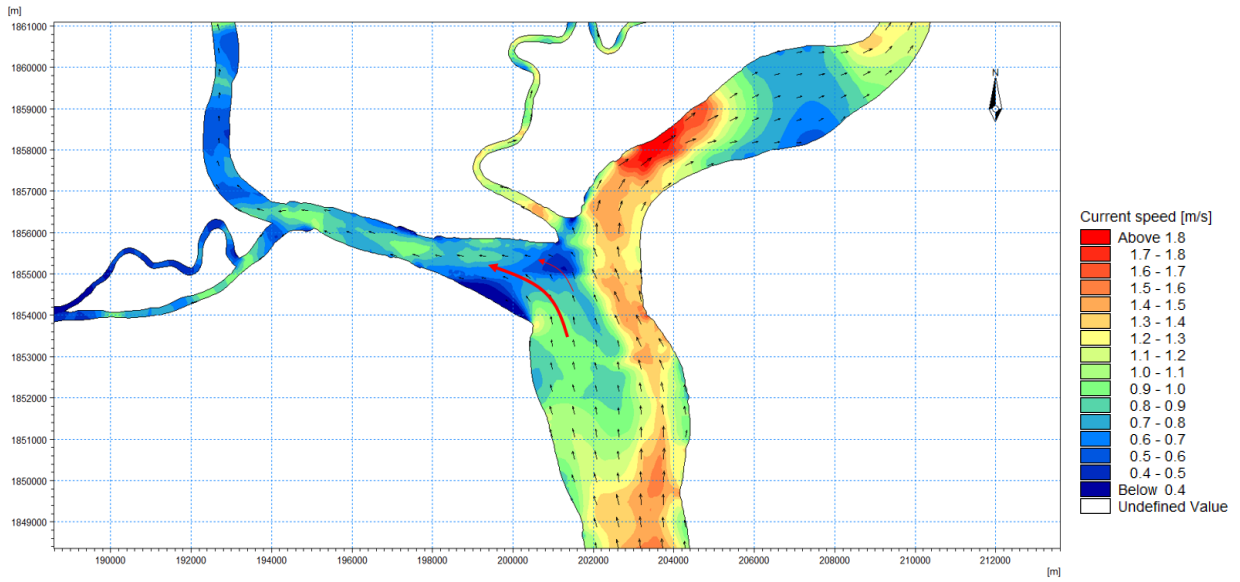
Figure 8.9: Flow velocities with direction during spring tide in dry season. The large red arrow indicates the dominant flow and the smaller red arrow indicates the minor flow.
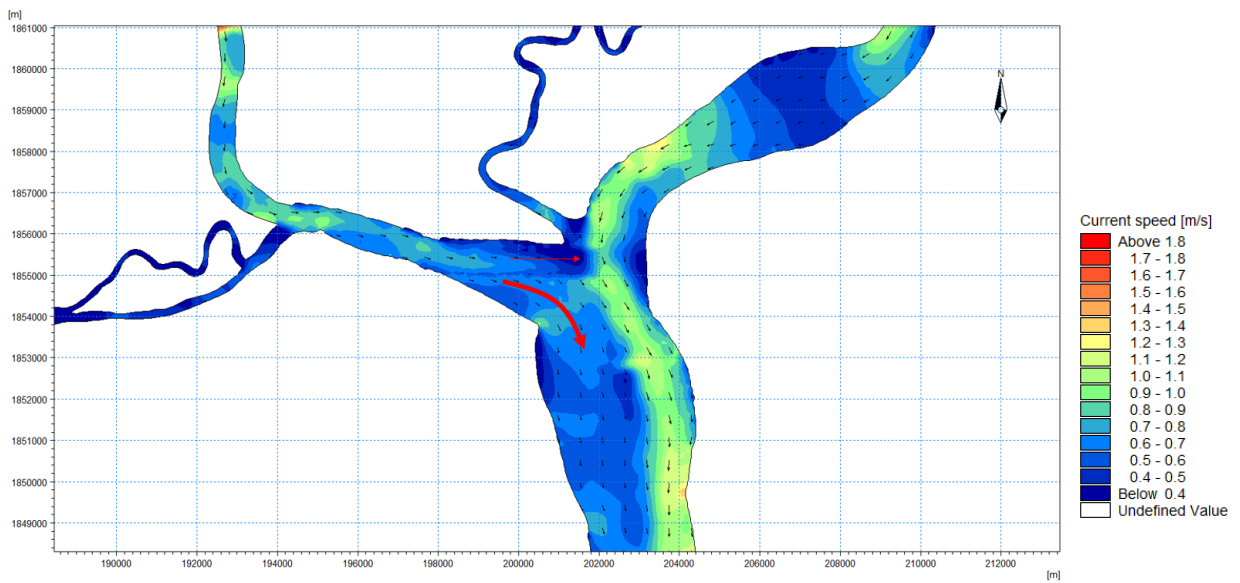
Figure 8.10: Flow velocities with direction during spring ebb in dry season. The large red arrow indicates the dominant flow and the smaller red arrow indicates the minor flow.
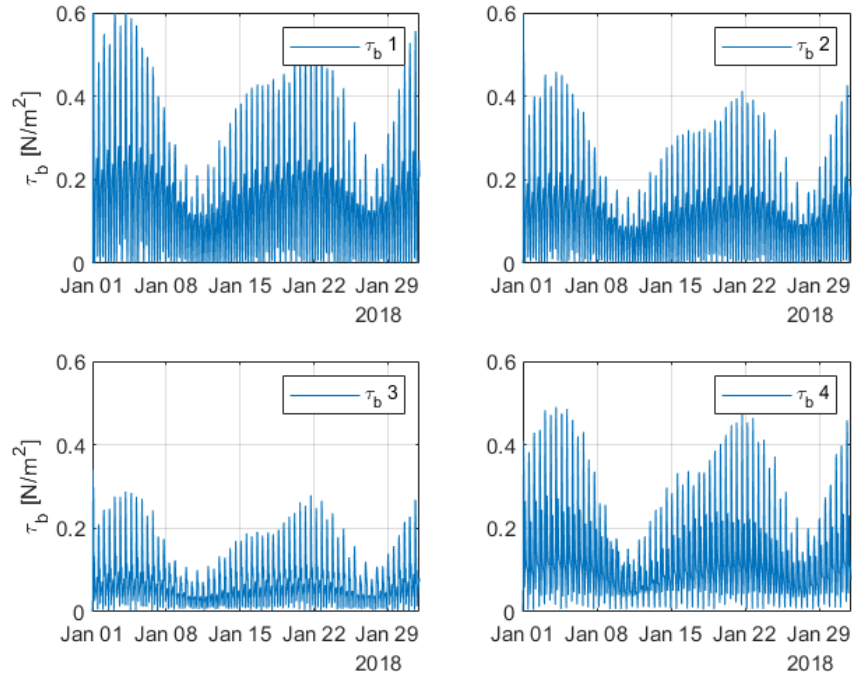
Figure 8.11: Bed shear stresses at point 1, 2, 3 and 4 in the enlarged Monkey Point Channel

Furthermore, Figure 8.11 shows that the bed shear stress has increased compared to Figure 6.15 with peaks exceeding 0.4 N/m^2. These peaks are during the flood. These peaks are sufficient to keep fresh deposited mud in suspension. However, during neap tide, the bed shear stresses drop down below 0.2 N/m^2, enabling fine sediments to deposit and consolidate during a couple of days. As a result, consolidated mud layers will be hard to erode and the risk on a permanent reduction of the water depth rises.

To conclude, the increased dimensions of Monkey Point Channel resulted in a higher discharge through the channel, but the flow velocities remain low. Hence, the bed shear stresses increase, particularly during spring tides, but the moderate neap tide conditions, the probability on mud layer formation rises. In combination with the observation that the 2D flow pattern is dominated by the confluence dynamics, it is decided that this adjustment to the Yangon Estuary is not a good option to improve the waterway towards Yangon Port.

8.2 Relocation of the navigation channel

Because the flow condition related to the confluence/bifurcation system dominant over the impact of bathymetry changes Hence, the relocation of the navigation channel is considered. The new navigation channel will connect the Yangon channel with the estuary channel as presented in Figure 8.12. The natural depth of the channels that need to be connected is 9.5 m below MSL. This will be done by a capital dredging project. But based on the bathymetry analysis, the natural equilibrium depth is insufficient to maintain the new navigation channel and sedimentation is expected when only a channel is dredged. Hence, two options of river training are considered. The goal of these options is to increase the flow in the new dredging channel. Consequently, the increased flow intensity must result in higher bed shear stresses that are sufficient to prevent sedimentation. The two options are first considered individually. The dredged material from the channel deepening will be used for the river training related land reclamation.
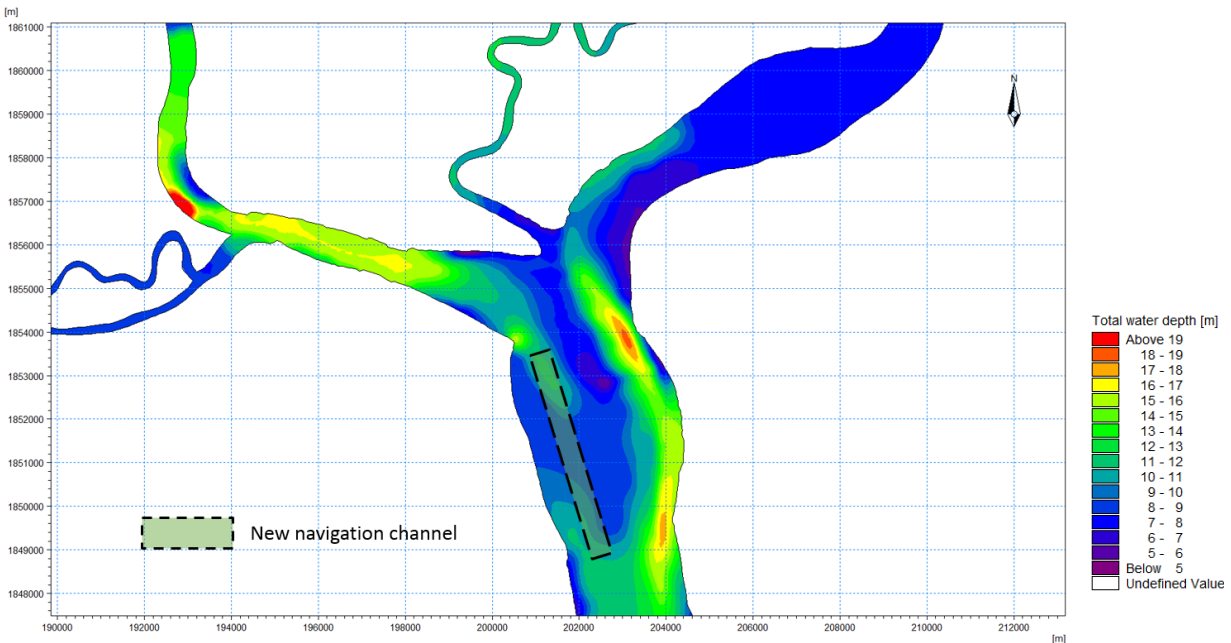
Figure 8.12: Location of the new channel.

Because the river training is expected to change the discharge distribution over the estuary junction, the SOBEK discharge boundaries are not correct anymore. Therefore, it is decided to calculate the hydrodynamic and morphologic response for dry season with the model grid defined by RHDHV (2016). Although the accuracy of the model results are arguable, it is assumed that the model results can give a good indication of the impact of the adaptation to the estuary.

8.2.1 Adjustment to the split

Based on the confluence/bifurcation analysis the flow is expected to lose energy by eddy formation in the stagnation/drive-up zone. To create a more efficient flow around the mouth of the Yangon River, the impact of a land reclamation at the split is analysed. The hypothesis is that the ebb flow from the Yangon River will be more concentrated like a jet and therefore capable of keeping the channel bed at a sufficient depth.
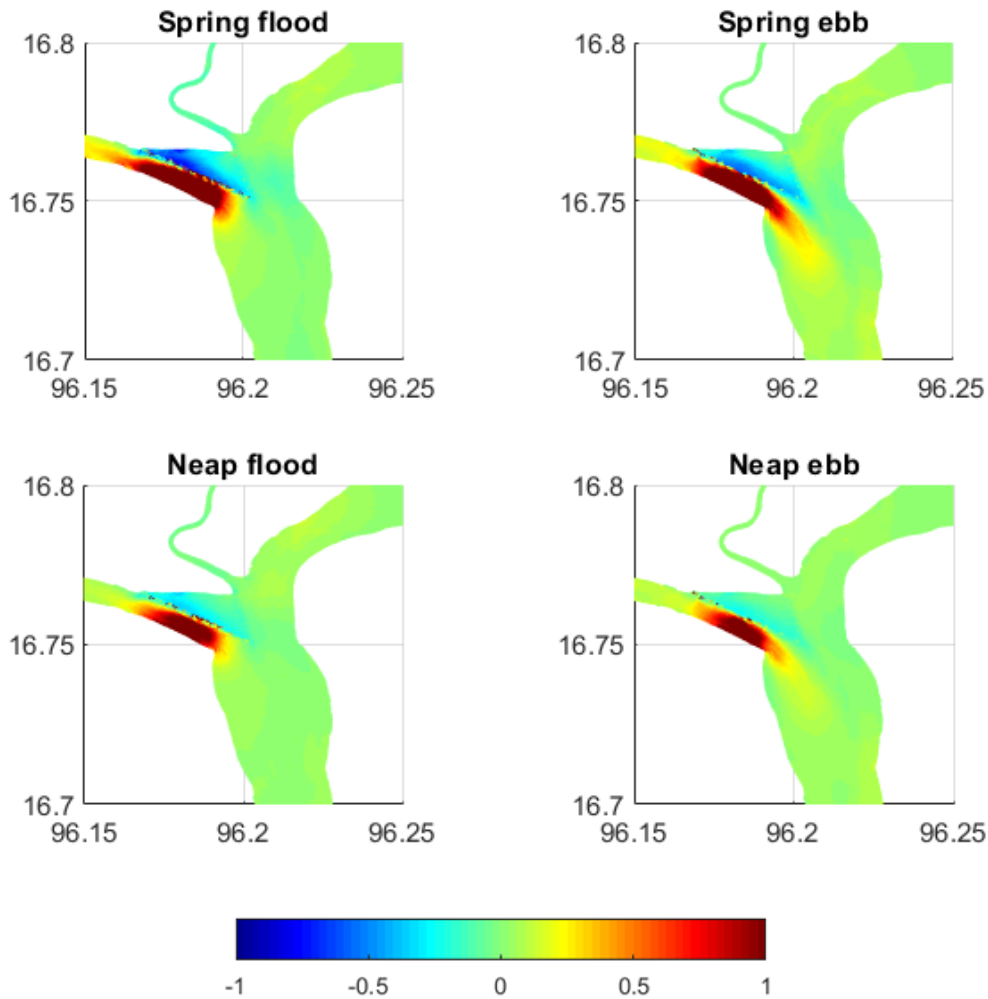
Figure 8.13: Increase in bed shear stress [N/m2] after construction of the adjustment at the split

The results show that the hypothesis is correct and the ebb flow causes for higher bed shear stresses in the channel downstream of the Yangon River mouth. However, it can be noticed that the increased water ebb flow does not reach the estuary channel as presented in Figure 8.13 and the impact of the jet seems not sufficient to maintain a deeper channel.

8.2.2 Adjustment to the western estuary bank

In this section the impact of land reclamation at the western bank is investigated. It is hypothesised that the land reclamation will cause for more efficient flow based on the two following arguments. First, the ebb flow loses energy due to eddy formation in the flow separation zone that was detected in **Error! Reference source not found.**. Secondly, the curve in the western bank seems unnecessary in relation to the flow and by changing the bank the estuary gets a more aerodynamic shape and the flow will keep (see bathymetry analysis). By reclaiming land on the western bank of the estuary, it is expected that the flow will be more concentrated leading to higher bed shear stresses in the estuary and the ability to maintain the navigation channel towards Yangon Port.
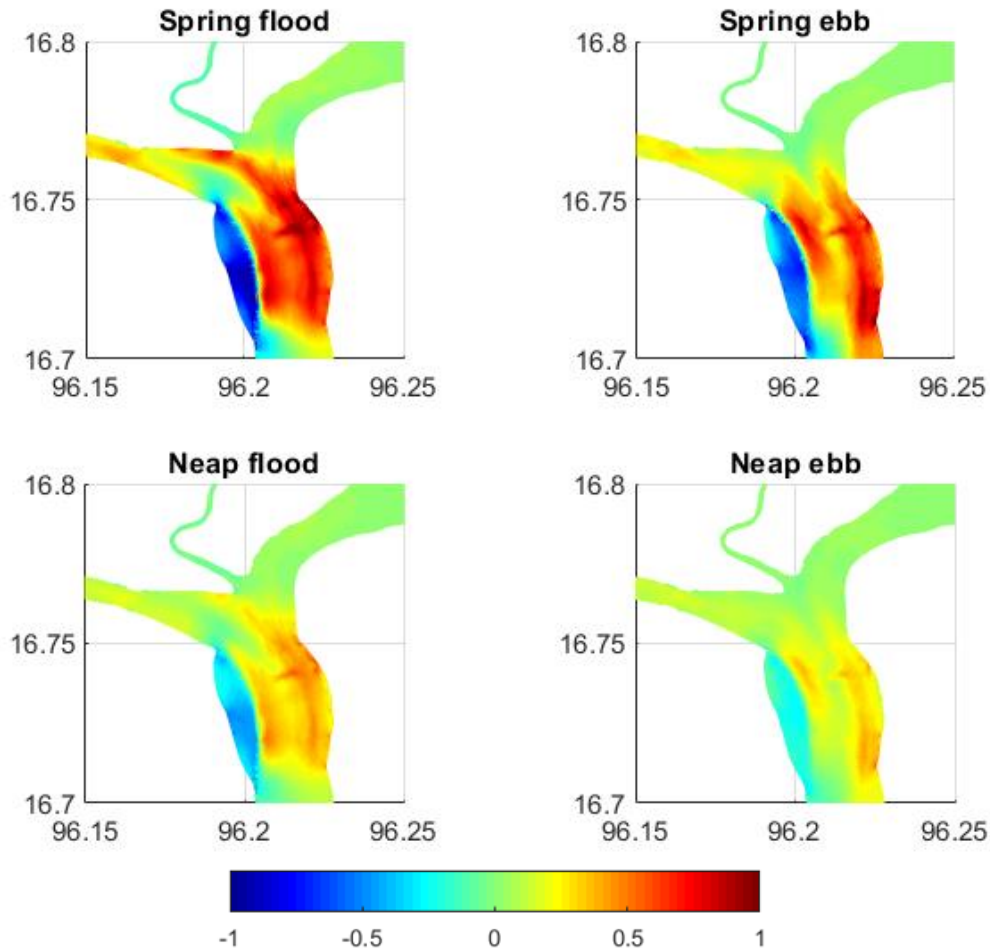
Figure 8.14: Increase in bed shear stress [N/m²] after construction of the adjustment at the western bank

The model results show that the adjustment to the estuary causes for an increase in bed shear stress in both the natural channel at the eastern bank as in the that is planned to be dredged. The bed shear stresses increases almost exact in the area where the new channel is planned to be dredged.

Relocation of the western bank is preferred over the land reclamation at the estuary split because the relocation of the western bank causes for higher bed shear stresses both during flood and ebb where the effect of the land reclamation at the split focusses on the ebb flow only. The increased bed shear stresses are right at the location which has the smallest depth in the current situation which reduces the risk on sedimentation in the channel. Hence it is chosen to test the land reclamation at the western bank in combination with a dredged channel.

8.3 Combination with dredged channel

The channel that will be dredged is 9 km long and 200 m wide. The channel will be 14 m deep in order enabling ships to reach Yangon Port through the whole tidal cycle.
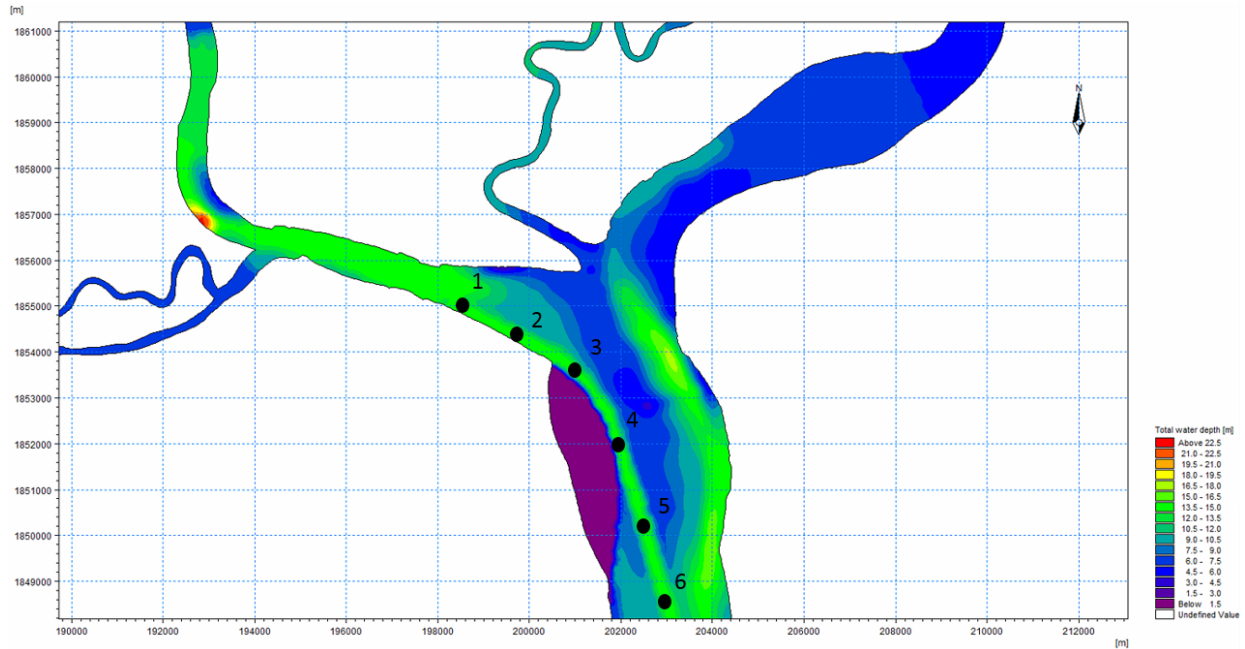
Figure 8.15: Bathymetry with dredged channel and the land reclamation.
The numbered dots are the output locations used by the model

With the dredging material the land reclamation will be done. Table 8-1 presents the volumes of the dredged channel and the land reclamation. 85% Of the volume of the land reclamation can be supplied by the dredged material from the new navigation channel.

Table 8-1: Volumes of the dredged channel and the land reclamation.

Location	Area $[10^6 \, m^2]$	Current depth [m+MSL]	New depth [m+MSL]	Volume $[10^6 \, m^3]$
Land reclamation	1.1	-4	5	9.9
Dredged channel 1	0.7	-9	-14	3.5
Dredged channel 2	0.7	-7	-14	4.9

In this section the effect of channel deepening on the bed shear stress is calculated. The model is run for one month in dry season to investigate the bed-shear stresses during spring tides and neap tides. Because this version of the model is not capable of calculating the hydrodynamic conditions properly in combination with high discharges, the calculations are done only for dry season conditions.
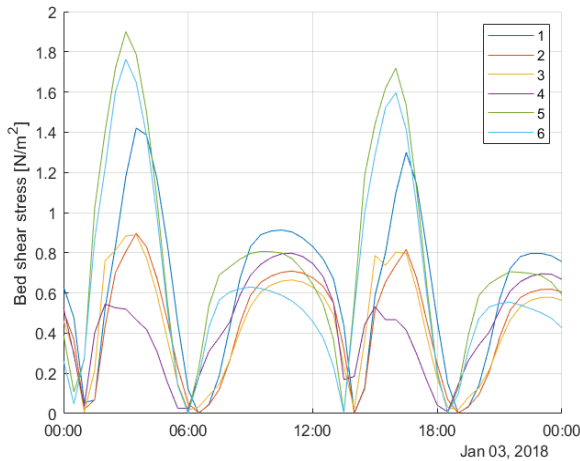
Figure 8.16: Bed-shear stress during spring tide in dry season
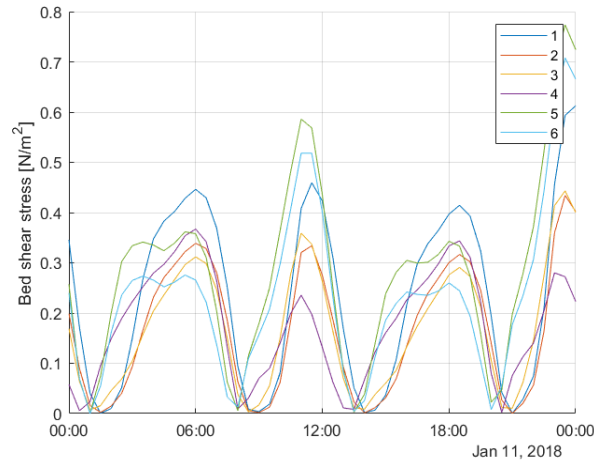
Figure 8.17: Bed-shear stress during neap tide in dry season

Figure 8.16: Bed-shear stress during spring tide in dry seasonFigure 8.16 and Figure 8.17 show the bed-shear stresses for the output locations as presented in Figure 8.15. From these results it can be concluded that the shear stresses are high enough to prevent the deposition of fine sediments. Based on a Shields parameter of 0.6, which represents the start of erosion (Schiereck, 2016), the critical bed-shear stress for medium sand (D_{50} = 0.3 mm) is 0.3 N/m². Consequently the sand is not expected to deposit. In order to verify this the sediment module is used to calculate the morphologic response of sand during a month in dry season.
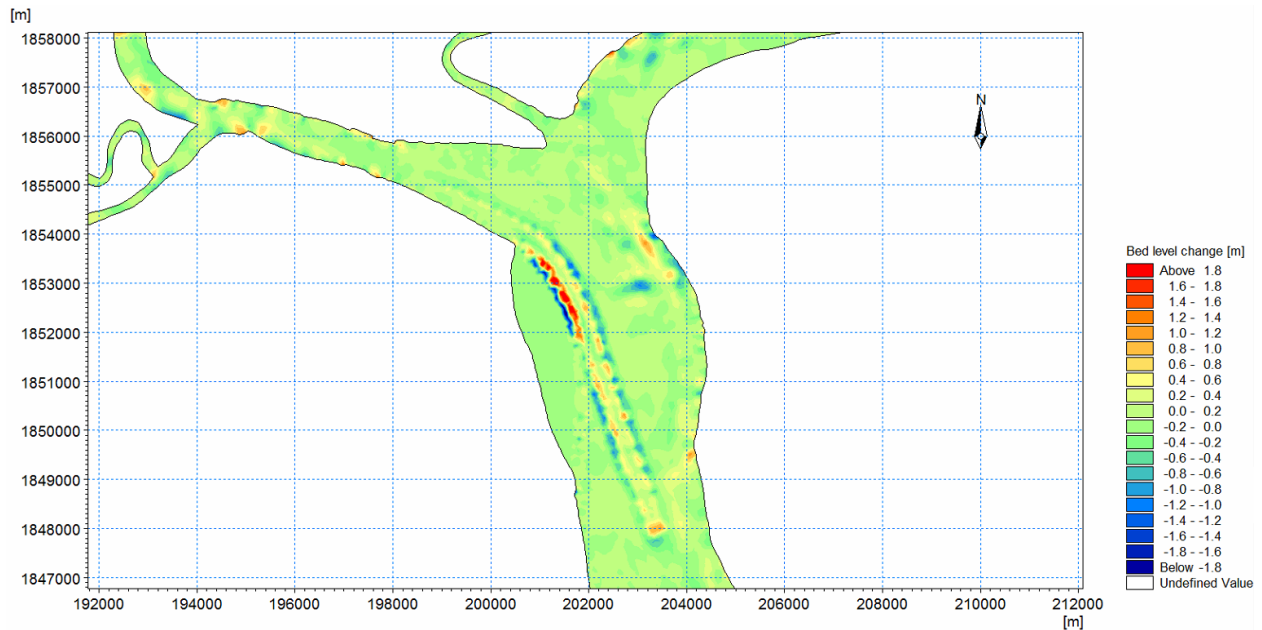
Figure 8.18: Morphodynamic response after one month of sand transport

As can be noticed from Figure 8.18, the slopes of the new channel show high morphologic activity. Accretion is accompanied by erosion. An explanation for the morphologic response can be the formation of the slopes because the initial height difference on the eastern slope is 20 m. Assuming a potential slope of 1/10 the slope length would be 200 m which agrees with the width

79

of the morphologic active area. A more important observation is that the center line of the channel seems quite stable, because the accretion is in the order of 0.01 to 0.10 m. It must be mentioned that this result is just an indication and must be interpreted very carefully. Comparing the sedimentation rate with the bed shear stresses of Figure 8.16 and Figure 8.17, one would expect the largest accretion at location 4, which agrees with the result in Figure 8.18.

9 Discussion

The influence of the different processes analysed in this research are discussed in Chapter 7. In this chapter the focus is on:

- Numerical model set-up

- Effect of the measures to improve the waterway to Yangon Port

9.1 Numerical model set-up

A goal of the numerical model was to analyse the hydrodynamics and the variations of it during spring/neap cycles and different seasons. Because the first version of the MIKE model was not appropriate to model monsoon scenarios and because of the large tidal intrusion length, it was decided to use the SOBEK model to define discharge time-series to use as boundary conditions for the MIKE 2DH model. The calibration of the MIKE water levels and discharges to the validated SOBEK water levels and discharges showed that the use of SOBEK discharges for the MIKE model works well. However, the combination of MIKE with SOBEK makes it inefficient to work with, because when different boundary conditions need to be implemented, one must first run the SOBEK model, extract the discharge time-series, implement them in the MIKE model, and finally run the MIKE model. This is experienced as a disadvantage of the used method..

During this research it was decided to focus on a 2D model instead of a 3D model. The reason for this was the consideration between the accuracy of the model, the related computational time and the added value of the results based on the expected uncertainties that the complex model would entail. As a consequence the current model is not appropriate to calculate the transport of fine sediments because important processes such as the considered lag effects and estuarine circulation depend on vertical varying flow conditions. Hence, the 2DH model results for fine sediment transport did not show a residual transport of fines (see Appendix).

The tidal boundary condition is defined based on tidal constituents and water level data along the Irrawaddy delta. However, other measurements that were not included in the determination of the tidal boundary condition that is used show a higher maximum water level of 0.5 m. Because the potential mixing conditions in the Yangon Estuary are determined by the ratio between the tidal prism and the river discharge, the difference in tidal range can have a big impact on these results. The low bed shear stresses in the stagnation-zone and drive-up zone, which is one of the important findings of this research, do not show a large variance during a spring/neap tidal cycle. Hence the conditions in the stagnation-zone and the drive-up zone seem less sensitive to changes in flow velocities compared to the other locations in the estuary.

9.2 Effect of measures on the estuary

The attempt to increase the flow resistance towards the Yangon River channel and force more discharge to Monkey Point Channel by increasing the Monkey Point Channel dimensions and dump the material at the Yangon River channel did result in higher shear stresses. However Figure 8.9 and Figure 8.10 show that the flow tends to follow the old path. Hence it could be expected that the morphology will quickly recover. The model result for the adjustments to the Monkey Point Channel dimensions suggest that the shape of the estuary split is dominant over the bed level variations in determining the flow over the estuary head. However, more research is required in order to conclude this suggestion.

With the sediment model the amount of sedimentation in the new channel is tried to predict (see 8.2.2). However, the model schematisation is not appropriate to calculate the hydrodynamic conditions for the monsoon season. Hence, only the sedimentation in dry season is calculated. From the results the development of the channel slopes can be noticed and in the middle of the channel the accretion is in the range of 0.01 – 0.10 m. However, the uncertainty of the model result is high because of the rough schematisation of the channel. More research to the sand transport would be required in order to give a better estimation on the amount of sand deposition in the new channel.

A risk of reducing the area of the shoals, is the potential rise in suspended sediments in the estuary just like happened in the Ems Estuary after decreasing of the intertidal areas (Van Maren, 2015). An incretion of suspended sediment concentrations can lead to problems in the port.

10   Conclusions

In this MSc thesis, research is done to the mixed sediment dynamics at the tide-dominated confluence of the Yangon Estuary. Focus has been on the cause for sedimentation in Monkey Point Channel that causes for hinder on the shipping route towards Yangon Port. In addition the main research question is formulated:

Which mechanisms are responsible for sedimentation at the confluence of the Bago and Yangon rivers, and how can sedimentation be mitigated?

In order to answer the main question a conceptual model has been developed in which the interaction between important processes are linked to the cause of sedimentation in Monkey Point Channel. The conceptual model is supported by a study to reference estuaries and the application of the numerical models SOBEK and MIKE21. The conceptual model has proven to be a good method whereby a good overview is kept of all processes that can play a role in the cause for the effect. Based on the conceptual model, answers to the sub questions are given in this section.

1.   Which hydrodynamic processes are important in relation to the morphology of the estuary?

Based on the typical morphology of the estuary and the model calculations which show that during eight months a year the tidal discharge entering the estuary is ten times larger than the river discharge. The tidal-dominance is reflected by the current velocities in the estuary which are maximum during spring tides, with the highest velocities during spring flood in dry season. The tidal currents show a strong tidal asymmetry resulting in flood dominance in the dry season. During monsoon season the river discharges causes the estuary to be ebb dominant. Additionally, the maximum flow velocities during dry season are much larger than during monsoon season.

The hydrodynamic processes at the estuary split have a large impact on the sediment distribution at the bay head delta by means of low dynamic areas and mid-channel bar growth. The characteristic confluence- and bifurcation-zones appeared to be present in the situation with bi-directional flow due to the tide. The stagnation-zone and the drive-up-zone have the most impact on the estuaries morphology because they are located in the same area and both causes for low flow velocities in the zone.

2.   How do sand and mud contribute to the sediment dynamics in the estuary?

Sand plays the major role in the formation of banks and channels. The MIKE model was able to give more insight in the formation of the estuary channels and the formation of the Inner Bar. Based on the bathymetry analysis and the model result the Inner Bar is expected to be formed by the deposition of sand from the Yangon River and reshaped by the interaction of the flow from the Yangon River and the Bago River related to mid-channel bar growth. Based on measurement data, theory on sand transport, Rouse profiles and model calculations, the distribution of the sand over the estuary is mainly limited to the channels and banks because the sand is transported as bed load and can therefore not leave the deep estuary channels. However, some sand will be able to reach the shoals by the flood channels.

Mud plays the major role in the suspended sediment concentrations in the estuary. Based on the study to the reference estuaries, the formation of mud layers is strongly related to the formation of an ETM. The type and the location of the ETM differs per season. The fortnightly rhythm of suspended sediment concentrations during the dry season in the Yangon Estuary shows similarities with the concentrations in the Severn estuary during low river discharges. This type of ETM, which is caused by the erosion of mud layers, is common for tide-dominated estuaries and

therefor also considered important to the sediment dynamics of Yangon Estuary. During spring tides the stationary fluid mud layers are eroded causing for a large increase in SSC. During the monsoon season the maximum flow velocities are believed to be insufficient to erode the stationary fluid mud layers. Hence, less sediment is brought into suspension explaining the seasonal variation in SSC.

3.   Why does sedimentation occur in Monkey Point Channel?

The analysis to confluences and bifurcations revealed the presence of the low dynamic stagnation-zone (confluence) and drive-up-zone (bifurcation). These zones are clearly represented by the MIKE model. Based on the model results it can be concluded that for all tidal and seasonal conditions the bed-shear stresses are low (<0.3 N/m2) in this area. Hence, fine sediments are almost continuously able to deposit in Monkey Point Channel. The measured consolidation behaviour of the sediment showed quick consolidation of the mud with consequently higher critical bed-shear stresses for erosion. The calculated sedimentation rate of the fine sediments corresponds with the required amount of dredging that is required in order to keep the channel at sufficient depth. It must be mentioned that due to the numerical model limitations, the processes based on density effects are not included which are expected to have a large influence on the residual sediment transport. However, based on the combination of the stagnation-zone and drive-up-zone and the found fine sediment, the deposition of fine sediments is a logical cause for the sedimentation in Monkey Point Channel.

4.   How can the sedimentation, and therefore the maintenance, in the navigation channel be reduced?

The sediment module of MIKE has been used to investigate the effect of adjustments to the estuary bathymetry in order to test potential solution to reduce the amount of sedimentation in the navigation channel. Because sedimentation in Monkey Point Channel is assumed to be caused by the deposition of fine sediments, adjustments have been tested on increasing the bed-shear stresses in the channel. Deepening of Monkey Point Channel resulted in a decrease in bed-shear stress and hence it is concluded that deepening of the current channel does not improve the conditions in relation to sedimentation in the channel. The attempt to increase the flow resistance in the direction of the Yangon River channel and force more flow towards the enlarged Monkey Point Channel did result in higher bed-shear stresses. However, the top view of the currents showed that the flow still follows the old pattern. Hence, it is expected that the morphology will quickly recover. Based on these two results it is concluded that changing the dimensions of Monkey Point Channel is not an effective solution to the sedimentation problem.

Consequently, relocation of the navigation channel has bene considered. Two options to improve the hydrodynamic conditions at the potential location of the new channel have been investigated. Land reclamation at the western bank just downstream of the Yangon Estuary mouth showed the most promising results since the bed shear stresses increased right in the area where deepening of the estuary is required. Test on the implementation of a 14 m deep channel showed minimum bed shear stresses of 0.3 N/m2, which are sufficient to prevent deposition of sand and fine sediments.

Finally the main conclusion of this research is given by answering the main question:

Sedimentation in the navigation channel at the confluence is caused by the deposition of fine sediment in the low dynamic zones caused by the specific hydrodynamic aspects of a confluence and bifurcation. The best option is to relocate the navigation channel outside this low dynamic zone. The relocation of the channel to the western bank in combination with land reclamation shows promising results.

11　Recommendations

This chapter contains recommendations based on the discussion and conclusions of this research. First, recommendations are made related to the sediment dynamics in Yangon Estuary and the improvement of the navigation channel towards Yangon Port. Next, recommendations are made related to further research.

11.1 Mitigation of the sedimentation in the navigation channel

It is concluded that in the stagnation-zone (confluence) and drive-up-zone (bifurcation) the fine sediment is able to deposit and causes for the high sedimentation rates. Attempts to increase the bed shear stresses in this zone by changing the channel dimension of Monkey Point Channel turned out to be ineffective. Therefore, it is recommended to relocate the navigation channel to a location outside the stagnation-zone and drive-up-zone.

As a potential new location of the navigation channel it is recommended to locate the channel between the natural channel of the Yangon River and the natural channel of the Estuary along the western bank (see Figure 8.12). The first results show that the bed shear stress in the new channel are too high for dine sediment to deposit and sedimentation of the channel due to fine sediment deposition is unlikely. Since, sand is mainly transported in the channel, sedimentation due to sand deposition must be further investigated. Furthermore, due to the construction of the new navigation channel, the potential area for mud deposition is reduced. Therefore, it must be investigated what effect this will have on the SSC in the estuary and if this can be problematic for example the harbour basins.

When the Myanma Port Authority prefers an improvement to the current dredging method, it is recommended to do more research to the application of water injection dredging because water injection dredging can be much cheaper per cube than dredging with a trailing suction hopper dredger (TSHD). Water injection dredging is, however, only applicable in situation of fine sediments which can be resuspended. This recommendation follows from the expectation that the sedimentation in Monkey Point Channel is dominated by the deposition of fine sediments. Based on the annual dredging volumes from Monkey Point Channel, the assumption is made that the annual deposits consists of 2.000.000 m^3 which agrees with about 13 m deposition a year. Hence, one must dredge 1 m every month in order to keep the navigation channel open. Hence, the mobilisation of a   As an option to reduce the amount of dredging operations, one must investigate if it is possible to do a capital dredging project when the channel is dredged to

11.2 Further research

In this research it is concluded that the Yangon Estuary is mainly a tide-dominated estuary. Hence the tidal propagation in the estuary is considered as the most important aspect of the numerical model. In order to optimize the accuracy of the model it is recommended to measure the water level at the estuary mouth and the split of the estuary for one year in order to include the seasonal variation. The measurement data on water levels at the estuary mouth can be used as a accurate boundary conditions and the water levels at the head of the estuary can be used for calibration. In addition, data on flow velocities should be available for model validation.

In this research only the data on SSC by Gibb and Nelson is used. Because these measurements are from 1976 and 1998, and the measurements show some important differences, it is

recommended to do new measurements on the SSC in the Bago and Yangon rivers and halfway the estuary at Thilawa Port. In addition the location of the mud layers should be identified because based on this research they are believed to be of major importance to the sediment dynamics. This can be done by using echo sounders. In addition the concentration of the fluid mud should be determined in order to define the relation between the concentration and the strength of the layer against erosion.

Because of the tide-dominance, the sediment concentrations in the estuary are thought to be correlated with the tide. When the measurements on water level and sediment concentrations are combined, one is able to check of these processes are correlated.

For further research it is recommended to use a 3D model because baroclinic processes have proved to be important to the sediment balance within Yangon Estuary. With a 3D model schematisation it would be possible to include the fine sediment dynamics properly, which was not possible in a 2DH framework. More insight in the fine sediment dynamics would really contribute understanding of the system.

As discussed in Chapter 5, the tidal propagation is difficult to implement properly in the model because the tidal intrusion length is very large (see Chapter 2) and hence bathymetry data is needed for a very large area which was not available when setting up this model. Problems risen when large monsoon river discharge had to flow through the Hlaing River. Because the bathymetry of the river banks was not included the model assumed the river banks as straight walls, resulting in a small cross-section for high water levels, while in reality the cross-section width would exponentially increase with the water depth due to the slope of the river banks. For further research with a numerical model, it is recommended to implement the river banks properly. In addition the erosion on the banks across the estuary main channel can be investigated. The model method consisting of the combination of MIKE with SOBEK turned out to be inefficient. Another (possibly better) method to make a model in which the tide can propagate properly, is to make a schematisation of the model by implementing a large basin at a river end to deal with the required tidal storage volume. The location of the basin should be chosen far enough from the area of interest to prevent disturbance from the basin. This is a good solution in order to minimalize the size of the model domain and ensure enough tidal storage volume.

12   Bibliography

Allen, G. (1977). *Transport and deposition of suspended sediment in the Grironde Estuary.*

Allen, G. (1991). *Sedimentary processes and facies in the Gironde Estuary: a recent model for macrotidal estuarine systems.* Saint Remy Les Chevreuse.

Ashworth, P. (1996). *Mid-channel bar growth and its relationship to local flow strength and direction.* Leeds: Leeds University.

Attema, Y. (2014). *Delft3D model for the Ayeyarwady delta Myanmar.* Delft: Delft University of Technology.

Aung, T. (2013). *Numerical simulation on sedimentation in the Yangon River and its navigation channel.* Tokyo: Societe franco-japonaise d'oceanographie.

Best, J. (1987). *Flow dynamics at river confluences.* Hull: University of Hull.

Bosboom, J., & Stive, J. (2015). *Coastal Dynamics 1.* Delft: VSSD.

Boskalis. (2016). *Yangon River Maintenance Dredgin.* Yangon: Boskalis.

DHI. (2018). *MIKE21 Manual.*

DMH. (2014). *Irrawaddy Discharge.* Yangon.

Dyer, K. (1994). *Estuarine Sediment Transport and Depostion.*

Gibb, S. A., & Partners. (1976). *Rangoon Sea Acces Channel and Associated Port Improvement Study.* Yangon: Birma Ports Cooperation.

JICA. (2014). *The Survey Programm for the Nationa Transport Development Plan in the Republic of the Union of Myanmar.* Tokyo: JICA.

JICA. (2016). *Data collection survey for improvement of the navigation channel of Yangon Port in the Republic of the Union of Myanmar.* Tokyo: JICA.

Kirby, R., & Parker, R. (1983). *Distribution and Behaviour of Fine Sediment in the Severn Estuary and Inner Bristol Channel, U.K.*

Koning, R. d., & Janssen, M. (2015). *Delft3D-FLOW Model of the Yangon Port Area.* Yangon: Delft University of Technology.

Manning, A. (2010). *A review of sediment dynamics in the Severn Estuary: Influence of flocculation.*

Maren, D. v. (2015). *Fine sediment transport into the hyper-turbid lower Ems River: the role of channel deepening and sediment induced drag reduction.* Delft: Springler.

Mosselman, E. (2017). *Lectures River Dynamics.* Delft: Technical University Delft.

Myanmar Port Authority. (2016). Retrieved from https://consult-myanmar.com/2016/09/19/myanma-port-authority-expression-of-interest-to-conduct-channel-development-project-for-yangon-river/

Myanmar Port Authority. (2019). Monkey Point Channel. (R. Bax, Interviewer)

Navionics. (2018). Retrieved from https://webapp.navionics.com/#boating@11&key=iygeB%7Bz%60jQ

Nelson, B. (2000). *Sediment Dynamics in the Yangon River.* Charlottesville: University of Verginia.

Oosterwegel, M. (2018). *Connecting Myanmar.* Delft: TU Delft + Arcadis.

PIANC. (2014). *Harbour approach channels design guidelines.* Bruxelles.

Pietrzak, J. (2016). *An Introduction to Stratified Flows for Civil and Offshore Engineers: From Shelf to Shore.* TU Delft.

Pritchard, D. (1967). *What is an estuary: physical viewpoint.*

RHDHV. (2017). *Yangon Estuary Project.* Yangon.

RHDHV. (2018). *Pan Hlaing Sluice Project.* Amersfoort.

Robinson, R. (2007). *The Irrawaddy River Sediment Flux to the Indian Ocean.* St. Andrews.

Ross, M., & Mehta, A. (1989). *On the mechanics of lutoclines and fluid mud .*

Schiereck, G. (2016). *Introduction to Bed, Bank and Shore Protection.* Delft: VSSD.

Sentinel. (2019, July). *Sentinel Hub.* Retrieved from https://www.sentinel-hub.com/explore/sentinel-playground

Van Rijn, L. (1993). *Principles of Sediment Transport in Rivers, Estuaries and Coastal Seas.*

Verruijt. (2010). *Soil Mechanics.* TU Delft.

Wells, J. (1995). *Tide-dominated estuaries and tidal rivers.* Elsevier .

Whitehouse, R., Soulsby, R., & Roberts, W. (2000). *Dynamics of Estuarine Mud.* London: HR Wallingford and Thomas Tellford Limited.

Winterwerp, J., & Prooijen, B. v. (2017). *Sediment Dynamics Lecture Notes.* Delft: Delft University of Technology.

WorldWaves offshore database. (2015). *Wind & Wave Roses Myanmar.*

13 Appendix

The appendix is set-up as the main text. Appendix A considers Chapter 2, Appendix B considers Chapter 3, Appendix C considers Chapter 4 and Appendix D considers Chapter 5 and 6.

13.1 A

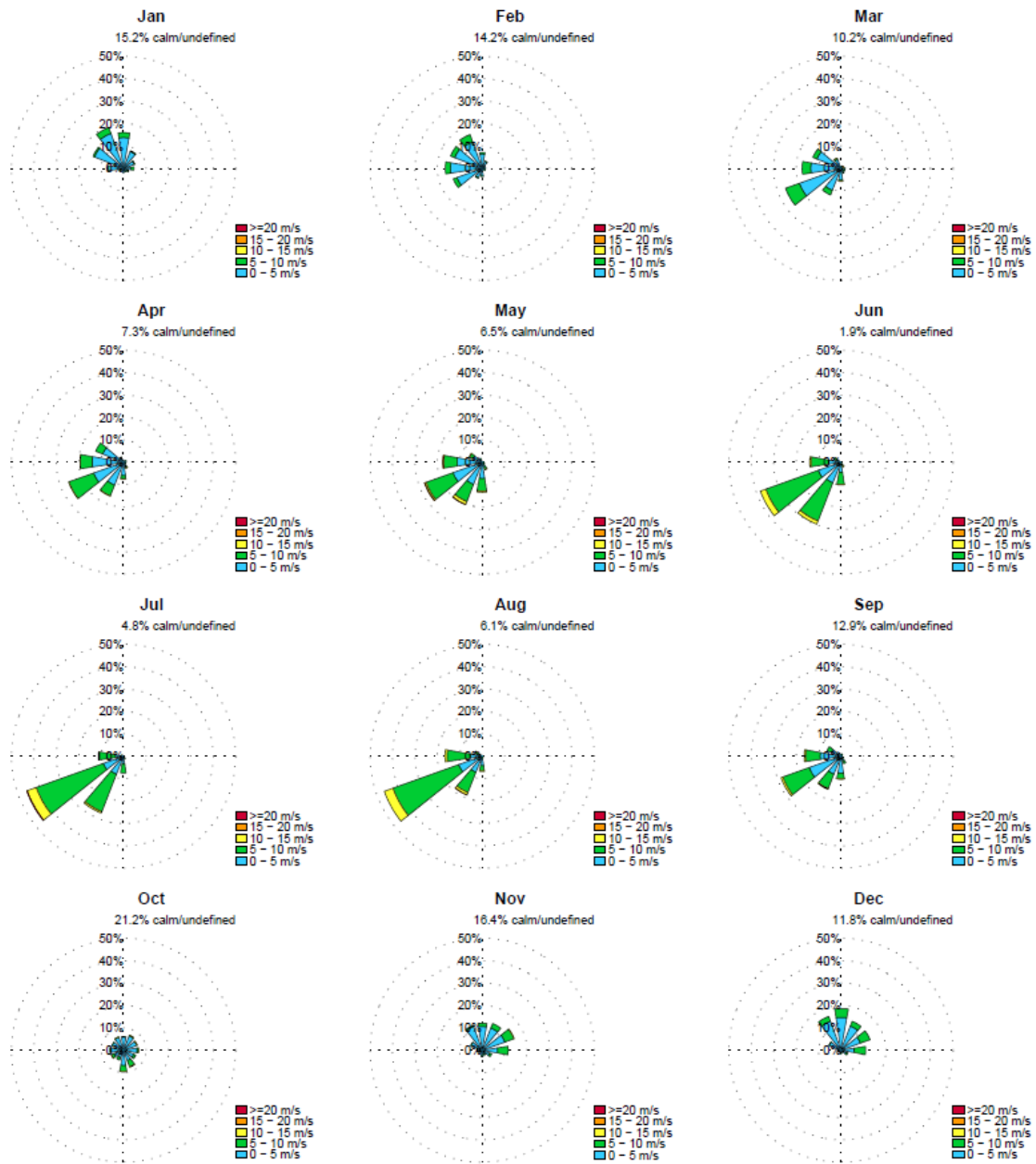Wind and waves roses for Gulf of Martaban.
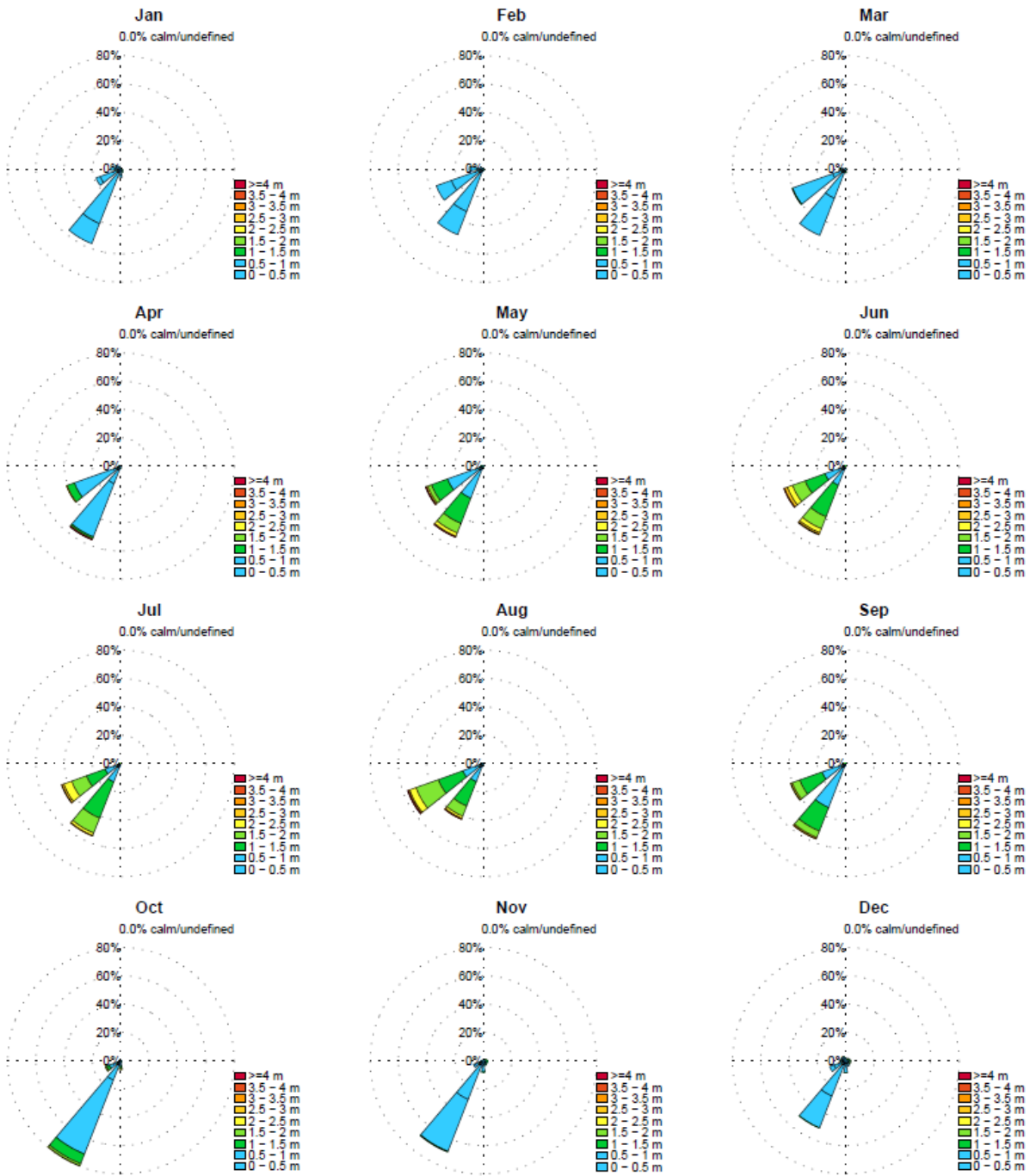

Figure 13.1: Wind roses for Gulf of Martaban

Figure 13.2: Wave roses for Gulf of Martaban

13.2 B

Stratification occurs when water masses with different density form layers that act as barriers to water mixing (Miller, 2004). The density of water depends on chemical composition, salinity, temperature and sediment concentration (Pietrzak, 2016). Salinity is the main driver for density differences in estuaries (Winterwerp & Van Prooijen, 2016). In estuaries, where saline water and fresh water interact, stratification may occur. The stratification may typically result in two-layered, bidirectional flow defined by a strong halocline (Pietrzak, 2016). Whether and where stratification occurs depends on the competition between how much buoyancy is input from fresh water and how much mixing takes place, principally from the tides (Pietrzak, 2016). This competition results in four different types of stratification (Pritchard, 1967):
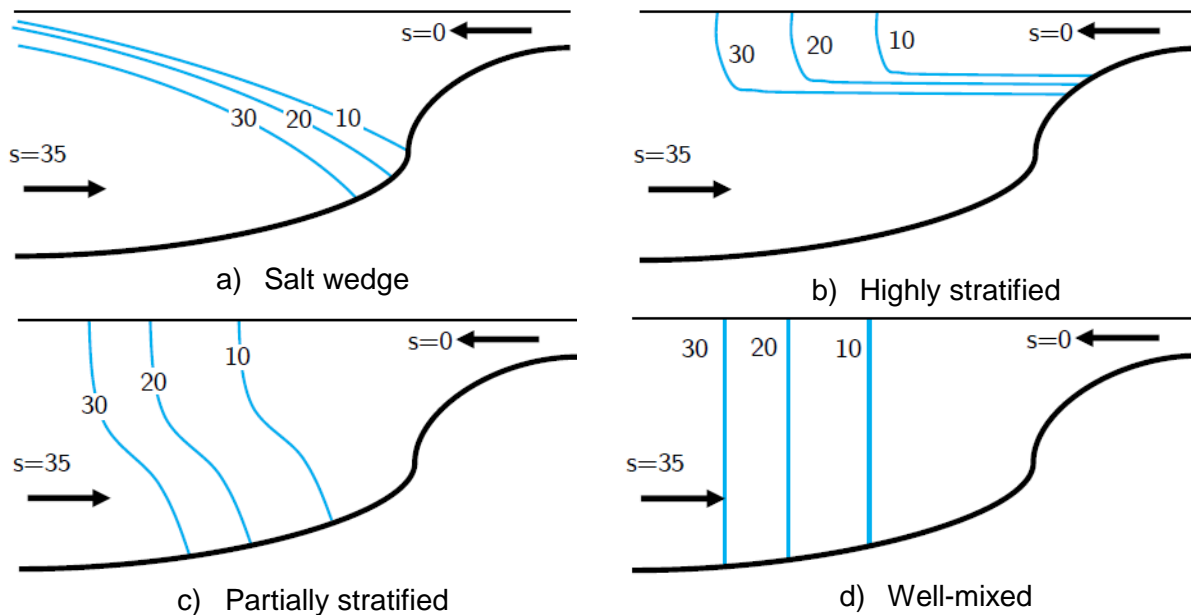

Figure 13.3: Types of stratification (Pritchard, 1967).

In order to predict what kind of estuary is considered, estuary classification is done by using the Estuary-Richardson Number:

$$Ri_E = g \frac{\varepsilon q_f}{u_T^3}$$

Where:

ε	Relative density difference
q_f	Fresh river discharge [m²/s]
u_T	Root mean square value of the tidal velocity near the estuary mouth [m/s]

The Estuary-Richardson Number gives a dimensionless number which indicates the amount of stratification based on the balance between the energy input by the tide to buoyancy available from the fresh water. The nominator, εq_f, is a measure for the amount of work needed to mix the fluids and is therefore the stabilising factor. The denominator, u_T, indicates the amount of turbulent mixing generated by the tide and therefore breaks down the stratification. Typical values of the Estuary-Richardson number are $Ri_E < 0.08$ for well-mixed estuaries and $Ri_E > 0.8$ for highly stratified estuaries. Based on the linear wave theory for waves in shallow water (Holthuijsen, 2016) the tidal current velocity can be calculated by using the tidal range data from Table 2-3**Error! Reference source not found.**.

$$u_T = \sqrt{\frac{1}{T} \int_0^T \hat{u}^2 \sin^2(\omega t)\, dt} \ = \frac{\hat{u}}{\sqrt{2}}$$

$$\hat{u} = \sqrt{\frac{g}{h}}\eta$$

Where:

h	Water depth [m]
η	Tidal amplitude [m]
$\hat{u}$	Velocity [m/s]

Because the correctness of the river discharge data is discussable and tide-dominated systems are expected to be well-mixed, the maximum river discharge related to well-mixed conditions is defined with the Estuary-Richardson Number. The representative average water depth for the Yangon Estuary is estimated as h = 14 m and the tidal amplitude for spring tide is η = 3 m. Hence the velocity, $\hat{u}$, is 2.51 m/s and the mean root square of the tidal velocity is 1.77 m/s. Assuming a density of 1025 kg/m^3 for saline water and a density of 1000 kg/m^3 the relative density difference is calculated. For Ri_E < 0.08, the fresh water discharge needs to be lower than 2.67 m^2/s. This river discharge depends on the width of the cross-section of the flow. Considering the width of the Yangon River and the Bago River mouth (B = 1500 m) the maximum fresh river discharge, Q_f, for well-mixed conditions is about 3000 m^3/s. During neap tides this maximum fresh river discharge is 100 m^3/s. Consequently the estuary is assumed to be well-mixed during spring tides when the fresh river discharge is lower than 3000 m^3/s. In addition the estuary is assumed to be partially-stratified during neap tides in dry season. During monsoon season, when the fresh river discharge may exceed 5000 m^3/s, the estuary can become highly stratified during neap tides, since the Estuary-Richardson number exceeds 0.8.

Horizontal salinity gradients can trigger estuarine circulation which is important for the residual transport of sediment.

13.3 C

Because the specific effect of estuarine circulation and lag effects on the Yangon Estuary is not determined, the analysis are shifted to the appendix. Furthermore Chapter 4 considers the SSC in the Severn Estuary and the formulas used to make the Rouse profiles.

Estuarine circulation

Estuarine circulation refers to the residual flow as a result of density differences. Estuarine circulation can occur due to both horizontal and vertical stratification. One of the first forms of estuarine circulation that was identified is gravitational circulation. Gravitational circulation is caused by horizontal stratification. Estuarine circulation due to vertical stratification is referred to as tidal straining. Both processes are discussed in this subsection.

Gravitational circulation is the circulation of water within the estuary, caused by the density differences along the estuary longitudinal axis (Winterwerp & Van Prooijen, 2016). Because the salt water has a higher density, the pressure on the sea side would be larger than on the river side. This is compensated with a slope in the water level. As a result the water level is slightly higher at the upstream part of the estuary where the density is lower. The downstream flow is therefore closer to the surface than the denser upstream flow. This causes for circulation which is shown in Figure 13.4. The effect of gravitational circulation depends on the mixing conditions of the estuary and on the water depth in the estuary. Gravitational circulation is most effective for partly stratified conditions (Wells, 1995). Gravitational circulation is enhanced for a larger water depth because the vertical distance between the net fresh water flow and the net saline water flow is larger causing for a larger momentum.
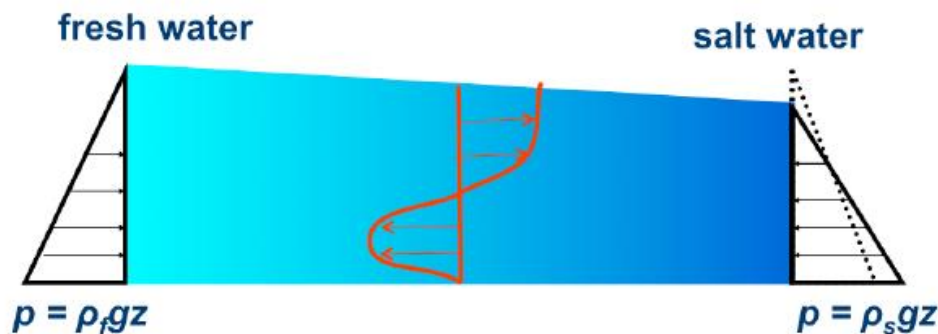

Figure 13.4: Gravitational circulation (Winterwerp & Van Prooijen, 2016)

In well-mixed estuaries tidal straining is an important process that causes for estuarine circulation. Tidal straining is defined as the stratified flow that occurs when fresh water is flowing on top of the saline water due to the density effect. Tidal straining of the density fields causes for stratification to be greater on ebb than flood (Jay & Musiak, 1994). During ebb tides, tidal currents stratify the water column through the straining of the density field by the interaction between a longitudinal density gradient and a vertically sheared velocity profile. During flood tides, this straining is reversed and the water column tends to be well-mixed, intensifying currents near the bottom. This asymmetric mixing and velocity profile can lead to a residual flow with the same structure as the density-driven circulation: seaward flow near the surface and landward flow at the bottom (Jay and Musiak 1996; Stacey et al. 2001).

Lag effects

Lag effects can have a large influence on the residual transport of fine sediment because lag effects cause asymmetries of the sediment particle's trajectory under a periodically reversing flow. Such asymmetries classically result in a landward transport of sediment over a tidal cycle (Gatto, 2016). Basically there are two important lags; scour lag and settling lag. Scour lag is caused by the difference in the required energy to keep cohesive sediments in suspension and the energy required for erosion of cohesive sediment. Due to the adhesive forces in cohesive sediment much more shear stress is required to erode the sediments from the bed than keep them in suspension. As a result, the transportation time is reduced by the acceleration time until the critical flow velocity for erosion is exceeded. When for instance the flow velocity decreases in upstream direction (see Figure 13.5b), the scour lag causes for a net upstream transportation of fine sediment for each tidal cycle (indicated by sediment particle position C). Settling lag is caused by the small settling velocity of fine sediment. When the shear stress falls below the critical shear stress to keep the fine sediment in suspension, the sediment starts settling while the particles still have a velocity in the direction of the tide. When for instance the bed level decreases in downstream direction (see Figure 13.5c), the deposition takes longer during ebb, causing for a net downstream transport of fine sediment. The combinations of local varying conditions with scour lag and deposition lag have a large influence on the residual sediment transport direction (Winterwerp & Van Prooijen, 2016).

a) Uniform conditions

b) Velocity damping

c) Increasing upstream bed level
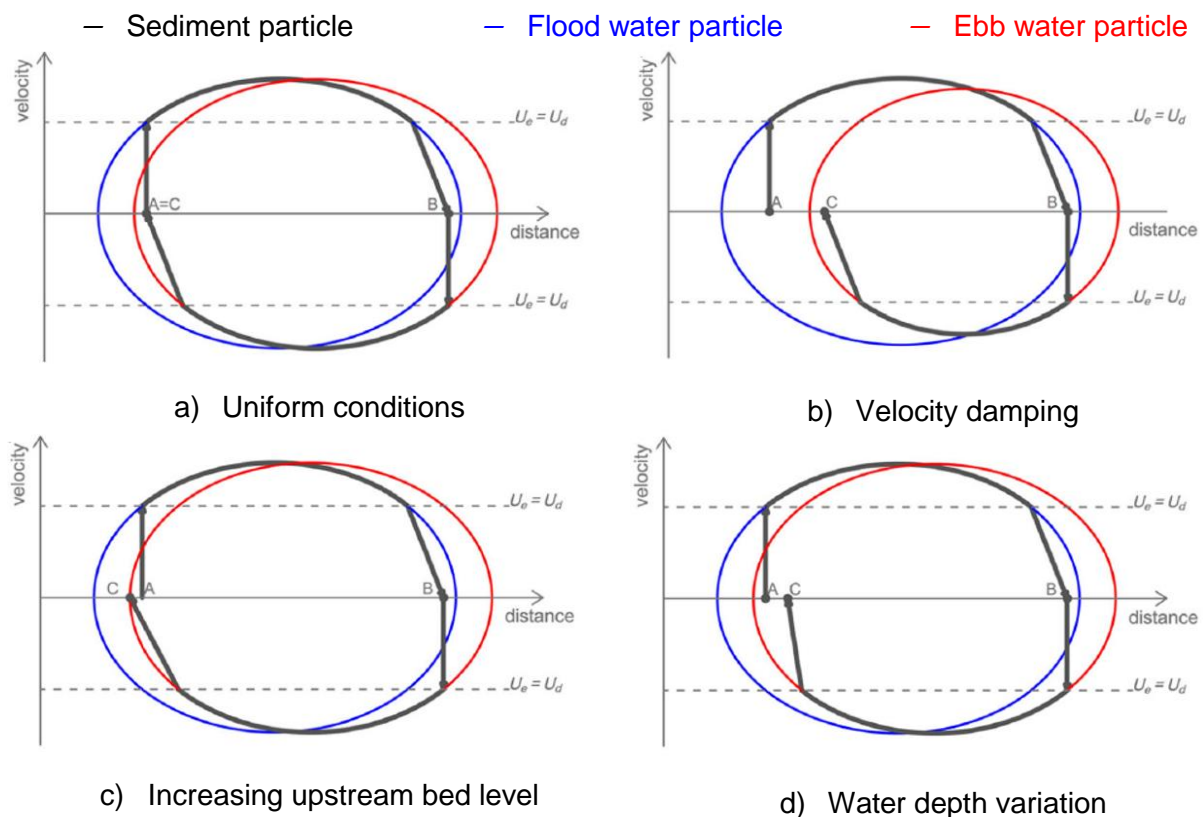
d) Water depth variation

Figure 13.5: Lag effects (Gatto, 2016)

Because Nelson (2000) reported the large amount of fine sediments within the estuary, the lag effects in combination with the flood dominant tide can be important in relation to the import of fine sediments from the delta into Yangon Estuary.
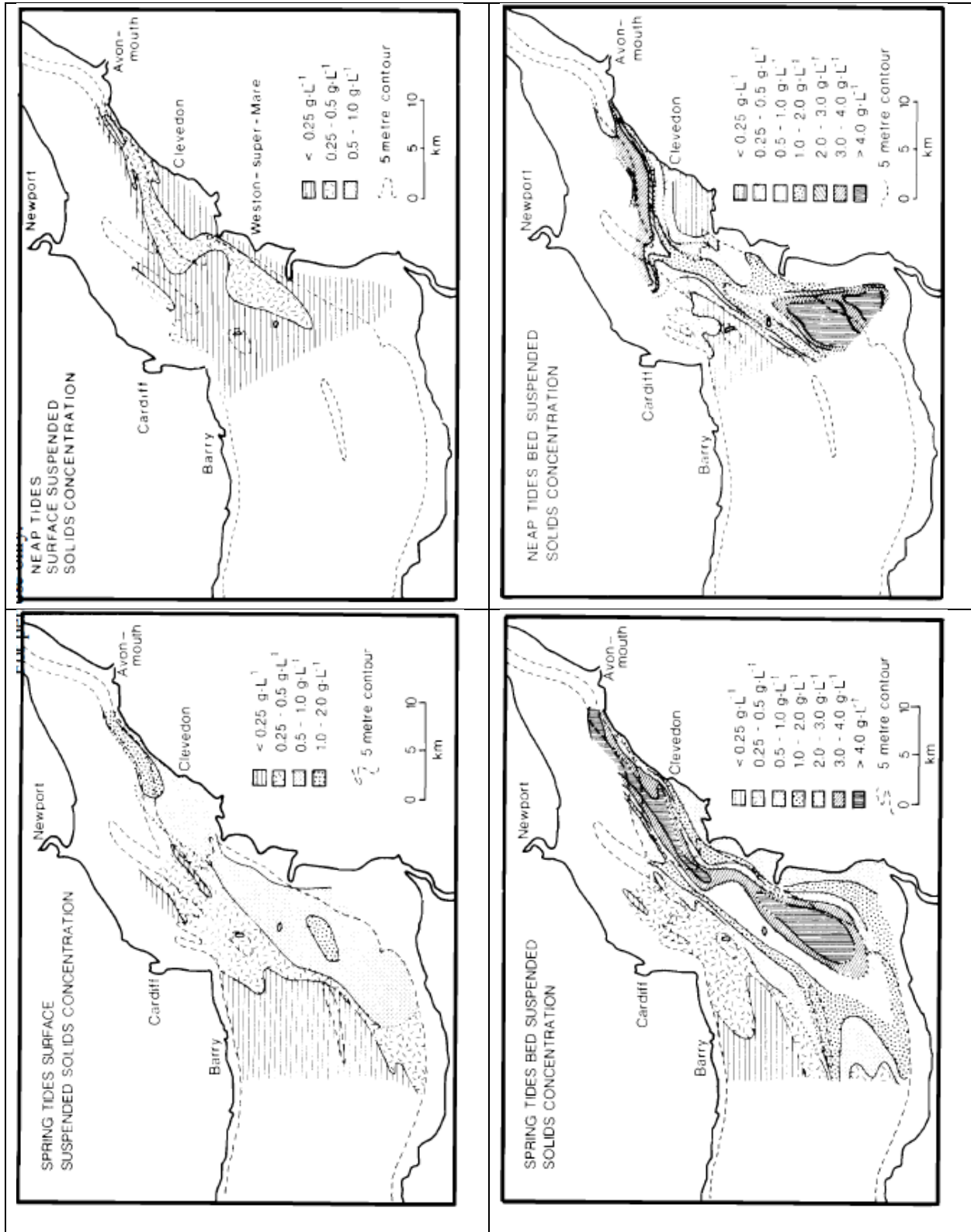
SSC in Severn Estuary

Figure 13.6: SSC in Severn Estuary

Formulas for Rouse Profile

The Rouse equation:

$$\frac{c}{c_a} = \left(\frac{a}{h-a} * \frac{h-z}{z}\right)^{\beta}$$

Where:

c	Concentration [g/l]
c_a	Concentration at reference height a [g/l]
a	Reference height [m]

For the reference height a of 5 times the D_{50} is used, resulting in a = 1.5 mm. The concentration at the reference height c_a is calculated with. :

$$c_a = \alpha \frac{D_{50}}{a} \frac{\left(\tau/\tau_c - 1\right)^{1.5}}{D_*^{0.3}}$$

Where:

α	Coefficient (1.0)
τ	Bed shear stress [N/m2]
τ_c	Critical bed shear stress [N/m2]
D_*	Dimensionless grain size parameter [-]

The critical bed shear stress is defined by Shields (Schiereck, 2016):

$$\tau_c = \psi_c(\rho_s - \rho)gD_{50}$$

Where:

ψ_c	Critical Shields parameter [-]
ρ_s	Sediment density (2650) [kg/m3]
ρ	Water density (1025) [kg/m3]
D_{50}	Median grain size [m]

For the critical Shields parameter a value of 0.06 is used which is recommended for sand transport calculations (Bed bank, 2016). The dimensionless grain size parameter is defined as:

$$D_* = \left(\frac{\Delta * g}{\upsilon}\right)^{\frac{1}{3}}$$

In which:

Δ	Relative density [-]
υ	Viscosity [m²/s]

The Rouse number is calculated with:

$$\beta = \frac{\sigma_T * w_s}{\kappa * u_*}$$

Where:

σ_T	Schmidt number (0.7) [-]
w_s	Setlling veolocity [m/s]
κ	Von Kármán constant (0.41) [-]
u_*	Shear velocity [m/s]

The settling velocity of non-cohesive sediment is described by Van Rijn(1993):

$$w_s \begin{cases} \dfrac{(s-1)gD^2}{18v} & 65\ \mu m < D \le 100\ \mu m \\[3ex] \dfrac{10v}{D} * \left(\sqrt{1 + \dfrac{0.01(s-1)gD^3}{v^2}} - 1 \right) & 100\ \mu m < D \le 1000\ \mu m \\[3ex] 1.1\sqrt{(s-1)gD} & 1000\ \mu m < D \end{cases}$$

Where:

s	Relative density ρ_s/ρ [-]

13.4 D

In this section first the model domains of the SOBEK and the MIKE model are presented. Next, the calibration and validation of the numerical models are presented.

Model domain SOBEK
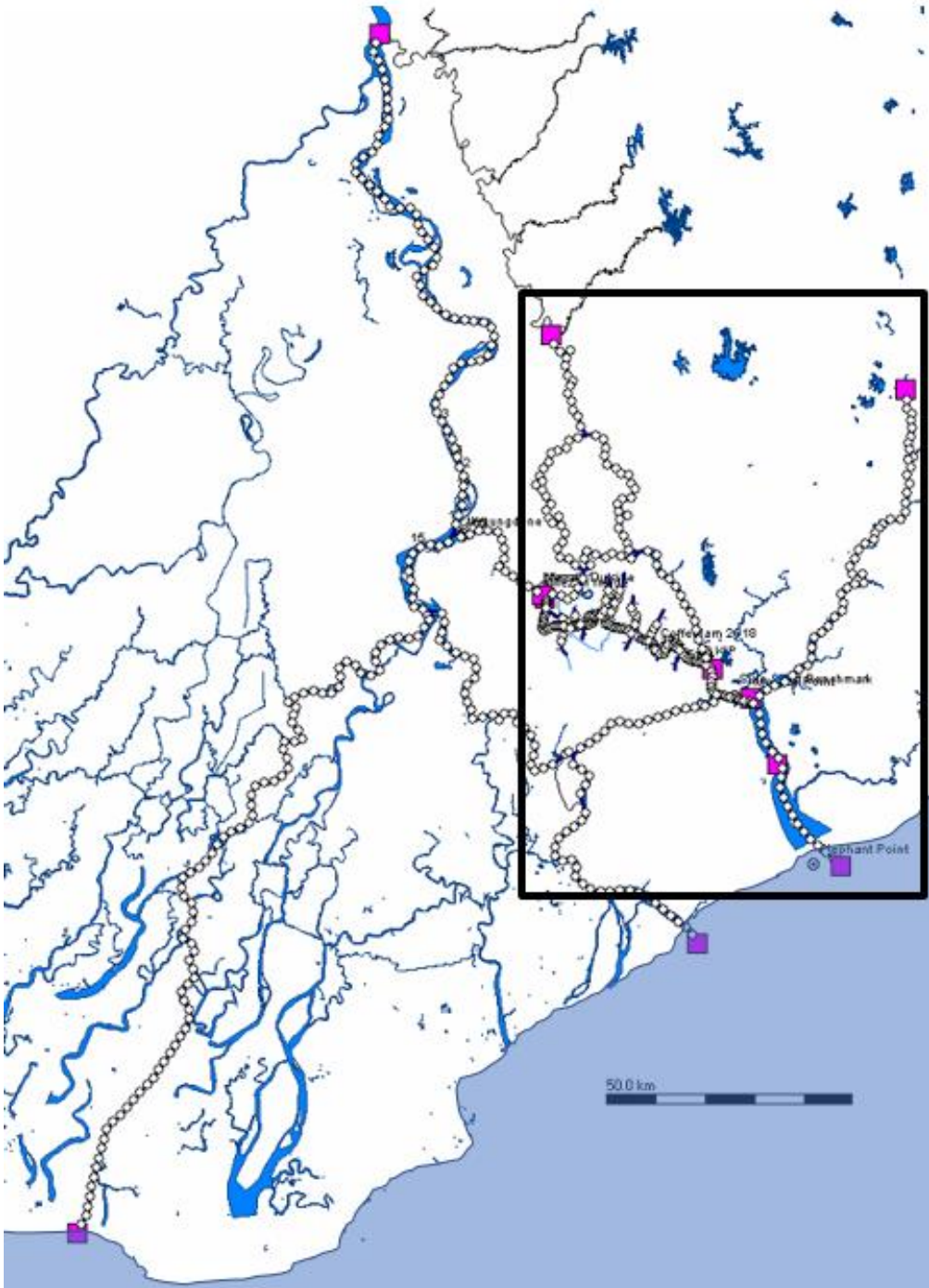
Figure 13.7: Model domain SOBEK

Model domain MIKE
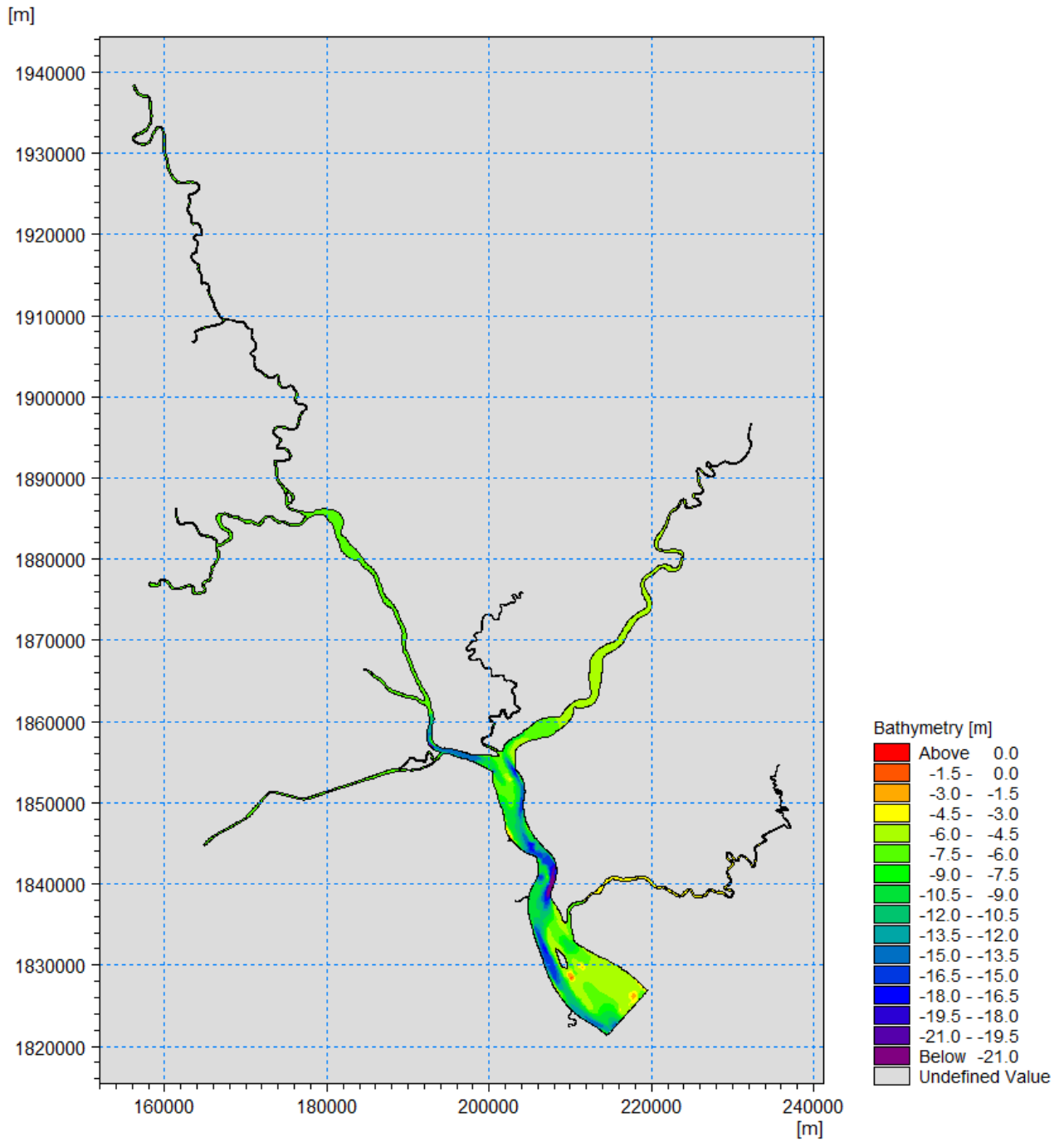
Figure 13.8: Model domain MIKE

SOBEK Calibration
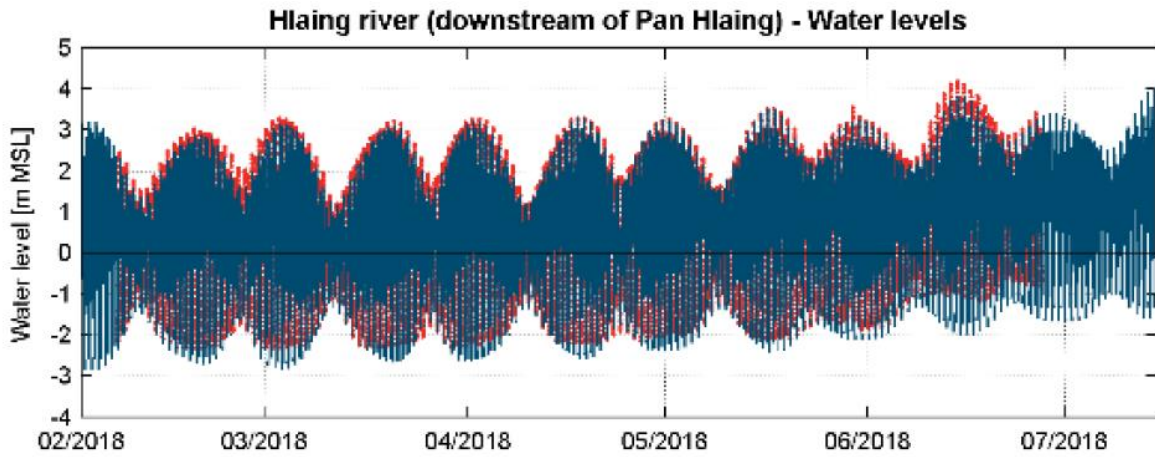
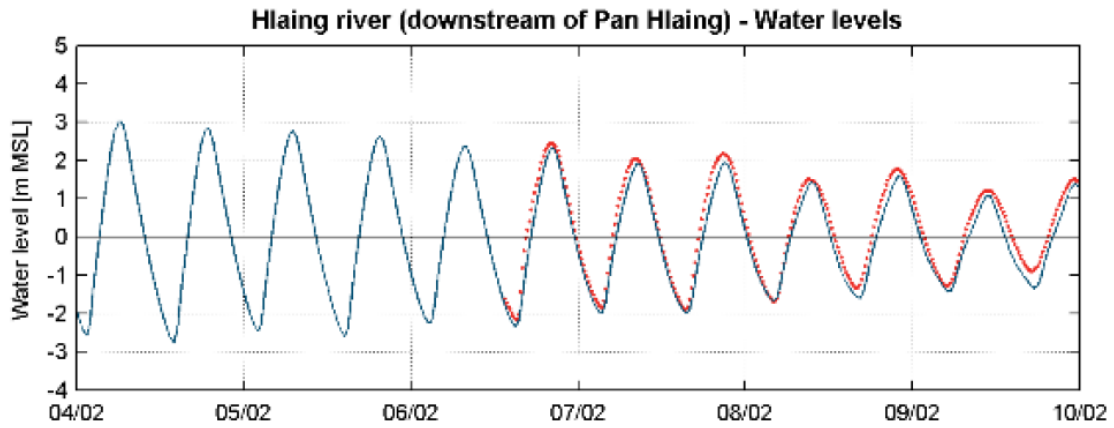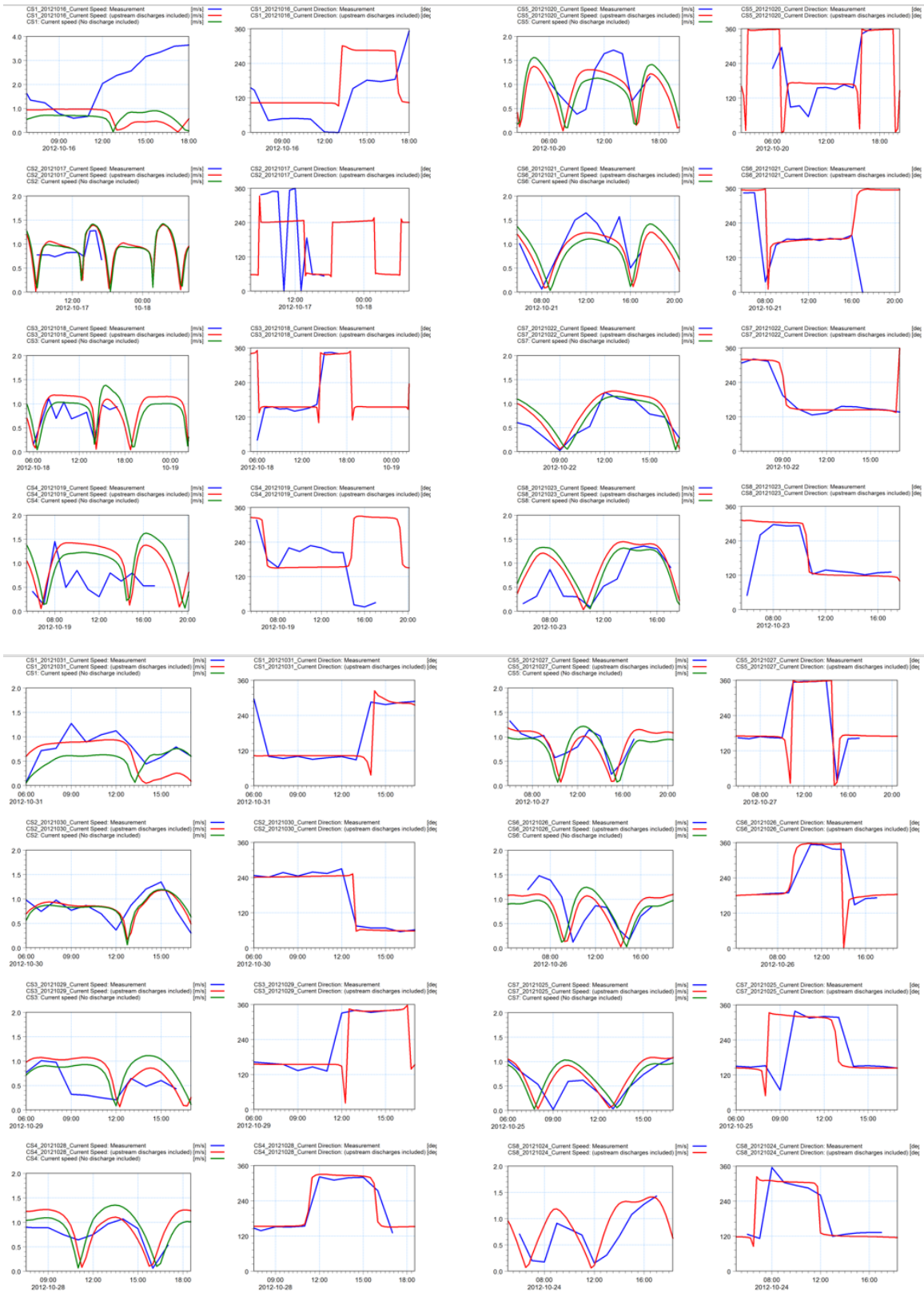Figure 13.9: Simulated (blue) versus measured (red) water level on Hliang River (station KIP) from February until July 2018

Figure 13.10: Simulated (blue) versus measured (red) water level at the confluence of the Pan Hlaing and Hliang River (station KIP) in the period of discharge measurements on the Pan Hlaing (February 5 2018)

100
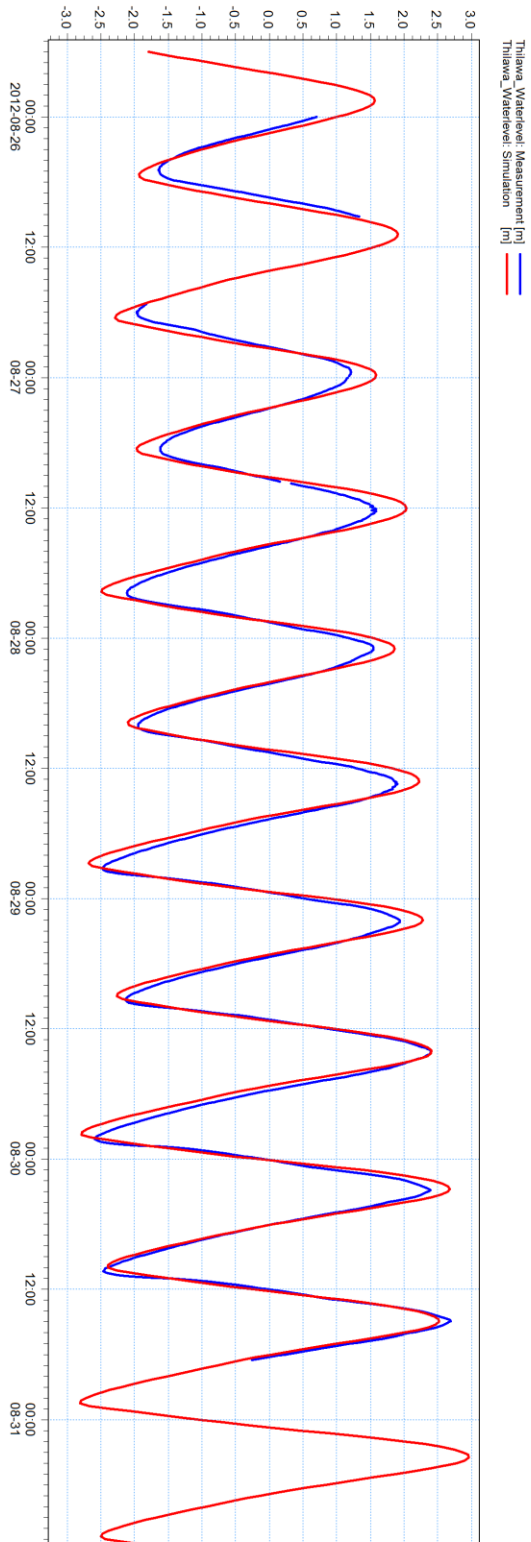
MIKE Calibration

Figure 13.11: Water level calibration results for water level at Thilawa

SOBEK MIKE Validation

It must be mentioned that the locations of output slightly differ which is thought to be the cause for the small differences between the discharge of the SOBEK model compared to the MIKE model with SOBEK boundary conditions.
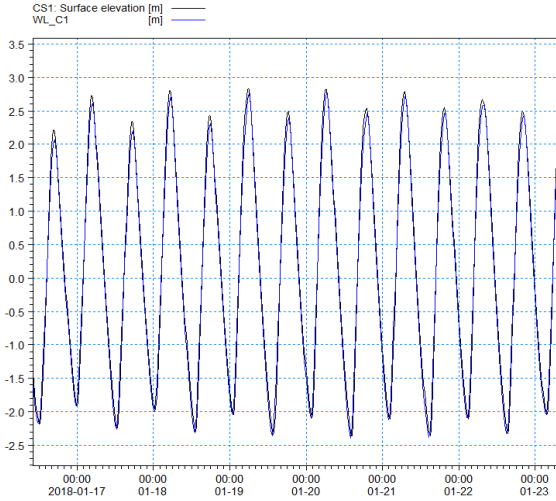

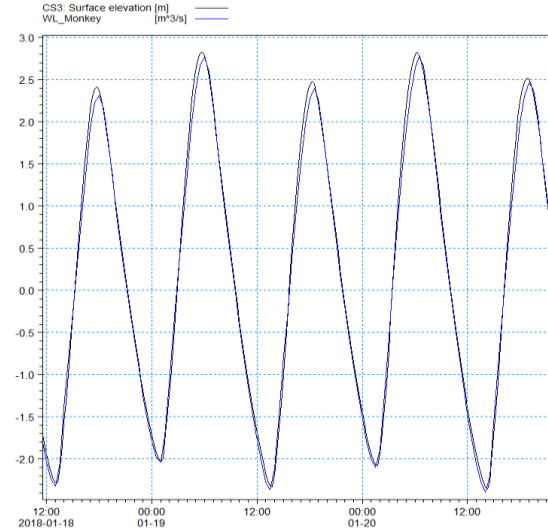Figure 13.12: Comparison of the water level in the Yangon River

Figure 13.13: Comparison of the water level downstream of the confluence of the Bago and Yangon Rivers
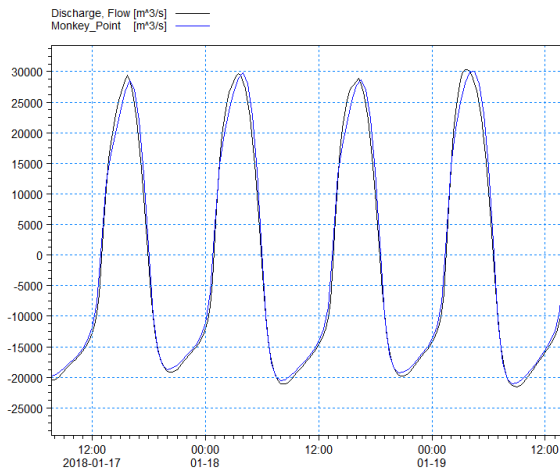

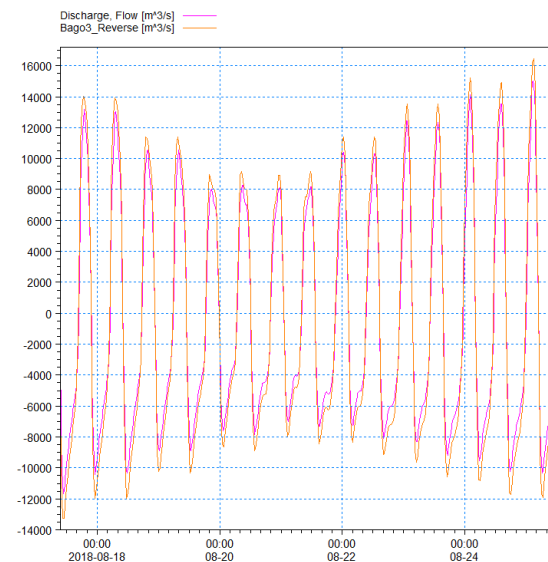Figure 13.14: Comparison of discharge downstream of the confluence of the Bago and Yangon rivers

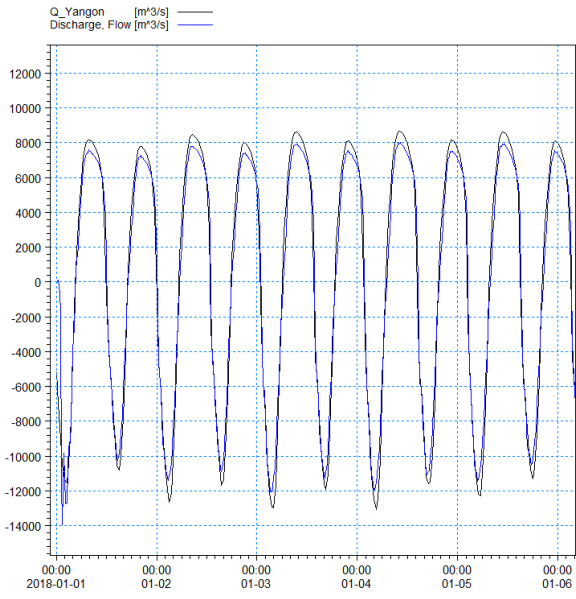Figure 13.15: Comparison of the discharge in the Bago River

Figure 13.16: Comparison of discharge in the Yangon River